May 2019

Wireless Electrostimulation to Eradicate Bacterial Biofilms

Hao Wang
Syracuse University

Abstract

Bacterial biofilms can form on medical implants and cause serious device-associated infections that are incurable by conventional antibiotics because of high-level tolerance to antimicrobials. Common strategies for controlling device-associated infections, such as coating with antimicrobials and modification of surface properties, can reduce or delay biofilm formation, but the inhibitory effect can be overcome by bacteria over time, and eradicating mature biofilms remains challenging. Direct currents (DCs) have been shown to have bactericidal effects and synergy with conventional antibiotics in concurrent treatment has been demonstrated for killing biofilm cells. However, these systems require a direct connection between electrodes and a power source, which requires skin-piercing wiring for current delivery. This is an invasive process that causes discomfort and can lead to secondary infections. In this study, we developed a new method to achieve DC treatment wirelessly towards the non-invasive control of device-associated infections. *Pseudomonas aeruginosa* PAO1 and *Staphylococcus aureus* ALC2085 were used as model organisms to investigate the killing efficacy of wirelessly delivered DC.

In the proof-of-concept experiments, we demonstrate that antibiotic tolerant biofilm cells can be effectively eradicated by electromagnetically induced DC from a remote power source. For example, the number of viable *P. aeruginosa* and *S. aureus* biofilm cells was reduced by approximately 3.4 and 2 logs, respectively, after treatment with 60 $\mu A/cm^2$ of wirelessly delivered DC using stainless steel electrodes for 6 hours. DC generated with graphite-based TGON^{TM} electrodes was also effective especially against *S. aureus*. For example, the viability of *P. aeruginosa* and *S. aureus* biofilm was reduced by 1.4 and 2.5 logs, respectively, after treatment with the 30 $\mu A/cm^2$ of wirelessly delivered DC for 3 hours. Synergy in biofilm killing was also

observed between lower level DC and antimicrobials (tobramycin and chlorhexidine for *P. aeruginosa* and *S. aureus*, respectively). These conditions were found safe to both human lung epithelial cells and mouse fibroblast cells. Additionally, the viability of *S. aureus* and *Streptococcus mutans* biofilms on the denture material were also reduced by 5 and 4 logs, respectively, by the concurrent treatment with the 28 μA/cm^2 of DC and 50 μg/mL chlorhexidine for 1 hour.

To further evaluate the potential of this technology, we engineered a prototype device after comparing different device designs with varying shapes, electrode layouts, and electrode materials. The prototype device based on the selected design demonstrated 1.0 and 2.6 logs of killing of *P. aeruginosa* and *S. aureus* biofilms, respectively, with 6 μA/cm^2 of wirelessly delivered DC for 6 h using an *ex vivo* model with porcine skin. Further *in vivo* test using a rabbit model showed that the prototype device inserted under the dermis tissue killed *S. aureus* biofilm cells by 65 % *in vivo* when receiving a magnetic field from outside of the body to generate DC. No tissue damage was found according to the histological analysis.

The killing mechanism of DC treatment was investigated in this study by comparing the killing effects of different electrochemical products. The results show that DC treatment using TGON electrodes killed bacterial cells by generating hypochlorite from the anode; while the DC treatment using stainless steel electrodes induced Fenton reaction and generated free radicals that have potent bactericidal effects.

In summary, the findings from this study indicate that wirelessly delivered DC has promising anti-biofilm effects on bacterial pathogens, both *in vitro* and *in vivo*. To our best knowledge, this is the first study to report the bactericidal activity of wirelessly delivered DC treatment. With the capability to kill bacterial biofilm without using a directly connected power source, this platform

technology has potential applications for noninvasive treatment of biofilm infections associated with orthopedic, cochlear and other implanted medical devices.

WIRELESS ELECTROSTIMULATION TO ERADICATE BACTERIAL BIOFILMS

by

Hao Wang

B.S. Pharmaceutical Engineering, Southeastern University, 2006
M.S. Chemical Engineering, University of Dayton, 2011

Dissertation
Submitted in partial fulfillment of the requirements for the degree of
Doctor of Philosophy in Chemical Engineering.

Syracuse University
May 2019

This is dedicated to my family and homeland

Acknowledgments

First, I would like to express my gratitude to my research advisor, Dr. Dacheng Ren, for having me in his Lab since 2014. I thank he invited me to join the group in the summer of 2014, which was a very hard time for myself. His generous supports, productive advice and encouragement support me to finish my Ph.D. career. I sincerely appreciated the countless time he spent on my study, and the invaluable knowledge he taught me.

Second, I would like to thank the committee members of my dissertation defense, Dr. Anthony Garza, Dr. James Henderson, Dr. Shikha Nangia, Dr. Pranav Soman and Dr. Zhen Ma to their invaluable suggestions and helps to my research. Through them, I would love to appreciate Syracuse University, the office of Research, the College of Engineering, the Department of Biomedical and Chemical Engineering.

Third, I would like to thank our collaborators, Dr. Brian Nicholas, Dr. Juntao Luo, and Dr. Guirong Wang, for their generous help during the research. I want to especially appreciate Dr. Alex Tampio. It's a very good experience to work with him, and I can't finish the animal study without his excellent knowledge and skills. I want to thank Dr. Changying Shi for the help in histology analysis. I want to acknowledge Dr. Duane L. Marcy, Dr. Eric Finkelstein, Dr. Pun To Yung, Sally Prasch, Michael Brandt, Timothy Breen and William Dossert for their technical support in my research.

Then I would like to express the grateful thank to all the group members in Ren lab. It is my pleasure to work with Dr. Huan Gu, Dr. Fangchao Song, Dr. Geetika Choudhary, Dr. Ali Adem Bahar, Dr. Xiangyu Yao, Grace Altimus, Li Zhang, Nicholas Kelly, Bo Peng, Sang Won Lee, Yousr Dhaouadi, Yanrui Zhao, Shuyuan Ma, Xinran Song, Zhaowei Jiang, Xikang Xu, Hao Li,

Melissa Gerwitz and Diego Cordero. I want to especially thank Sweta Roy for kindly helping me in the animal study.

My grateful thanks also go out to Dr. Tagbo H. R. Niepa for initiating and establishing the fundament of the research of electric stimulation in our group.

I would also like to acknowledge the generous help provided by Jason Markle, Mario Montesdeoc, Karen Low, Amy Fobes, Sabina Redington, Dawn Long, Kristin Lingo. And I want to express my thanks to the financial support from the Gerber endowment funding of Syracuse University.

My upmost gratitude goes to my parents and parents in law Quanyu Wang, Xinlian Zhao, Jianguo Wang and Qihong Zhang for their love, and encouragements in my Ph.D. career. Special thanks are given to my wife, another Hao Wang, for loving, supporting and inspiring me in these years. Also, thank Leo for your patience and cooperation.

Table of Contents

List of figures

Chapter 3

Chapter 4

Chapter 5

Chapter 6

List of tables

Chapter 2

Chapter 4

Chapter 5

Chapter 7

Chapter 1

Motivation and hypothesis

1.1 Implant device-associated infections

The application of surgically implanted medical devices is on the rise due to advances in device design and improvement in patients' life quality [1]. However, device-associated infections remain challenging despite the improvement in sterilization techniques during the last decade [2]. Approximately 4.3% of the total 2.6 million orthopedic devices implanted in the United States every year are infected [3]. The risk of hearing aid implants (e.g. cochlear and bone anchored implant) associated infection is also approximately 4%; but more detrimental to younger patients [4, 5]. Such infections lead to ulcer, swelling or inflammation of affected tissues [6], and further surgeries for implant relocation, fixation and even explanation [7].

The standard therapeutic approach for controlling and curing the bacterial infection is antibiotic treatment. Since the discovery of penicillin in the 1940s, antibiotics have saved millions of lives from microbial infections. However, bacterial pathogenic also developed resistance to all kinds of commercially available antibiotics, which has become one of the most serious threats to public health. Based on CDC's report in 2013, there are at least 2 million people infected by the antibiotic-resistant strains annually and at least 23,000 people die in the U.S. alone [8]. Bacteria have multiple strategies to survive the killing of antibiotic resistance including acquired mechanism based on resistant genes and intrinsic mechanisms due to the formation of dormant persister cells and surface-attached biofilms. Among these factors, biofilms play an important role in recalcitrant device-associated infections since the abiotic surface of implanted medical devices are fairly susceptible to microbial adhesion [7 9].

1.2 Central hypothesis and specific aims

Due to the high-level antibiotic resistance, biofilm infections present serious challenges to infection control. Consequently, the use of conventional antimicrobials constantly fails to eradicate the biofilm cells on the implant surfaces even at high concentrations. Instead, treating biofilms at sub-lethal levels can promote the development of antibiotic-resistant strains, such as superbugs that resist all currently available antibiotics.

In 1994, Costerton et al. [10] demonstrated that low-level direct current (DC) had antimicrobial effects, and DC had synergy with the antibiotic in bacterial killing. This phenomenon, known as bioelectric effects, provides a new direction for engineering new antimicrobial strategies. However, the electric current must be delivered by wires in conventional electric treatment, which requires skin-piercing in clinical application. This could bring the risk of secondary infection and pain or discomfort. This severely limits the application of electric treatment. Using implantable battery is an option without skin-piecing, but the capacity of a battery limits the *in vivo* lifetime of the device and brings the risk of battery leak. We were motivated to develop a wireless system to deliver electric current from an external power to the implant device *in vivo*. We hypothesize that therapeutic levels of direct electric current (DC) could be delivered from a power source the medical device wirelessly. To test this central hypothesis and explore the underlying mechanisms, this study was conducted to systematically investigate the effects of wirelessly delivered DC on bacterial biofilms using *in vitro*, *ex vivo* and *in vivo* models. The proposed study was carried out in three specific aims:

Aim 1. To evaluate the effects of wirelessly delivered DC on bacterial biofilms by varying the electrode materials and treatment conditions and testing the synergy between DC and antibiotics

in vitro. *P. aeruginosa* and *S. aureus* were selected as model species and treated with the different levels of wirelessly delivered DC with or without antibiotics. Both graphite-based TGON and stainless steel coupons were tested as electrode materials. The mechanism of bacterial killing by DC was investigated by testing the effects of ions, solutions, and redox reactions.

Aim 2. To design a prototype device that integrates the wireless DC delivery and electric treatment system and evaluate its antimicrobial activities. The design was optimized to reduce the size to fit in a <30 mm^3 case, which is the same as cochlear implants, pacemakers and GI tract stimulators. The layout of the electrodes was also optimized.

Aim 3. To evaluate the effects of skin tissue on electromagnetic coupling and the killing effects of the DC treatment device in both *ex vivo* and *in vivo* models. The killing effects of the prototype device on biofilms was evaluated in an *ex vivo* model with porcine skin as the barrier and an *in vivo* model using rabbits. The cytotoxicity to host tissues was also studied by histological analysis.

1.3 Reference

1. Vinh, D.C. & Embil, J.M. Device-related infections: a review. *Journal of long-term effects of medical implants* **15**, 467-488 (2005).
2. Campoccia, D., Montanaro, L. & Arciola, C.R. A review of the biomaterials technologies for infection-resistant surfaces. *Biomaterials* **34**, 8533-8554 (2013).
3. Darouiche, R.O. Treatment of infections associated with surgical implants. *The New England journal of medicine* **350**, 1422-1429 (2004).
4. Germiller, J.A., El-Kashlan, H.K. & Shah, U.K. Chronic Pseudomonas infections of cochlear implants. *Otology & neurotology : official publication of the American Otological Society, American Neurotology Society [and] European Academy of Otology and Neurotology* **26**, 196-201 (2005).
5. Granstrom, G., Bergstrom, K., Odersjo, M. & Tjellstrom, A. Osseointegrated implants in children: experience from our first 100 patients. *Otolaryngology--head and neck surgery : official journal of American Academy of Otolaryngology-Head and Neck Surgery* **125**, 85-92 (2001).
6. Cunningham, C.D., 3rd, Slattery, W.H., 3rd & Luxford, W.M. Postoperative infection in cochlear implant patients. *Otolaryngology--head and neck surgery : official journal of American Academy of Otolaryngology-Head and Neck Surgery* **131**, 109-114 (2004).
7. Skrivan, J. & Drevinek, P. A case report of a cochlear implant infection - A reason to explant the device? *Cochlear implants international* **17**, 246-249 (2016).
8. Prevention, C.f.D.C.a. (2013).

9. Veerachamy, S., Yarlagadda, T., Manivasagam, G. & Yarlagadda, P.K. Bacterial adherence and biofilm formation on medical implants: a review. *Proc Inst Mech Eng H* **228**, 1083-1099 (2014).

10. Costerton, J.W., Ellis, B., Lam, K., Johnson, F. & Khoury, A.E. Mechanism of electrical enhancement of efficacy of antibiotics in killing biofilm bacteria. *Antimicrobial Agents and Chemotherapy* **38**, 2803-2809 (1994).

Chapter 2

Literature review

2.1 Microbial biofilm formation

Biofilms are a complex structure composed of bacterial cells and an extracellular matrix produced by the attached cells. Biofilms are constantly formed on implanted biomaterials and medical devices. When a device is implanted in a host, it is coated quickly coated with proteins such as fibrin and fibronectin, which provide a better anchor for bacterial adhesion [1]. Once a mature biofilm is established, it is difficult to eradicate due to slow growth and high level of antimicrobial tolerance [2].

Extracellular polymeric substance (EPS) is a major contributor to the antimicrobial resistance of biofilm cells, which prevents the common antimicrobial agents from effectively penetrating. This extracellular matrix is composed of polysaccharide, proteins, nucleotides, and lipids, which could protect cells from the oxidizing biocides, some antibiotics and metallic cations [3] by retarding the diffusion or neutralization [4].

Another mechanism of antimicrobial resistance of biofilm cells is its lower metabolic activities of biofilm cells. While EPS retards penetration of hazardous compounds into biofilm, the nutrients are also depleted in the biofilm, especially in deep layers, along with the accumulation of toxic metabolism wastes [5]. These factors lead to dormancy of biofilm cells and the formation of persister cells, a subpopulation with extremely high-level antibiotic tolerance but without genotype changes. In 1944, Joseph Bigger [6] first found that there was a small but constant subpopulation of *Staphylococcus,* which could survive after long-time treatment with high-concentration penicillin and named this subpopulation “persisters”. Resistant cells didn’t cause significant attention due to the success of antibiotic therapies until 2000s. Kim Lewis reported persister phenotype in *Escherichia coli* [7]. Numerous studies have shown that the persister cells formation is not due to

genetic mutation but rather phenotypic variants [8-12]. When the cells survived were sub-cultured in the absence of antibiotics and rigorously antibiotic treatment, the new culture exhibits the same level of antibiotic susceptibility, which indicates it is tolerance, rather than resistance.

2.2 Biofilm formation on the implanted medical devices

Microbial pathogens that cause biofilm-associated infections usually come from the patients' skin, surgical equipment or hospital environment [13]. The infection may occur immediately after surgery or during the post-surgery period ranging from several months to years depending on the causative agents and the patient's immunity. The standard treatment of such conditions is using antibiotics. If the antibiotic therapy fails, the patient needs two-step surgeries. This requires explanation, cleaning the infected area with a high concentration of antibiotics, and implantation of a new device [14]. This procedure is expensive and negatively impacts the life quality of the patient.

Biofilm formation is a dynamic process including initial attachment, microcolony formation, maturation and dispersion [15]. The concept of "race for the surface" well describes the nature of biofilm-associated infections on implants; e.g., if bacterial adhesion occurs on implanted biomaterial before tissue integration, it is difficult to prevent further biofilm formation by host defense [16]. There are many factors that affect bacteria adhesion, such as the roughness [17-19], topography [20-22], hydrophobicity [23-25], net charge of the surface [25, 26] and van der Waals forces between cells and surface [27]. Bacterial cells can produce specific proteins and other molecules to enhance the initial attachment on medical device surfaces [27-29].

After bacterial cells irreversibly attach to the surface, the cells proliferate to form clusters with multiple layers of cells in mature biofilms. During this stage, the extracellular polysaccharide is produced, and form an extracellular matrix along with proteins and extracellular DNA [28, 30, 31].

Bacterial cell-cell signaling system, such as quorum sensing (QS) system is also active in the biofilms, which have major impacts on biofilm formation, motility, and production of EPS [32]. For example, *S. aureus* uses the Agr QS system to regulate the production of virulence factors that promote surface attachment and protect the cells from clearance by the host immune system [33].

Along with biofilm maturation, bacterial cells become inactive (e.g. persister formation) or due to the lack of nutrient and accumulation of toxin [34, 35]. Under certain conditions, biofilm cells may dispense from the biofilm matrix, and migrate to another location with motility and/or flow [5, 36, 37]. This leads to the spread of infection from the implant site to the bloodstream and other organ tissues, which can be life-threatening [38, 39]. As a result, even if the patient has received the anti-infection therapy or new implantation, bacterial cells may come back from surrounding tissues and cause infection again, leading to chronic infections with recurring symptoms [40]. Most causative agents of device-associated infections are opportunistic pathogens, consistent with the protection of biofilms. These species include *P. aeruginosa* [8, 40], *S. aureus* [16, 41], *Klebsiella pneumonia* [42] and *Acinetobacter baumannii* [43].

2.3 Representative implant device-associated infections

Dental implants are widely used implanted devices serving for different purposes. Unfortunately, the human mouth is an ideal environment for microbial growth; e.g. there are approximately 10^9 bacterial cells of more than 1,000 species in each mL human saliva [15, 44]. Because the dental surfaces are coated with saliva which contains mucus, varying enzymes and many other components, such as epithelial cells, lysozyme and secretory IgA [15], these surfaces are prone to microbial attachment, growth and the formation of dental biofilms (also known as dental plaques) in the oral cavity. One pathogen with significance in dental biofilm is *S. aureus*. Unlike other

common oral species, such as *Streptococcus mutans* and *Streptococcus gingivitis* that produce acid to cause tooth decay, *S. aureus* is frequently linked to infections associated with the dental implant infection [45, 46]. *S. aureus* biofilms cause inflammation of surrounding tissues (e.g. gum), pain, and may lead to implant failure. Because infections often happen in the deeper site of soft tissue, daily oral hygiene has limited impact [45].

Orthopedic implants are another type of devices facing challenges by biofilms. The surfaces of commonly used orthopedic components contain stainless steel, titanium, ceramic, cobalt-chromium alloy, hydroxyapatite, and polymethylmethacrylate (PMMA) cement. All these materials are susceptible to colonization by bacterial cells [47, 48]. In general, 34% of infections are caused by *S. aureus*, followed by *S. epidermidis* (32%), and *P. aeruginosa* (7%) [49]. It is alarming that the Methicillin-resistant *S. species* (MRSA *S. aureus*) is fund in increasing cases orthopedic infections [50]. The conventional strategies to prevent orthopedic implant infections focus on controlling environmental and personal factors related to the surgical operation. In recent research, antifouling/antimicrobial techniques have been applied to modify orthopedic materials, such as bactericidal coating or antifouling surface modification by altering charges, roughness, hydrophobicity of the implanted materials.

Modern devices, such as cardiovascular implants, cochlear implants, insulin pumps, and GI tract stimulators, are also susceptible to biofilm-associated infections. Due to their rather short history of application, there are only a few epidemiological reports about the infections of these electronic devices; however, the problem is expected to become more serious due to the rapid increase in the use of electronic implants. Based on the limited data from the recent literature, *Staphylococcal* biofilm is still the primary cause [4, 51, 52], and *P. aeruginosa* is more correlated with chronic infections [53]. Infections associated these devices could lead to more serious or even life-threatening

conditions than orthopedic and dental infection since the implant sites are usually close to important organs or central nervous system (e.g. brain, heart). As other device-associated infections, Antibiotic treatment is the primary choice for therapy. If antibiotic treatment fails, patients have to take surgeries to explant the devices. Because these devices usually have essential life-saving functions, the surgery of electronic medical devices have higher risks, and thus are complicated than orthopedic or dental surgery. Those surgeries bring more suffering to patients due to longer recovery time from the surgical trauma [54].

In summary, biofilm-associated infections have a significant risk for medical implants because these devices are widely applicable in the human body to improve life quality, facilitate therapies process or sustain life. High-level resistance to antibiotics of biofilm cells necessitates multidisciplinary research to develop more and more comprehensive solutions to these challenging problems.

2.4 Current antifouling and antimicrobial approaches for controlling device-associated infections

An effective approach to preventing infection is to use materials that have antimicrobial activities. Some metals have intrinsic bacterial killing activities, such as silver, zinc, and copper. Multiple mechanisms are involved in bacterial killing. For examples, silver ions can interact with thiol (sulfhydryl) groups and interfere with the respiratory chain of bacterial cells [55]. Zinc oxides nanoparticles can cause morphological changes and measurable membrane leakage of bacterial cells [56]. However, the bactericidal effect of metal ions is not highly specific to prokaryotic cells, which lead to cytotoxicity to host cells [57-59]. Moreover, the corrosion of metal materials *in vivo* could accumulate excessive metal ions and possibly precipitates, which have detrimental effects

on host tissue and organs. For example, silver ions and silver chloride precipitates were found to have cytotoxicity to red blood cells and human mesenchymal stem cells [57]. Although the metals are not used as bulk for implanted devices, these materials are promising candidates for using in nanoparticles, hydrogel or bioactive alloys with other non-toxic metal materials. Chitosan is another biomaterial with promising antimicrobial activities. It is a polycationic polymer compound derived from chitin. By modifying the chitosan structure, a number of derivatives have been developed with improved functions [60, 61].

Another strategy for combating device-associated infections is coating the metal (e.g. titanium) or polymerase material (e.g. silicone, hydrogel) of the device with a bioactive antibacterial layer. Most commonly used coating materials include antibiotics, chlorhexidine, chitosan and the derives, antimicrobial peptides, and materials that can release copper and silver ions (See Table 1). The bactericidal substances are loaded into the bulk materials via covalent bonding, charging force, or forming a complex. These coatings kill bacterial cells either via direct contacting or by releasing antimicrobial agents to surroundings.

An alternative strategy to modification antimicrobials surface for killing is preventing attachment of cells or disturbing biofilm formation by altering chemical and physical properties of the surface. Biofilm formation can be prevented by changing the topography, charge, hydrophobicity, roughness, or stiffness of the materials [15, 72, 73].

Table 1. Examples of antimicrobial coating and biomaterials

Coating substance	Surface material	Target bacterial species	Reference
Chlorhexidine	Titanium	*S. aureus*	[62]
Benzalkonium chloride	Polyurethane	*S. epidermidis*	[63]
Antimicrobial peptide	Hydroxyapatite	*S. aureus* *P. aeruginosa* *S. epidermidis*	[64]
Antimicrobial peptides	Hydrogel	*S. aureus*	[65]
Chitosan	Titanium alloy	*E. coli*	[66]
Chitosan	Collagen hydrogel	*S. aureus*	[60]
Copper and fluorine	Polyester	*S. aureus*	[67]
Silver	Hydroxyapatite	*S. epidermidis* *S. aureus*	[68]
Chlorhexidine	CHG gel	*S. aureus* *E. coli*	[69]
Trimethylammonium chloride	Silicone	*S. aureus* *Enterococcus faecalis*	[70]
S-nitrosothiol	Xerogel	*P. aeruginosa*	[71]

Most bacterial cells have a negative charge on the outer membrane. Thus, a surface with a positive charge is more attractive for bacterial cells than the negative charge that can repulse bacterial cells from attachment [15]. Based on this principle, many coating materials have been developed to modify the surface charge of biomaterials to prevent biofilm formation. For example, polyethylene (PE) surfaces were modified with a large of negatively charged sodium sulfite using glycidyl methacrylate (GMA) as the linking agent, which reduces *E. coli* cell density by 10 times compared to positively charged surface [74]. Similarly, Carmona-Ribeiro et al. [75] reported that the cationic antimicrobial substances such as dioctadecyldimethylammonium bromide (DODAB), could reduce the viability of *E. coli*, *P. aeruginosa, S. aureus* as well as *C. albicans*. However, the

antimicrobial and antifouling properties of surface charge could be hindered by dead cells, which cover/neutralize the charges and provide protection to later colonies.

Hydrophobicity is another important factor influencing the antifouling property of biomaterials. In general, a hydrophilic surface could provide high affinity to water and tissue cells but is also prone to attachment of bacterial cells. However, the superhydrophilic surface is non-fouling due to the strong dipoles of the zwitterions and electrostatic interactions [76]. Making some materials hydrophobic or superhydrophobic was also found to affect biofilm formation. For instance, Tripathy et al. [77] showed the coating of copper hydroxide nanowires on polydimethylsiloxane (PDMS) could reduce the cell density of *E. coli* up to 5 logs compared to the uncoated surface. Loo et al. [78] also found the reduced attached *P. aeruginosa* cells on the polyvinyl chloride (PVC) surface with the micron-sized particulates and porous structures made by ethanol (35% (v/v)) treatment. In contrast to typical gram-negative strains, some gram-positive strains demonstrated a lower affinity to hydrophilic surfaces than hydrophobic ones because of their different surface proteins [79]. *Streptococcus mutans* biofilms were reduced by 8 times on the surface of resin blended with 2,2-bis[4-(2-hydroxy-3-methacryloylpropoxy)]-phenyl propane (bisGMA), bis[2-(methacryloyloxy)ethyl]phosphate (BisMP) and 2-hydroxyethyl methacrylate (HEMA) than hydrophobic resin. *S. epidermis* biofilm formation was also reduced on the hydrophilic Pluronic F127 coated polystyrene surfaces [80].

Surface topography is another feature that attracted much attention, and the specific topographic patterns can control bacterial cell attachment and biofilm formation. Gu et al. [79] reported the hexagon-shaped topographic patterns with 15 μm side length, 10 μm height and 2 μm inter-pattern distance could reduce 85% of biofilm formation and 46% of associated conjugation than a smooth surface. They also found that the topographic pattern could affect interfere cells cluster formation

[81]. Manabe et al. [82] demonstrated the porous polystyrene surface could prevent *P. aeruginosa* attachment when the pore size was 5 to 11 μm although the pores out of this range promoted cells' attachment. Xu et al. [83] reported that the adhesion of *S. epidermis* cells on the polyurethane urea surface was reduced by micro- and nano-size pillar patterns on the surface. The nano-size patterns not only reduced bacterial adhesion but also exhibited biocidal effects. Yi et al. [56] reported the significant killing of bacteria and fungi using the ZnO nanopillar coated surfaces that was inspired by dragonfly wings.

Although stiffness is an important material property, the effects of stiffness on biofilm formation have not been systematically studied until recently. Song et al. [15, 84, 85] reported that the attachment of *E. coli* and *P. aeruginosa* was 1 – 2 logs lower on the stiff (5:1) PMDS surface than soft (40:1) in early biofilm (5h). Besides attachment, bacterial motility was also found differences between stiff and soft surfaces, which suggests that these cells preferred to settle down on soft PDMS [85]. However, the antifouling effect of surface stiffness seems also to be affected by material types. For example, Kolewe et al. [86] found softer hydrophilic PEGDMA and agar hydrogels had less attached *E. coli* and *S. aureus* cells.

2.5 Limitation of present antifouling and antimicrobial approaches

Although many materials have been demonstrated for antimicrobial/antifouling activities during the last decades, most of these techniques still have drawbacks that limit applications *in vivo*. For example, some new bactericidal materials can eradicate pathogens efficiently by direct-contact or releasing biocidal agents into surroundings, but those materials could also induce the drug-resistant species during the treatment [87, 88]. Furthermore, a few studies reported the cytotoxicity of surface-coated antimicrobial peptides [89, 90] and silver nanoparticles (Ag-NPs) [91-93] in mammalian cells. The

antifouling materials with alternated surface chargers, hydrophobicity, topography or stiffness may be limited to the effect on early biofilm formation, and less effective against later colonizer. Also, the effects are not complete eradication. Once a few cells have attached and established early biofilm colonies, they will overcome the antifouling effects over time [15, 85]. Thus, it is important to develop new techniques that not only have long-term antimicrobial/antifouling effects to present biofilm formation but also can eradicate existing biofilms. This is of particular importance to medical device-associated biofilm infections because all the patients have established biofilms.

2.6 Electrochemical control of biofilm

Bacterial control by electrochemical approaches has been explored as an alternative strategy. An early approach to electric sterilization approach is utilizing high energy electric pulse, also called pulsed electric field (PEF), to eradicate the microorganisms in a liquid [94]. PEF was also found to inactivate yeast cells in 1980s [95]. Since PEF is a nonthermal process, it has been applied in the food industry to achieve decontamination of liquid or semi-liquid products, such as milk, juice and beverages [96-98]. The process of PEF shows little effects on proteins, so it could also be applied to biological products like porcine plasma [99]. The potential of the external electric field for PEF treatment ranges from volts to kilovolts [98, 100]. The killing mechanism of PEF is believed to changes in membrane permeability and integrity leading to cell lysis [101]. When a microbial cell is in a strong electric field, it could induce a transmembrane potential that is proportional to the external electric field strength. The cell membrane could break once the transmembrane is over critical value (1V) [102]. If the change is applied for a fairly short time, the cell membrane may still return to normal state (still weaker than normal cell) when the external electric field is removed, which is a well-known process of electroporation. However, if the strength and duration of electric field exceed the critical values, the cell membrane would incur permanent damages that lead to the lysis of the

cell [94, 101]. Recently, Pillet [103] reported that PEF also led to cell wall deterioration, such as decreasing stiffness and hydrophobicity. According to the technique specifications, PEF is not suitable for applying in human body directly because of its high energy that exceeds the safety limit.

In 1915, Beattie [104] reported the use of alternating current (AC) to control bacterial cells. It was found that biocidal effects of AC can be obtained when a very high potential (3000 – 4000 V) was applied to sterilize milk. In 1962, Brandt et al. [105, 106] first proposed that the free radicals generated during electric treatment contribute to the killing of bacteria. Rosenberg [107] reported that *E. coli* could be killed with 2 A of AC using platinum electrodes. Low-level AC was also found to have bactericidal effects. Pareilleux et al. [105] reported that the viability of *E. coli* was reduced after treatment with 10 to 200 mA of AC in 10s, using stainless-steel electrodes.

Compared to AC, direct current (DC) has received more attention as an alternative antimicrobial method recently. Rowley [108] first showed the biocidal effects on *E. coil* with 1- 140 mA DC conducted with platinum electrodes in 1970s. Baranco [109] demonstrated the killing of *S. aureus* cells using 400 μA DC delivered with silver, platinum, gold or stainless steel electrodes. In general, DC requires lower current levels for bacteria-killing compared to AC. Table 2 shows the representative examples of studies on controlling bacteria cells using electric current. Most of these researches used metal electrodes because of their high conductivity, stable electrochemical properties (e.g. platinum, titanium, gold) [110, 111], application in medical device (e.g. titanium, stainless steel) [112, 113], and antimicrobial effects (e.g. copper, silver). The carbon materials recently become attractive in the researches due to its good corrosion resistance [114] and biocompatibility [115]. Both metal and carbon electrodes show potent bactericidal effects in DC treatment on pathogenic cells, such as *P. aeruginosa*, *S. aureus*, *S. epidermidis,* and *E. coli*, although their

electrochemical products could be different [116, 117]. The reported reduction effects of electric current on bacterial cells varied in different experimental conditions (current level, treatment duration and position of samples). In general, the longer treatment duration could kill more bacterial cells than short treatment [118-120], and the biofilm on the electrode surface was more vulnerable to DC treatment than biofilm away from the electrodes [116, 117, 121, 122]. Although a higher level of electric current absolutely has stronger bactericidal efficacy [118], the recent researches focus on controlling biofilm with a lower level of DC (1-500 μA) because of the safety issues [116, 117, 120-125].

It is exciting that bacterial killing by DC/AC can be enhanced through synergistic effects with antibiotics. For example, 2 additional logs of killing of *E. coli* effects by gentamicin and oxytetracycline were obtained with concurrent treatment with 6 mA/cm^2 of DC [126]. Similar synergistic effects were also found for AC although the current level of AC was up to 150 mA [126]. In 1994, Costerton et al. [30] also reported that low-level DC could also promote the killing of antibiotics against bacterial biofilms using *P. aeruginosa* as the model species.

Table 2. The examples of researches used electric current to eradicate bacteria cells.

Current/Voltage Level	**AC/DC**	**Electrodes material**	***Bacterial Species***	**Findings**	**Ref**
3000 – 4000 V	AC	Copper	Mixed species in milk	Bactericidal effect	[104]
2 A	AC	Platinum wire	*E. coli*	Division inhibition	[107]
10 - 200 mA	AC	Stainless steel	*E. coli*	Bactericidal effect	[105]
1 - 140 mA	DC	Platinum wire	*E. coli*	Growth inhibition	[108]
40 and 400 μA	DC	Silver, platinum, gold, stainless steel wires	*S. aureus*	Bactericidal effect	[109]
5 – 10 μA	DC	Silver wires	Mixed Oral bacteria	Growth inhibition	[127]
0.7-1.8 mA/cm^2	DC	Platinum wires	*S. epidermidis* *P. aeruginosa*	6-7 logs reduction	[128]
50 μA	DC	Platinum wires	*K. pneumoniae* *P. fluorescens* *P. aeruginosa*	74% reduction to biofilm via anodic current	[123]
60 - 100 μA	DC	Stainless-steel	*S epidermidis*	76% reduction to biofilm	[124] [125]
20-2000 μA	DC	Stainless steel or graphite	*P. aeruginosa* *S. aureus*	3.5 – 5 logs reduction in 2-7 days treatment	[118]
200 μA	DC	stainless steel	*S. epidermidis*	3 logs reduction in 24 h treatment	[129]
1 – 5 mA	DC	Stainless steel	*E. coli* and *S. aureus*	5 logs reduction in 40 min treatment	[130]
2 - 2000μA	DC	Stainless steel, graphite, titanium or platinum	*S. aureus,* *P. aeruginosa* *S. epidermidis*	0.2 – 4.8 logs reduction to biofilm in 4-7 days treatment	[119]
100 - 500 μA	DC	platinum	*S. aureus* *S. epidermidis* *P. aeruginosa* *E. coli* *Candia* species	1.5 – 3 logs reduction to biofilm in 24 h treatment. 3 – 5 logs reduction to biofilm in 4 days treatment.	[120]
800 mV	DC	Gold	*E. coli, S. aureus*	0.5 – 1 logs reduction in 24 h treatment	[131]
−1.8 V for cathode	DC	Titanium	*S. aureus*	97% reduction *in vitro* 98% reduction *in vivo*	[132, 133]
1.25 – 2V/cm	DC/AC	stainless steel	*E. coli*	Bactericidal effect	[134]
10 mA	DC	Titanium	*Anaerobic species*	4-7 logs reduction to biofilm	[135]
1.5 V	DC	Carbon nanotube	*E. coli*	32 - 67% reduction	[136]
-0.6V	DC	Carbon fabric	*P. aeruginosa*	7.8 logs reduction to biofilm with antibiotics	[137]
70 μA/cm^2	DC	Stainless steel/Graphite	*P. aeruginosa*	2-7 logs reduction to persister cells	[116, 117, 121]
30 μA/cm^2	DC	Stainless steel	*S. mutans* and *S. aureus*	4-5 logs reduction to biofilm with antimicrobial	[122]

2.7 Killing mechanisms of DC

The exact killing mechanism of electric current is still unclear though there are many proposed theories. For the treatment with high voltage (kV) level electric pulses, the permanent damage of the cell membranes was observed [101]. In comparison, the effects of low-level DC are thought to occur via electrochemical products, rather than directly affecting cell membrane integrity. There are many possible redox reactions that happen at the interface between electrode and electrolyte solution during electrolysis procedure:

Oxidation reactions on the anode [138]:

$$2H_2O \rightarrow 4H^+ + O_2 + 2e^-$$

$$Fe \rightarrow Fe^{2+} + 2e^-$$

$$Fe^{2+} \rightarrow Fe^{3+} + e^-$$

$Cr \rightarrow Cr^{3+} + 3e^-$ (Trace in steel anode)

$$2Cl^- \rightarrow Cl_2 + 2e^-$$

$$Cl^- + H_2O \rightarrow HClO + 2e^- + H^+$$

$$Cl_2 + 2H_2O \rightarrow 2HClO + 2e^- + 2H^+$$

Reduction reactions on the cathode:

$$H_2O + 2e^- \rightarrow H_2 + 2OH^-$$

$$O_2 + 2H^+ + 2e^- \rightarrow H_2O_2$$

$$O_2 + H_2O + e^- \rightarrow HO_2 \cdot + OH^-$$

$$O_2 + 2H_2O + 2e^- \rightarrow H_2O_2 + 2OH^-$$

Redox reactions in the electrolyte solution [139]:

$$Fe^{2+} + H_2O_2 \rightarrow Fe^{3+} + OH\cdot + OH^-$$

$$Fe^{3+} + H_2O_2 \rightarrow Fe^{2+} + OOH\cdot + H^+$$

$$2Fe^{3+} + 2H_2O \rightarrow 2Fe^{2+} + H_2O_2 + 2H^+$$

During DC treatments, the anode material, especially silver, copper or steel, is oxidized and metal ions (Ag^+, Cu^{2+}/Cu^+, Cr^{3+}, Fe^{2+}/Fe^{3+}, et al.) are released [121]. These ions could accumulate and become toxic to bacterial cells by interrupting cells' and metabolic activities. Moreover, the generated metal ions could move under an electric field, which can disrupt the integrity of cell membrane [116, 121]. Based on the principles of electrochemistry, reactive oxygen species (ROS) and free radicals are also generated from the redox reaction involving electrodes. However, this is difficult to prove directly since many of these species react quickly and thus only have the transient presence. Hydrogen peroxide (H_2O_2) is one of several proofed ROS generated in electric treatment. H_2O_2 affects the structure and permeability of the cell membrane [140]. The concentration of H_2O_2 closed to electrode surface ranges from 1ppm to more than 15ppm depending on the current density [141]. However, the concentration decreases quickly over the distance away from the electrode [141]. Another reported ROS generated during DC treatment is hypochlorite if the electrolyte solution contains chloride ions. The chloride ions are oxidized on the anode to produce chlorine and hypochlorite [135]. Hypochlorite could disrupt a series of metabolic activities of bacteria, such as oxidative phosphorylation and sulfhydration, as well as DNA synthesis [142]. The generation of hypochlorite depends on the current level and concentration of chloride [135].

The mechanism of synergy between antibiotics and electric current treatment is of research interest. It is speculated that DC weakens the cell membrane leading to higher permeability to antibiotic molecules [30]. Electrochemical products could also disrupt extracellular matrix, and expose biofilm cells more to antibiotics molecules [143]. Many antibiotics have charges after dissolved, and these cationic or anionic antibiotic molecules have better penetration to the cell membrane in the presence of electric field [144]. Moreover, some anionic molecules could interact with metal ions to form a complex that has a higher affinity to cellular targets, such as RNA [145].

2.8 Limitation of conventional DC treatment

An essential requirement for DC treatment with the conventional setup is that the treatment facility (electrodes) must be connected to a power source by wires. This limits the *in vivo* applications, especially for treatment in deeper tissues. To deliver electric current, the electric wires must be introduced into the body to reach the treatment site. There are two options to achieve this: 1) insert wires through natural pores (oral, nasal, ear canal, etc.) if the treatment site is in the mouth, nose or ear. 2) pierce skin directly to insert wire from outside to the treatment position. Both options would bring discomfort to the patient. Moreover, skin-piercing increases the risk of secondary infection [146], since the piercing breaks the skin barrier. The wiring requirement needs to be solved if we want to apply electric current for human therapy. This motivated us to develop a platform to deliver DC wirelessly for bacterial control.

2.9 Wireless charging technologies

Wireless charging (also known as inductive charging) is a technique that uses an electromagnetic field to transfer electric energy between two objects. The transfer medium is radio wave, and the phenomena are called resonant inductive coupling between two conducts. In 1894, Nikola Tesla

first used this principle to light up a phosphorescent and incandescent lamp without direct connection with a power cord [147]. The early devices of wireless electric delivery needed a very high voltage at high frequency (~150 kHz) in the 19th century. In 1960s, the first wireless electric delivery system was developed for the pacemaker, and the distance of wireless delivering was less than 20 cm [148].

Recent research on wireless electric delivery can be divided into three major fields. One focuses on improving charge efficiency (up to 75 – 80%) and the other on developing rapid charging at kilowatt power levels for those high-power electric consumers, such as road electrification devices. The third field is working on low milliwatt power levels that could provide stable and safe electric power to implantable and wearable devices [148].

Today many types of medical devices carry a wireless electric delivery system, such as pacemaker, cochlear and gastric stimulation implants [149] [150, 151]. The major advantages of wireless charging for medical implants include low risk of infection and good reliability. Since the magnetic field could penetrate the skin tissue and pass the energy to the device *in vivo*, there is no requirement for skin piecing, which could reduce the risk of post-surgical infection. Wireless charging device also avoids the use of batteries, which need replacement, and are associated with the issues of corrosion.

To achieve wireless electric delivery by resonant inductive coupling, it requires two basic sub-systems are required: a transmitter unit and a receiver unit. The transmitter unit is composed with a transmitter coil (primary coil) and controller chips. The transmitter coil can transfer alternating current to a time-changing magnetic field because the conduct with electric current could generate a magnetic field on the surrounding. The controller chips are used for adjusting the frequency and current level of AC in the coil to obtain the desired strength and frequency of the magnetic field.

The magnetic field can use radio wave to transport and penetrate the barrier, so no wire or other physical medium is required. The receiver unit is composed of a magnetic coil and another controller chips. The magnetic coil works as an antenna to receive the magnetic field and then transfers back to altering current according to the Faraday's law of induction. The function of controller chips in receiver unit is to convert AC to a stable DC. This DC level can be adjusted from μA to mA level for effective control bacterial biofilms.

2.10 Materials and methods used in research

2.10.1 Strains

Wild-type *Staphylococcus aureus* and *Pseudomonas aeruginosa* PAO1 strains were chosen as representative species in this study. *S. aureus* is a gram-positive strain and commonly found in the human bodies, such as nose, respiratory tract, and skin. It is also an important pathogen that causes community and hospital-acquired infections. There have been almost 500,000 cases of *S. aureus* infections reported in U.S. and 58% of these are related to Methicillin-resistant *S. aureus* (MRSA) strains [152]. For implant-associated infections, the prevalence of *S. aureus* is 35.5% in orthopedic implant infection cases based on an epidemiology study [153]. *P. aeruginosa* is a gram-negative strain and one of the most significant pathogens. Since *P. aeruginosa* can form robust biofilms on the surface of biomaterials, it is commonly linked to chronic infections after implant surgery [53]. According to the CDC, there are about 51,000 healthcare-associated *P. aeruginosa* infections annually in the U.S., causing approximately 400 deaths.

NCI-H1299 (ATCC® CRL-5803™) human epithelial cells and C3H/10T1/2, Clone 8 (ATCC® CCL-226™) mice fibroblast cells are chosen as mammalian cells to investigate the effect of wireless DC treatment on mammalian cell lines. We used these mammalian cells to mimic the host

tissue cells around implant sites to evaluate the cytotoxicity of wirelessly delivered DC. The cells are grown on the bottoms of mammalian culture petri dishes and treated under the same conditions as bacteria cells.

2.10.2 Substrate material for biofilm formation

Poly(dimethylsiloxane) (PDMS) is chosen as the substratum material for biofilm growth in this study. This material is broadly used in medical devices, especially as biocompatible case material for electronic implant devices (such as cochlear implants, pacemakers, GI track stimulators, et al.) [154, 155]. According to the previous researches, the silicone shells are the primary sites for biofilm formation since this material is susceptible to bacterial attachment [38]. Hence, the biofilm formed on PDMS surface is a suitable infection model for our research.

2.10.3 Wireless charging system

The electromagnetic field used in this research is the extremely low field (ELF) with a frequency of 100,000 Hz. The *in vitro* system of wireless DC delivery was connected to a treatment facility (petri dish with two electrodes) in the series circuit. It contained an AC power source, transmitter coil & controller chip, receiver coil & controller chip, and an external resistor (Figure 1). The transmitter and receiver coils were used to achieve wireless electric delivery by coupling induction. The main functions of the controller chip are AC/DC conversion as well as controlling the frequency of the electromagnetic field. An external resistor was used to adjust DC level in the treatment circuit. A multimeter was included into the circuit during setup to monitor the voltage across the external resistor. The current level was calculated based on below equation:

$$I_{total} = \frac{U_{\ resistor}}{R_{resistor}}$$

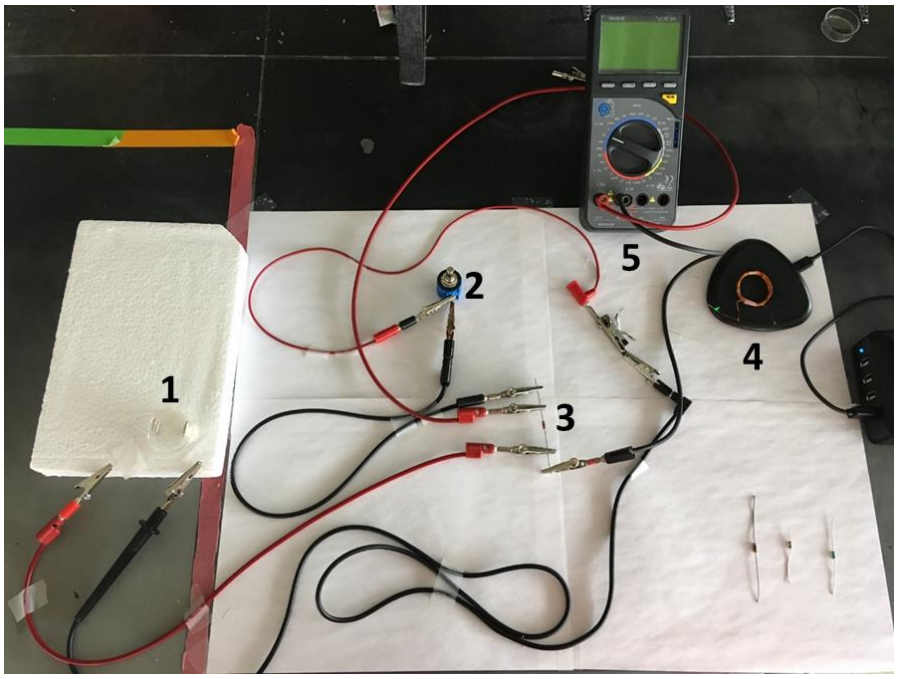

Figure 1. The actual circuit of wireless DC delivery system in our research (1: Treatment petri dish. 2: Adjustable resistor. 3: Fixed resistor. 4: transmitter and receiver coils. 5: Multimeter.)

2.10.4 Cytotoxicity test

To evaluate the safety of DC to human tissue, it is essential to test cytotoxicity to mammalian cell lines after the treatment with wirelessly delivered DC. In this study, we used Live/Dead staining to differentiate health cells and dead injured cells after treatment. This Live/Dead staining is based on the difference in membrane permeability between live and dead cells, and thus the labeling efficiency between green (live cells) or red (dead cells) fluorescence. The staining kit contains two different dyes: Calcein AM and Ethidium homodimer-1. Calcein AM has green fluorescence with ex/em wavelength of 494/517 nm, while Ethidium homodimer-1 has red fluorescence with ex/em wavelength of 528/617 nm. The Calcein AM is polyanionic and retains on live cells membrane. The Ethidium homodimer-1 can only penetrate the damaged membrane of dead or unhealthy cells

and bind to nucleic acid. Once binding to DNA, Ethidium homodimer-1 has 40-fold enhancement of fluorescence, so that the dead cells would have a bright red color under fluorescence microscopy. The membrane of intact cell blocks the penetration of Ethidium homodimer-1 so that they have a green color under fluorescence microscopy.

2.11 Reference

1. Dwayne C. Savage , M.F. Bacterial adhesion: mechanisms and physiological significance, Edn. 2nd. (Springer, University of Michigan; 1985).
2. Shen, Y., Stojicic, S. & Haapasalo, M. Antimicrobial efficacy of chlorhexidine against bacteria in biofilms at different stages of development. *J Endod* **37**, 657-661 (2011).
3. Flemming, H.C. & Wingender, J. The biofilm matrix. *Nat Rev Microbiol* **8**, 623-633 (2010).
4. Antonelli, P.J., Lee, J.C. & Burne, R.A. Bacterial biofilms may contribute to persistent cochlear implant infection. *Otology & neurotology : official publication of the American Otological Society, American Neurotology Society [and] European Academy of Otology and Neurotology* **25**, 953-957 (2004).
5. Sauer, K. et al. Characterization of nutrient-induced dispersion in Pseudomonas aeruginosa PAO1 biofilm. *J Bacteriol* **186**, 7312-7326 (2004).
6. Bigger, J.W. The bactericidal action of penicillin on staphylococcus pyogenes. *Irish Journal of Medical Science* **19**, 11 (1944).
7. Lewis, K. Persister cells. *Annual Review of Microbiology* **64**, 357-372 (2010).
8. Keren, I., Kaldalu, N., Spoering, A., Wang, Y. & Lewis, K. Persister cells and tolerance to antimicrobials. *FEMS Microbiol Lett* **230**, 13-18 (2004).
9. Balaban, N.Q., Merrin, J., Chait, R., Kowalik, L. & Leibler, S. Bacterial persistence as a phenotypic switch. *Science* **305**, 1622-1625 (2004).
10. Keren, I., Shah, D., Spoering, A., Kaldalu, N. & Lewis, K. Specialized persister cells and the mechanism of multidrug tolerance in Escherichia coli. *J Bacteriol* **186**, 8172-8180 (2004).

11. Mulcahy, L.R., Burns, J.L., Lory, S. & Lewis, K. Emergence of Pseudomonas aeruginosa strains producing high levels of persister cells in patients with cystic fibrosis. *Journal of Bacteriology* **192**, 6191-6199 (2010).

12. Lewis, K. Persister cells: molecular mechanisms related to antibiotic tolerance. *Handbook of Experimental Pharmacology* **(211):121-33. doi**, 121-133 (2012).

13. Veerachamy, S., Yarlagadda, T., Manivasagam, G. & Yarlagadda, P.K. Bacterial adherence and biofilm formation on medical implants: a review. *Proc Inst Mech Eng H* **228**, 1083-1099 (2014).

14. Skrivan, J. & Drevinek, P. A case report of a cochlear implant infection - A reason to explant the device? *Cochlear implants international* **17**, 246-249 (2016).

15. Song, F., Koo, H. & Ren, D. Effects of Material Properties on Bacterial Adhesion and Biofilm Formation. *Journal of dental research* **94**, 1027-1034 (2015).

16. Hetrick, E.M. & Schoenfisch, M.H. Reducing implant-related infections: active release strategies. *Chemical Society Reviews* **35**, 780-789 (2006).

17. Quirynen, M. & Bollen, C.M. The influence of surface roughness and surface-free energy on supra- and subgingival plaque formation in man. A review of the literature. *J Clin Periodontol* **22**, 1-14 (1995).

18. Truong, V.K. et al. The influence of nano-scale surface roughness on bacterial adhesion to ultrafine-grained titanium. *Biomaterials* **31**, 3674-3683 (2010).

19. Carlén, A., Nikdel, K., Wennerberg, A., Holmberg, K. & Olsson, J. Surface characteristics and in vitro biofilm formation on glass ionomer and composite resin. *Biomaterials* **22**, 481-487 (2001).

20. Teughels, W., Van Assche, N., Sliepen, I. & Quirynen, M. Effect of material characteristics and/or surface topography on biofilm development. *Clin Oral Implants Res* **17 Suppl 2**, 68-81 (2006).

21. Chung, K.K. et al. Impact of engineered surface microtopography on biofilm formation of Staphylococcus aureus. *Biointerphases* **2**, 89-94 (2007).

22. Valle, J. et al. Evaluation of Surface Microtopography Engineered by Direct Laser Interference for Bacterial Anti-Biofouling. *Macromol Biosci* **15**, 1060-1069 (2015).

23. Cerca, N., Pier, G.B., Vilanova, M., Oliveira, R. & Azeredo, J. Quantitative analysis of adhesion and biofilm formation on hydrophilic and hydrophobic surfaces of clinical isolates of Staphylococcus epidermidis. *Res Microbiol* **156**, 506-514 (2005).

24. Di Bonaventura, G. et al. Influence of temperature on biofilm formation by Listeria monocytogenes on various food-contact surfaces: relationship with motility and cell surface hydrophobicity. *J Appl Microbiol* **104**, 1552-1561 (2008).

25. Guo, K. et al. Effects of surface charge and hydrophobicity on anodic biofilm formation, community composition, and current generation in bioelectrochemical systems. *Environ Sci Technol* **47**, 7563-7570 (2013).

26. Dunne, W.M. Bacterial adhesion: seen any good biofilms lately? *Clin Microbiol Rev* **15**, 155-166 (2002).

27. Chen, Y., Harapanahalli, A.K., Busscher, H.J., Norde, W. & van der Mei, H.C. Nanoscale cell wall deformation impacts long-range bacterial adhesion forces on surfaces. *Appl Environ Microbiol* **80**, 637-643 (2014).

28. Habash, M. & Reid, G. Microbial biofilms: their development and significance for medical device-related infections. *J Clin Pharmacol* **39**, 887-898 (1999).

29. Camilli, A. & Bassler, B.L. Bacterial small-molecule signaling pathways. *Science* **311**, 1113-1116 (2006).

30. Costerton, J.W., Ellis, B., Lam, K., Johnson, F. & Khoury, A.E. Mechanism of electrical enhancement of efficacy of antibiotics in killing biofilm bacteria. *Antimicrobial Agents and Chemotherapy* **38**, 2803-2809 (1994).

31. Stoodley, P., Sauer, K., Davies, D.G. & Costerton, J.W. Biofilms as complex differentiated communities. *Annual Review of Microbiology* **56**, 187-209 (2002).

32. Xiong, Y. & Liu, Y. Biological control of microbial attachment: a promising alternative for mitigating membrane biofouling. *Appl Microbiol Biotechnol* **86**, 825-837 (2010).

33. Wesson, C.A. et al. Staphylococcus aureus Agr and Sar global regulators influence internalization and induction of apoptosis. *Infect Immun* **66**, 5238-5243 (1998).

34. Arciola, C.R., Campoccia, D., Speziale, P., Montanaro, L. & Costerton, J.W. Biofilm formation in Staphylococcus implant infections. A review of molecular mechanisms and implications for biofilm-resistant materials. *Biomaterials* **33**, 5967-5982 (2012).

35. Semenyuk, E.G. et al. Spore formation and toxin production in Clostridium difficile biofilms. *PLoS One* **9**, e87757 (2014).

36. Uppuluri, P. & Lopez-Ribot, J.L. Go Forth and Colonize: Dispersal from Clinically Important Microbial Biofilms. *PLoS Pathog* **12**, e1005397 (2016).

37. Petrova, O.E. & Sauer, K. Escaping the biofilm in more than one way: desorption, detachment or dispersion. *Curr Opin Microbiol* **30**, 67-78 (2016).

38. Vinh, D.C. & Embil, J.M. Device-related infections: a review. *Journal of long-term effects of medical implants* **15**, 467-488 (2005).

39. Hall-Stoodley, L. et al. Towards diagnostic guidelines for biofilm-associated infections. *FEMS Immunol Med Microbiol* **65**, 127-145 (2012).

40. Costerton, J.W., Stewart, P.S. & Greenberg, E.P. Bacterial biofilms: a common cause of persistent infections. *Science* **284**, 1318-1322 (1999).

41. Harris, L.G. & Richards, R.G. Staphylococci and implant surfaces: a review. *Injury* **37 Suppl 2**, S3-14 (2006).

42. Anderl, J.N., Franklin, M.J. & Stewart, P.S. Role of antibiotic penetration limitation in Klebsiella pneumoniae biofilm resistance to ampicillin and ciprofloxacin. *Antimicrob Agents Chemother* **44**, 1818-1824 (2000).

43. Santajit, S. & Indrawattana, N. Mechanisms of Antimicrobial Resistance in ESKAPE Pathogens. *Biomed Res Int* **2016**, 2475067 (2016).

44. Dewhirst, F.E. et al. The human oral microbiome. *Journal of Bacteriology* **192**, 5002-5017 (2010).

45. Cuesta, A.I., Jewtuchowicz, V., Brusca, M.I., Nastri, M.L. & Rosa, A.C. Prevalence of Staphylococcus spp and Candida spp in the oral cavity and periodontal pockets of periodontal disease patients. *Acta Odontologica Latinoamericana : AOL* **23**, 20-26 (2010).

46. O'Donnell, L.E. et al. Dentures are a Reservoir for Respiratory Pathogens. *Journal of prosthodontics : official journal of the American College of Prosthodontists* (2015).

47. Gristina, A.G. Biomaterial-centered infection: microbial adhesion versus tissue integration. *Science (New York, N.Y.)* **237**, 1588-1595 (1987).

48. Archer, N.K. et al. Staphylococcus aureus biofilms: properties, regulation, and roles in human disease. *Virulence* **2**, 445-459 (2011).

49. Campoccia, D., Montanaro, L. & Arciola, C.R. The significance of infection related to orthopedic devices and issues of antibiotic resistance. *Biomaterials* **27**, 2331-2339 (2006).

50. Patel, A. et al. Methicillin-resistant Staphylococcus aureus in orthopaedic surgery. *J Bone Joint Surg Br* **90**, 1401-1406 (2008).

51. Im, G.J. et al. Analysis of Bacterial Biofilms on a Cochlear Implant Following Methicillin-Resistant Staphylococcus Aureus Infection. *Journal of audiology & otology* **19**, 172-177 (2015).

52. Xu, Y. et al. Nanoscale Plasma Coating Inhibits Formation of Staphylococcus aureus Biofilm. *Antimicrob Agents Chemother* **59**, 7308-7315 (2015).

53. Germiller, J.A., El-Kashlan, H.K. & Shah, U.K. Chronic Pseudomonas infections of cochlear implants. *Otology & neurotology : official publication of the American Otological Society, American Neurotology Society [and] European Academy of Otology and Neurotology* **26**, 196-201 (2005).

54. Carter, R. & Hailey, D. Economic evaluation of the cochlear implant. *Int J Technol Assess Health Care* **15**, 520-530 (1999).

55. Lansdown, A.B. Silver in health care: antimicrobial effects and safety in use. *Curr Probl Dermatol* **33**, 17-34 (2006).

56. Yi, G., Yuan, Y., Li, X. & Zhang, Y. ZnO Nanopillar Coated Surfaces with Substrate-Dependent Superbactericidal Property. *Small* **14**, e1703159 (2018).

57. Zhang, S. et al. Reduced cytotoxicity of silver ions to mammalian cells at high concentration due to the formation of silver chloride. *Toxicol In Vitro* **27**, 739-744 (2013).

58. Feltis, B.N. et al. Independent cytotoxic and inflammatory responses to zinc oxide nanoparticles in human monocytes and macrophages. *Nanotoxicology* **6**, 757-765 (2012).

59. Tchounwou, P.B., Newsome, C., Williams, J. & Glass, K. Copper-Induced Cytotoxicity and Transcriptional Activation of Stress Genes in Human Liver Carcinoma (HepG(2)) Cells. *Met Ions Biol Med* **10**, 285-290 (2008).

60. Cui, F. et al. Development of chitosan-collagen hydrogel incorporated with lysostaphin (CCHL) burn dressing with anti-methicillin-resistant Staphylococcus aureus and promotion wound healing properties. *Drug Deliv* **18**, 173-180 (2011).

61. Norowski, P.A., Jr. & Bumgardner, J.D. Biomaterial and antibiotic strategies for peri-implantitis: a review. *Journal of biomedical materials research.Part B, Applied biomaterials* **88**, 530-543 (2009).

62. Riool, M. et al. A chlorhexidine-releasing epoxy-based coating on titanium implants prevents Staphylococcus aureus experimental biomaterial-associated infection. *Eur Cell Mater* **33**, 143-157 (2017).

63. Tebbs, S.E. & Elliott, T.S. Modification of central venous catheter polymers to prevent in vitro microbial colonisation. *Eur J Clin Microbiol Infect Dis* **13**, 111-117 (1994).

64. Townsend, L. et al. Antimicrobial peptide coatings for hydroxyapatite: electrostatic and covalent attachment of antimicrobial peptides to surfaces. *J R Soc Interface* **14** (2017).

65. Haisma, E.M. et al. Antimicrobial Peptide P60.4Ac-Containing Creams and Gel for Eradication of Methicillin-Resistant Staphylococcus aureus from Cultured Skin and Airway Epithelial Surfaces. *Antimicrob Agents Chemother* **60**, 4063-4072 (2016).

66. D'Almeida, M. et al. Chitosan coating as an antibacterial surface for biomedical applications. *PLoS One* **12**, e0189537 (2017).

67. Leyland, N.S. et al. Highly Efficient F, Cu doped TiO2 anti-bacterial visible light active photocatalytic coatings to combat hospital-acquired infections. *Sci Rep* **6**, 24770 (2016).

68. Chen, W. et al. In vitro anti-bacterial and biological properties of magnetron co-sputtered silver-containing hydroxyapatite coating. *Biomaterials* **27**, 5512-5517 (2006).

69. Karpanen, T.J., Casey, A.L., Conway, B.R., Lambert, P.A. & Elliott, T.S. Antimicrobial activity of a chlorhexidine intravascular catheter site gel dressing. *J Antimicrob Chemother* **66**, 1777-1784 (2011).

70. Zhou, C. et al. In Vivo Anti-Biofilm and Anti-Bacterial Non-Leachable Coating Thermally Polymerized on Cylindrical Catheter. *ACS Appl Mater Interfaces* **9**, 36269-36280 (2017).

71. Nablo, B.J., Prichard, H.L., Butler, R.D., Klitzman, B. & Schoenfisch, M.H. Inhibition of implant-associated infections via nitric oxide release. *Biomaterials* **26**, 6984-6990 (2005).

72. Hasan, J., Crawford, R.J. & Ivanova, E.P. Antibacterial surfaces: the quest for a new generation of biomaterials. *Trends in biotechnology* **31**, 295-304 (2013).

73. Chen, N. et al. Polymer Thin Films and Surface Modification by Chemical Vapor Deposition: Recent Progress. *Annual review of chemical and biomolecular engineering* **7**, 373-393 (2016).

74. Terada, A., Okuyama, K., Nishikawa, M., Tsuneda, S. & Hosomi, M. The effect of surface charge property on Escherichia coli initial adhesion and subsequent biofilm formation. *Biotechnol Bioeng* **109**, 1745-1754 (2012).

75. Carmona-Ribeiro, A.M. & de Melo Carrasco, L.D. Cationic antimicrobial polymers and their assemblies. *Int J Mol Sci* **14**, 9906-9946 (2013).

76. Damodaran, V.B. & Murthy, N.S. Bio-inspired strategies for designing antifouling biomaterials. *Biomater Res* **20**, 18 (2016).

77. Tripathy, A. et al. Fabrication of Low-Cost Flexible Superhydrophobic Antibacterial Surface with Dual-Scale Roughness. *ACS Biomater. Sci. Eng.* **4** (2018).

78. Loo, C.Y. et al. Superhydrophobic, nanotextured polyvinyl chloride films for delaying Pseudomonas aeruginosa attachment to intubation tubes and medical plastics. *Acta Biomater* **8**, 1881-1890 (2012).

79. Navarre, W.W. & Schneewind, O. Surface proteins of gram-positive bacteria and mechanisms of their targeting to the cell wall envelope. *Microbiol Mol Biol Rev* **63**, 174-229 (1999).

80. Boardman, A.K., Allison, S., Sharon, A. & Sauer-Budge, A.F. Comparison of anti-fouling surface coatings for applications in bacteremia diagnostics. *Anal Methods* **5**, 273-280 (2013).

81. Gu, H. et al. How Escherichia coli lands and forms cell clusters on a surface: a new role of surface topography. *Sci Rep* **6**, 29516 (2016).

82. Manabe, K., Nishizawa, S. & Shiratori, S. Porous surface structure fabricated by breath figures that suppresses Pseudomonas aeruginosa biofilm formation. *ACS Appl Mater Interfaces* **5**, 11900-11905 (2013).

83. Xu, L.C. & Siedlecki, C.A. Staphylococcus epidermidis adhesion on hydrophobic and hydrophilic textured biomaterial surfaces. *Biomed Mater* **9**, 035003 (2014).

84. Song, F. & Ren, D. Stiffness of cross-linked poly(dimethylsiloxane) affects bacterial adhesion and antibiotic susceptibility of attached cells. *Langmuir : the ACS journal of surfaces and colloids* **30**, 10354-10362 (2014).

85. Song, F. et al. How Bacteria Respond to Material Stiffness during Attachment: A Role of Escherichia coli Flagellar Motility. *ACS applied materials & interfaces* **9**, 22176-22184 (2017).

86. Kolewe, K.W., Peyton, S.R. & Schiffman, J.D. Fewer Bacteria Adhere to Softer Hydrogels. *ACS Appl Mater Interfaces* **7**, 19562-19569 (2015).

87. Hong, J., Hu, J. & Ke, F. Experimental Induction of Bacterial Resistance to the Antimicrobial Peptide Tachyplesin I and Investigation of the Resistance Mechanisms. *Antimicrob Agents Chemother* **60**, 6067-6075 (2016).

88. Guilhelmelli, F. et al. Antibiotic development challenges: the various mechanisms of action of antimicrobial peptides and of bacterial resistance. *Front Microbiol* **4**, 353 (2013).

89. Bacalum, M. & Radu, M. Cationic Antimicrobial Peptides Cytotoxicity on Mammalian Cells: An Analysis Using Therapeutic Index Integrative Concept. *International Journal of Peptide Research and Therapeutics* **21**, 8 (2015).

90. Pacor, S., Giangaspero, A., Bacac, M., Sava, G. & Tossi, A. Analysis of the cytotoxicity of synthetic antimicrobial peptides on mouse leucocytes: implications for systemic use. *J Antimicrob Chemother* **50**, 339-348 (2002).

91. Guo, D. et al. The cellular uptake and cytotoxic effect of silver nanoparticles on chronic myeloid leukemia cells. *J Biomed Nanotechnol* **10**, 669-678 (2014).

92. Wang, X. et al. Use of coated silver nanoparticles to understand the relationship of particle dissolution and bioavailability to cell and lung toxicological potential. *Small* **10**, 385-398 (2014).

93. Zhang, T., Wang, L., Chen, Q. & Chen, C. Cytotoxic potential of silver nanoparticles. *Yonsei Med J* **55**, 283-291 (2014).

94. Sale, A.J. & Hamilton, W.A. Effects of high electric fields on micro-organisms. 3. Lysis of erythrocytes and protoplasts. *Biochim Biophys Acta* **163**, 37-43 (1968).

95. Hülsheger, H., Potel, J. & Niemann, E.G. Electric field effects on bacteria and yeast cells. *Radiat Environ Biophys* **22**, 149-162 (1983).

96. Delsart, C. et al. Impact of pulsed-electric field and high-voltage electrical discharges on red wine microbial stabilization and quality characteristics. *J Appl Microbiol* **120**, 152-164 (2016).

97. Guionet, A. et al. Effect of nanosecond pulsed electric field on Escherichia coli in water: inactivation and impact on protein changes. *Journal of applied microbiology* **117**, 721-728 (2014).

98. Jeyamkondan, S., Jayas, D.S. & Holley, R.A. Pulsed electric field processing of foods: a review. *Journal of food protection* **62**, 1088-1096 (1999).

99. Boulaaba, A., Egen, N. & Klein, G. Effect of pulsed electric fields on microbial inactivation and physico-chemical properties of whole porcine blood. *Food science and technology international = Ciencia y tecnologia de los alimentos internacional* **20**, 215-225 (2014).

100. Grahl, T. & Märkl, H. Killing of microorganisms by pulsed electric fields. *Appl Microbiol Biotechnol* **45**, 148-157 (1996).

101. Aronsson, K., Rönner, U. & Borch, E. Inactivation of Escherichia coli, Listeria innocua and Saccharomyces cerevisiae in relation to membrane permeabilization and subsequent

leakage of intracellular compounds due to pulsed electric field processing. *Int J Food Microbiol* **99**, 19-32 (2005).

102. Kinosita, K. & Tsong, T.T. Hemolysis of human erythrocytes by transient electric field. *Proc Natl Acad Sci U S A* **74**, 1923-1927 (1977).

103. Pillet, F., Formosa-Dague, C., Baaziz, H., Dague, E. & Rols, M.P. Cell wall as a target for bacteria inactivation by pulsed electric fields. *Sci Rep* **6**, 19778 (2016).

104. Beattie, J.M. & Lewis, F.C. The Electric Current (apart from the Heat Generated): A Bateriological Agent in the Sterilization of Milk and other Fluids. *J Hyg (Lond)* **24**, 123-137 (1925).

105. Pareilleux, A. & Sicard, N. Lethal effects of electric current on Escherichia coli. *Appl Microbiol* **19**, 421-424 (1970).

106. Edebo, L. & Selin, I. The effect of the pressure shock wave and some electrical quantities in the microbicidal effect of transient electric arcs in aqueous systems. *J Gen Microbiol* **50**, 253-259 (1968).

107. ROSENBERG, B., VANCAMP, L. & KRIGAS, T. INHIBITION OF CELL DIVISION IN ESCHERICHIA COLI BY ELECTROLYSIS PRODUCTS FROM A PLATINUM ELECTRODE. *Nature* **205**, 698-699 (1965).

108. Rowley, B.A. Electrical Current Effects on E. coil Growth Rates. *Experimental Biology and Medicine* **139** (1972).

109. Barranco, S.D., Spadaro, J.A., Berger, T.J. & Becker, R.O. In vitro effect of weak direct current on Staphylococcus aureus. *Clin Orthop Relat Res*, 250-255 (1974).

110. Cataldi, T.R., Rubino, A., Laviola, M.C. & Ciriello, R. Comparison of silver, gold and modified platinum electrodes for the electrochemical detection of iodide in urine samples

following ion chromatography. *J Chromatogr B Analyt Technol Biomed Life Sci* **827**, 224-231 (2005).

111. Aziz-Kerrzo, M., Conroy, K.G., Fenelon, A.M., Farrell, S.T. & Breslin, C.B. Electrochemical studies on the stability and corrosion resistance of titanium-based implant materials. *Biomaterials* **22**, 1531-1539 (2001).

112. Chen, X. et al. In vitro studying corrosion behavior of porous titanium coating in dynamic electrolyte. *Mater Sci Eng C Mater Biol Appl* **70**, 1071-1075 (2017).

113. Perren, S.M., Regazzoni, P. & Fernandez, A.A. How to Choose between the Implant Materials Steel and Titanium in Orthopedic Trauma Surgery: Part 2 - Biological Aspects. *Acta Chir Orthop Traumatol Cech* **84**, 85-90 (2017).

114. Tiwari, A. & Singh Raman, R.K. Durable Corrosion Resistance of Copper Due to Multi-Layer Graphene. *Materials (Basel)* **10** (2017).

115. Petersen, R. Carbon Fiber Biocompatibility for Implants. *Fibers (Basel)* **4** (2016).

116. Niepa, T.H., Gilbert, J.L. & Ren, D. Controlling Pseudomonas aeruginosa persister cells by weak electrochemical currents and synergistic effects with tobramycin. *Biomaterials* **33**, 7356-7365 (2012).

117. Niepa, T.H.R., Wang, H., Gilbert, J.L. & Ren, D. Eradication of Pseudomonas aeruginosa cells by cathodic electrochemical currents delivered with graphite electrodes. *Acta Biomater* **50**, 344-352 (2017).

118. del Pozo, J.L., Rouse, M.S., Mandrekar, J.N., Steckelberg, J.M. & Patel, R. The electricidal effect: reduction of Staphylococcus and pseudomonas biofilms by prolonged exposure to low-intensity electrical current. *Antimicrobial Agents and Chemotherapy* **53**, 41-45 (2009).

119. Schmidt-Malan, S.M. et al. Antibiofilm Activity of Low-Amperage Continuous and Intermittent Direct Electrical Current. *Antimicrobial Agents and Chemotherapy* **59**, 4610-4615 (2015).

120. Voegele, P. et al. Antibiofilm Activity of Electrical Current in a Catheter Model. *Antimicrobial Agents and Chemotherapy* **60**, 1476-1480 (2015).

121. Niepa, T.H. et al. Sensitizing Pseudomonas aeruginosa to antibiotics by electrochemical disruption of membrane functions. *Biomaterials* **74**, 267-279 (2016).

122. Wang, H. & Ren, D. Controlling Streptococcus mutans and Staphylococcus aureus biofilms with direct current and chlorhexidine. *AMB Express* **7**, 204-017-0505-z (2017).

123. Stoodley, P., deBeer, D. & Lappin-Scott, H.M. Influence of electric fields and pH on biofilm structure as related to the bioelectric effect. *Antimicrob Agents Chemother* **41**, 1876-1879 (1997).

124. van der Borden, A.J., van der Mei, H.C. & Busscher, H.J. Electric block current induced detachment from surgical stainless steel and decreased viability of Staphylococcus epidermidis. *Biomaterials* **26**, 6731-6735 (2005).

125. van der Borden, A.J. et al. Prevention of pin tract infection in external stainless steel fixator frames using electric current in a goat model. *Biomaterials* **28**, 2122-2126 (2007).

126. Caubet, R. et al. A radio frequency electric current enhances antibiotic efficacy against bacterial biofilms. *Antimicrob Agents Chemother* **48**, 4662-4664 (2004).

127. Thibodeau, E.A., Handelman, S.L. & Marquis, R.E. Inhibition and killing of oral bacteria by silver ions generated with low intensity direct current. *J Dent Res* **57**, 922-926 (1978).

128. Sandvik, E.L., McLeod, B.R., Parker, A.E. & Stewart, P.S. Direct electric current treatment under physiologic saline conditions kills Staphylococcus epidermidis biofilms via electrolytic generation of hypochlorous acid. *PLoS One* **8**, e55118 (2013).

129. Del Pozo, J.L. et al. The electricidal effect is active in an experimental model of Staphylococcus epidermidis chronic foreign body osteomyelitis. *Antimicrob Agents Chemother* **53**, 4064-4068 (2009).

130. Zhu, A., Liu, H.K., Long, F., Su, E. & Klibanov, A.M. Inactivation of bacteria by electric current in the presence of carbon nanotubes embedded within a polymeric membrane. *Appl Biochem Biotechnol* **175**, 666-676 (2015).

131. Zituni, D. et al. The growth of Staphylococcus aureus and Escherichia coli in low-direct current electric fields. *Int J Oral Sci* **6**, 7-14 (2014).

132. Nodzo, S.R. et al. Cathodic Voltage-controlled Electrical Stimulation Plus Prolonged Vancomycin Reduce Bacterial Burden of a Titanium Implant-associated Infection in a Rodent Model. *Clin Orthop Relat Res* **474**, 1668-1675 (2016).

133. Ehrensberger, M.T. et al. Cathodic voltage-controlled electrical stimulation of titanium implants as treatment for methicillin-resistant Staphylococcus aureus periprosthetic infections. *Biomaterials* **41**, 97-105 (2015).

134. Kim, Y.W. et al. Effect of electrical energy on the efficacy of biofilm treatment using the bioelectric effect. *NPJ Biofilms Microbiomes* **1**, 15016 (2015).

135. Sahrmann, P. et al. Effect of low direct current on anaerobic multispecies biofilm adhering to a titanium implant surface. *Clin Implant Dent Relat Res* **16**, 552-556 (2014).

136. Ronen, A., Duan, W., Wheeldon, I., Walker, S. & Jassby, D. Microbial Attachment Inhibition through Low-Voltage Electrochemical Reactions on Electrically Conducting Membranes. *Environ Sci Technol* **49**, 12741-12750 (2015).

137. Sultana, S.T., Call, D.R. & Beyenal, H. Eradication of Pseudomonas aeruginosabiofilms and persister cells using an electrochemical scaffold and enhanced antibiotic susceptibility. *NPJ Biofilms Microbiomes* **2**, 2 (2016).

138. Kalbacova, M. et al. The effect of electrochemically simulated titanium cathodic corrosion products on ROS production and metabolic activity of osteoblasts and monocytes/macrophages. *Biomaterials* **28**, 3263-3272 (2007).

139. Anfruns-Estrada, E. et al. Inactivation of microbiota from urban wastewater by single and sequential electrocoagulation and electro-Fenton treatments. *Water Res* **126**, 450-459 (2017).

140. Samoĭlenko, I.I., Vasil'eva, E.I., Pavlova, I.B. & Tumanian, M.A. [Mechanisms of the bactericidal action of hydrogen peroxide]. *Zh Mikrobiol Epidemiol Immunobiol*, 30-33 (1983).

141. Drogui, P., Elmaleh, S., Rumeau, M., Bernard, C. & Rambaud, A. Oxidising and disinfecting by hydrogen peroxide produced in a two-electrode cell. *Water Res* **35**, 3235-3241 (2001).

142. Fukuzaki, S. Mechanisms of actions of sodium hypochlorite in cleaning and disinfection processes. *Biocontrol Sci* **11**, 147-157 (2006).

143. Blenkinsopp, S.A., Khoury, A.E. & Costerton, J.W. Electrical enhancement of biocide efficacy against Pseudomonas aeruginosa biofilms. *Appl Environ Microbiol* **58**, 3770-3773 (1992).

144. del Pozo, J.L. et al. Effect of electrical current on the activities of antimicrobial agents against Pseudomonas aeruginosa, Staphylococcus aureus, and Staphylococcus epidermidis biofilms. *Antimicrobial Agents and Chemotherapy* **53**, 35-40 (2009).

145. Niepa, T.H., Wang, H., Dabrowiak, J.C., Gilbert, J.L. & Ren, D. Synergy between tobramycin and trivalent chromium ion in electrochemical control of Pseudomonas aeruginosa. *Acta Biomater* **36**, 286-295 (2016).

146. Stirn, A. Body piercing: medical consequences and psychological motivations. *Lancet* **361**, 1205-1215 (2003).

147. Treffers, M.T. <div _ngcontent-c6="" class="document-title-container col-12" style="box-sizing: border-box; position: relative; width: 947.5px; min-height: 1px; padding: 0.4em 1em 0.8em; -webkit-box-flex: 0; flex: 0 0 100%; max-width: 100%; margin: 0px; background-color: rgb(255, 255, 255); outline: 0px !important;"><h1 _ngcontent-c6="" class="document-title" style="margin: 0px 10px 0px 0px; line-height: 1.3; outline: 0px !important;"> History, Current Status and Future of the Wireless Power Consortium and the Qi Interface Specification. *IEEE Circuits and Systems Magazine* **15** (2015).

148. Payne, J., Song, K., Yang, S.Y. & Kim, J. in Proceedings of SPIE - The International Society for Optical Engineering (Society of Photo-Optical Instrumentation Engineers, 2009).

149. Zeng, F.G., Rebscher, S., Harrison, W., Sun, X. & Feng, H. Cochlear implants: system design, integration, and evaluation. *IEEE reviews in biomedical engineering* **1**, 115-142 (2008).

150. Abid, A. et al. Wireless Power Transfer to Millimeter-Sized Gastrointestinal Electronics Validated in a Swine Model. *Scientific reports* **7**, 46745 (2017).

151. Rao, S. et al. in 2014 Texas Symposium on Wireless and Microwave Circuits and Systems (WMCS) (IEEE, Waco, TX, USA; 2014).

152. Klein, E., Smith, D.L. & Laxminarayan, R. Hospitalizations and deaths caused by methicillin-resistant Staphylococcus aureus, United States, 1999-2005. *Emerg Infect Dis* **13**, 1840-1846 (2007).

153. Montanaro, L. et al. Scenery of Staphylococcus implant infections in orthopedics. *Future Microbiol* **6**, 1329-1349 (2011).

154. Stover, T. & Lenarz, T. Biomaterials in cochlear implants. *GMS current topics in otorhinolaryngology, head and neck surgery* **8**, Doc10 (2009).

155. Dalu, A., Blaydes, B.S., Lomax, L.G. & Delclos, K.B. A comparison of the inflammatory response to a polydimethylsiloxane implant in male and female Balb/c mice. *Biomaterials* **21**, 1947-1957 (2000).

Chapter 3

The proof-of-concept study of wirelessly delivered DC treatment on biofilm cells

3.1 Abstract

Bacteria such as *Pseudomonas aeruginosa* and *Staphylococcus aureus* can form biofilms on medical implants and cause serious infections that are incurable by conventional antibiotics due to high-level tolerance to antimicrobials. In this study, we developed a new method towards the non-invasive treatment of biofilm infections. We demonstrate that antibiotic tolerant biofilm cells can be effectively eradicated by electromagnetically induced direct current (DC) from a remote power source. For example, after treatment with 60 μA/cm^2 of wirelessly delivered DC using stainless steel electrodes for 6 hours, the viability of *Pseudomonas aeruginosa* and *Staphylococcus aureus* biofilm cells was reduced by approximately 3.4 and 2 logs, respectively. DC generated with graphite-based TGON^{TM} electrodes was also effective especially against *S. aureus*. For example, the viability of *P. aeruginosa* and *S. aureus* biofilm was reduced by 1.4 and 2.5 logs, respectively, after treatment with the 30 μA/cm^2 of wirelessly delivered DC for 3 hours. Synergy in biofilm killing was also observed between lower level DC and antibiotics. The viability of *P. aeruginosa* biofilm was reduced by 1.6 logs after concurrent treatment with 12 μA/cm^2 wireless delivered DC and 4.5 μg/ml tobramycin. In comparison, treatment with the same level of DC or tobramycin alone only showed 0.8 and 0.5 log of killing, respectively. The viability of *S. aureus* biofilm was reduced by 2.2 logs after concurrent treatment with 6 μA/cm^2 DC and 10 μg/mL chlorhexidine, while treatment with the same level of DC or chlorhexidine alone only showed 1.1 logs and 0.6 logs of killing, respectively. These conditions were found safe to the human epithelial cell line CLR 5803 and mice fibroblast cell line C3H/10T1/2, Clone 8.

3.2 Introduction

Application of surgically implanted medical devices is on the rise, thanks to the advances in device design and major benefits to patients' life quality [1]. However, device-associated infections remain challenging despite the improvement on sterilization techniques over the past decades [2]. Approximately 4.3% of the total 2.6 million orthopedic devices implanted in the United States every year are infected [3]. The risk of infections associated with hearing aid implants (e.g. cochlear and bone anchored implants) is also approximately 4 % but higher among younger patients [4, 5]. Such infections lead to ulcer, swelling or inflammation of affected tissues [6], and in some cases, additional surgeries for implant relocation, fixation or even explanation [7]. In severe cases, device-associated infections can lead to life-threatening conditions such as meningitis [6, 8-10].

It is well documented that bacterial biofilms play an important role in recalcitrant implant-associated infections [7]. The source of these bacteria is commonly linked to the ambient environment, surgical equipment, or the patient's own skin [11]. The concept of "race for the surface" well describes the nature of device-associated infections; e.g., if bacterial adhesion occurs on implanted biomaterial before tissue integration, it is difficult to prevent further biofilm formation by host defense [12]. However, infections can also occur years after the operation [13, 14]. The major causative agents of implant-associated infections include *Staphylococcus aureus, Staphylococcus epidermidis, Pseudomonas aeruginosa* and *Streptococcus* species [6, 14-18]. Gram-positive *S. aureus* and Gram-negative *P. aeruginosa* are the most commonly isolated strains from infected implanted devices [6, 14, 17].

A common strategy for controlling device-associated infection is coating with antimicrobials that are either released from the implant surface [19, 20] or immobilized on the surface [21]. Besides, biofilm

formation can be reduced by chemical and physical modification of material properties, such as charges, hydrophobicity, topography and stiffness [22-24]. Although these approaches can reduce/delay biofilm formation, many of these mechanisms can be overcome by bacteria over time, and eradicating mature biofilms remains challenges. Direct currents (DCs) have been shown to have bactericidal effects against established biofilm cells; and synergy between DC and antibiotics in bacterial killing has been observed in multiple systems including *in vivo* models [25-32]. However, these systems require a direct connection between electrodes and a power source, which requires skin-piercing wiring for current transduction. This is an invasive process, which causes discomfort and can lead to secondary infections. These limiting its application in the treatment of device associated infections.

To improve infection control by DC, we developed a method to induce DC wirelessly using a magnetic field. *P. aeruginosa* and *S. aureus* were used as model species in this study to test this new strategy. The results demonstrate that wirelessly delivered DC has strong effects in killing planktonic and biofilm cells of *P. aeruginosa* and *S. aureus*, and the treatment conditions are safe to human epithelial cells.

3.3 Materials and methods

3.3.1 Bacteria strains and growth media

P. aeruginosa PAO1 and *S. aureus* ALC2085 (strain RN6390 containing pALC2084) were routinely cultured in Luria-Bertani (LB) medium [33] containing 10 g/L tryptone, 5 g/L Yeast extract and 10 g/L NaCl at 37 °C with shaking at 200 rpm. Chloramphenicol was supplied at 10 μg/mL for *S. aureus* cultures.

3.3.2 Biofilm formation

Polydimethylsiloxane (PDMS) blocks (1 cm x 0.5 cm; 0.1 cm thick) were used to form biofilms because it is a commonly used biomaterial for medical devices, such as cochlear implants and pacemakers [34, 35]. Briefly, 25 µL overnight culture of planktonic cells was used to inoculate a petri dish containing 25 mL of LB medium and PDMS blocks. The biofilm cultures were incubated at 37°C for 24 h without shaking. After biofilm growth, the PDMS blocks with attached biofilms were removed from the petri dish and washed gently with 0.85% NaCl solution prior to DC treatment.

3.3.3 Wirelessly delivered DC treatment

The setup of the experimental system for wirelessly delivered DC generation is shown in Figure 1. Briefly, the treatment circuit was constructed with two stainless steel (McMaster-Carr, Elmhurst, IL, U.S.) or TGON™ 805 (Laird Technologies, Schaumburg, IL, U.S.) electrodes positioned on the opposite sides of a 35 mm petri dish (Thermo Fisher Scientific, Pittsburg, PA, U.S.). To deliver DC wirelessly, the electrodes were connected to a rectifier (XKT-3168, Xinketai, China) and then to a copper receiver coil (10 turns, 5 cm diameter, 0.7 mm thickness) (McMaster-Carr, Elmhurst, IL, U.S.). The total current level of treatment circuit was controlled using adjustable resistors (10 k – 10 M ohm). The receiver coil was placed on a phone wireless charging pad (Yootech, T100, JinJiang, China) or a wireless charging module (XKT-412, Xinketai, China) as a power source. Electric power was delivered wirelessly based on the principle of coupling induction between the transmitter coil and receiver coil. The electric power consumption of DC treatment can be calculated using the Equation 1 [36]:

$$Power = \frac{(U_{total} - U_R)^2}{R} \qquad (1)$$

Where U_{total} is the total potential output of rectifier chip (5V in our system), U_R is the average potential applied on the adjustable resistors, and R is resistance value of resistors. All of them were monitored by using a multimeter (Metex, M4640A, Toronto, ON, Canada).

To understand if the presence of skin tissue may affect wireless DC delivery, a porcine skin purchased from a local grocery store was inserted between transmitter and receiver coils, and the current density in the internal circuit was monitored in the same method.

3.3.4 DC treatment of biofilms

DC treatment of biofilms was carried out in 3 mL 0.85% NaCl solution. The PDMS blocks with attached *P. aeruginosa* PAO1 or *S. aureus* ALC2085 biofilm were placed in the middle of the electric field with approximately 2-3 mm from each electrode. The biofilm was treated with DC for 2-6 hours. The untreated samples were used as controls. After treatment, each PDMS block was transferred to a 10 mL tube containing 1 mL 0.85% NaCl solution. The biofilm cells were removed from the surface by gentle sonication (Model B200, Branson, Danbury, CT, USA) for 1 min. The number of viable cells detached from PDMS blocks was quantified by counting CFU.

Tobramycin (Tob) and chlorhexidine (CHX) were used to evaluate possible synergy with low-level DC in bacterial killing. PDMS blocks with *P. aeruginosa* PAO1 biofilm were concurrently treated with 12 μA/cm^2 DC and 4.5 μg/mL Tob for 6 h and compared with individual treatment. PDMS blocks with *S. aureus* biofilm were concurrently treated with 6 μA/cm^2 DC and 10 μg/mL CHX for 6 h and compared with individual treatments. The number of viable biofilm cells was quantified by counting CFU.

3.3.5 Scanning Electron Microscopy (SEM)

SEM was performed to evaluate the effects of the wireless electrochemical treatments on *P. aeruginosa* and *S. aureus* biofilm cells compared to the untreated control. The treated and control PDMS with biofilm samples were gently rinsed with PBS and fixed with 2.5% glutaraldehyde in 1X PBS buffer (pH 7.4) for 3 days at 5 °C. Then the samples were fixed in 2.0% osmium tetroxide (MilliporeSigma, St. Louis, MO, US) for 1 h, and washed by DI water again followed by dehydration in a graded ethanol series (15%, 30%, 50%, 70%, 90%, and 100%). The final dehydration in 100% ethanol was repeated three times. After dehydration, the samples were critical point dried with 100% ethanol in a Tousimis samdri-810 (Tousimis, Rockville, MD). Finally, the samples were coated with approximately a 5 nm gold and imaged using a Scanning Electron Microscope (JEOL 5600, JEOL, Japan) at an accelerating voltage of 7 kV.

3.3.6 Cytotoxicity to human cells

Human epithelial lung cancer cell line (CLR-5803) was grown in 35 mm glass bottom petri dish (Thermo Fisher Scientific, Pittsburg, PA, U.S.), with RPMI 1640 medium supplemented with 10% Fetal Bovine Serum (FBS) (Thermo Fisher Scientific, Pittsburg, PA, U.S.) [37, 38] for 2 days. Mice fibroblast cell line (C3H/10T1/2) was grown in the same petri dish with Eagle's Basal medium supplemented with 10% Fetal Bovine Serum (FBS) and 2mM L-glutamine [39, 40] (Thermo Fisher Scientific, Pittsburg, PA, U.S.) for 2 days. Then two electrodes (stainless or TGON) were inserted into the petri dish to deliver 30 - 60 $\mu A/cm^2$ wirelessly induced DC at 37 °C supplemented with 5% CO_2. After DC treatment, the mammalian cells on the bottom of petri dish were stained using the Cell-Mediated Cytotoxicity Kit (Life Technologies, Grand Island, NY, USA) 30 min,

followed by observation with a fluorescence microscope (Axio Imager M1, Carl Zeiss Inc., Berlin, Germany) to evaluate viability.

3.3.7 Statistical analysis

All data are presented as a mean ± standard deviation. Statistical significance was assessed with one-way or two-way ANOVA followed by Tukey test. Results with $p < 0.05$ were considered statistically significant. All analyses were performed using SAS 9.4 software (SAS Institute, Cary, NC, USA).

3.4 Results

3.4.1 Engineering a new system for wireless delivery of DC at therapeutic levels

Our design is based on the principle of induction coupling. The system we developed for wireless DC delivery included an AC power, a pair of transmitter and receiver coils, and a rectifier chip connected to the biofilm treatment unit. In the first test, the system was evaluated in a petri dish with two electrodes (Figure 1A&B). The AC power and transmitter coil composed the power transmitter unit; while the receiver coil, rectifier chip and an adjustable resistor composed DC generation unit. Using this setup, the electric power was transferred to a time-changing magnetic field by the transmitter unit first and then transferred back to electric current in the receiver unit by induction coupling. The AC current was transformed to stable DC by the rectifier and delivered to the treatment unit (Figure 1B). Although a larger receiver coil could provide higher efficiency of coupling induction, we chose the coil with 3 cm of diameter in this study (Figure S3), because it is close to the diameter of typical electric medical implants, such as pacemaker, cochlear implant, and GI tract stimulator [38, 41, 42].

The current densities of our wireless DC delivering system were tested from 6 to 120 μA/cm^2, which was stable during 3 - 6 h treatment. We also measured the current density with varying distance between the charging pad and receiver coil. The current density remained at the stable and high level when the distance varied from 0 to 10 mm, beyond which the current density started to decrease (Figure 1C). When the distance increased to 15 mm, the current density decreased to approximately 2/3 of the maximum level. This result indicates that the wireless delivery of DC can penetrate skin and tissues without significant decay (Figure 1C). The maximum power required to obtain 60 μA/cm^2 output current in our experimental system is approximately 0.1 mW based on the calculation using Equation 1 shown in the Methods section. By enhancing the power output, the distance for DC delay can be substantially increased if needed.

3.4.2 Effects of DC on *P. aeruginosa* and *S. aureus* biofilms using stainless steel electrodes

The maximum killing effect on *P. aeruginosa* biofilms among the tested conditions was observed when treated with 60 μA/cm^2 DC for 6 h, which was 3.4 ± 0.03 logs (p = 0.03). This killing was reduced to 2.4 ± 0.17 logs when the DC treatment was shortened to 2 h (Figure 4). At lower current levels, the 6 h treatment with 6 or 30 μA/cm^2 DC killed 0.4 ± 0.04 ($p < 0.05$) and 1.8 ± 0.001 logs (p = 0.04), respectively. Thus, biofilm cells are more tolerant to DC treatment as expected. No significant killing was observed at any of these current levels when the treatment time was shortened to 2 h (Figure 2A). These results demonstrated the dosage-dependent killing of *P. aeruginosa* by wirelessly delivered DC.

Wirelessly delivered DC was also found effective against *S. aureus* biofilms under the same treatment conditions. Specifically, the number of viable *S. aureus* biofilm cells was reduced by 1.6 ± 0.02 and 2.2 ± 0.2 logs after treatment with 60 μA/cm^2 DC for 2 and 6 h ($p < 0.01$), respectively.

DC at 30 μA/cm^2 showed similar killing activities against *S. aureus* biofilms (1.2 ± 0.01 and 1.9 ± 0.02 log for 2 and 6 h treatment, respectively; $p < 0.01$); while 6 μA/cm^2 DC only exhibited significant killing effect (1.1 ± 0.05 log) with 6 h treatment ($p < 0.01$) (Figure 2B). When current density increased up to 120 μA/cm^2, the number of viable *S. aureus* cells was reduced by 2.4 ± 0.01 logs for 6 h treatment ($p < 0.01$).

To better understand the killing effects of wireless electrochemical treatment on biofilm cells, SEM analysis was performed to examine the morphology of *P. aeruginosa* and *S. aureus* biofilm cells with and without treatment by wirelessly delivered DC. The SEM results revealed major damage to the treated cells, consistent with the potent killing effects of DC observed. For example, after treatment with 60 μA/cm^2 DC for 6 h, The majority *P. aeruginosa* and *S. aureus* cells were disrupted, and cell debris was seen for treated samples (Figure 3), which is consistent with CFU results described above.

3.4.3 Synergy between DC and antimicrobials in killing *P. aeruginosa* and *S. aureus* biofilms using stainless steel electrodes

Low-level electric currents are known to have synergy with antibiotics in killing bacterial biofilm cells [43, 44]. To understand if wirelessly induced DC also has such effects, tobramycin (Tob) was tested on *P. aeruginosa* PAO1 biofilms. When *P. aeruginosa* biofilms were treated with 12 μA/cm^2 DC and 4.5 μg/mL tobramycin (Tob) for 6 h, the maximum killing effect (1.6 ± 0.1 logs, $p = 0.003$) was observed under the condition of concurrent treatment with both DC and Tob present. In comparison, treatment with 12 μA/cm^2 DC or 4.5 μg/mL Tob alone only showed 0.8 ± 0.3 logs and 0.5 ± 0.3 log of killing, respectively (Figure 2C). Thus, synergy was observed between wirelessly delivered DC and Tob.

Similar to the results of *P. aeruginosa*, concurrent treatment with wirelessly delivered DC and chlorhexidine (CHX) was found to have synergetic effects in killing *S. aureus* biofilms. For example, the number of viable *S. aureus* biofilm cells was reduced by 2.2 ± 0.05 logs ($p < 0.01$) after concurrent treatment with 6 μA/cm^2 DC and 10 μg/mL CHX for 6 h. In comparison, treatment with 6 μA/cm^2 DC or 10 μg/mL CHX alone only showed 1.1 ± 0.05 log and 0.6 ± 0.03 log of killing, respectively (Figure 2D).

3.4.4 Effects of DC on *P. aeruginosa* and *S. aureus* biofilms using TGON^{TM} 805 electrodes

Carbon is a good nonmetal material for medical implants because of its corrosion resistance and good biocompatibility [2, 45]. Unlike stainless steel, carbon-based electrodes don't produce salt precipitation, which helps keep the biomaterial clean after DC treatment [46]. To understand if it is also effective for bacterial killing by wirelessly delivered DC using carbon-based electrodes, we treated *P. aeruginosa* and *S. aureus* biofilms using the same test system but replaced by replacing stainless steel electrodes with the TGON^{TM} 805. TGON is a graphite-based material that has higher flexibility and conductivity than normal carbon electrodes [46]. The results showed that treatment with 30 μA/cm^2 DC for 3 h led to the killing of *P. aeruginosa* and *S. aureus* biofilm cells by 1.8 ± 0.08 ($p < 0.01$) and 2.9 ± 0.5 logs ($p = 0.01$) (Figure 2 E&F), respectively. These effects are compatible to those by stainless electrodes and more potent in killing *S. aureus.*

3.4.5 The effective DC levels for bacterial killing are safe to human cells

To understand if the conditions effective in bacterial killing are safe to human cells, human lung epithelial cell line (CLR-5803) was used to evaluate the effects of DC. The microscopic images of epithelial cells stained with Cell-Mediated Cytotoxicity kit showed no notable difference between DC treated epithelial cells and untreated control. As shown in Figure 4, nearly all mammalian cells

remain viable (stained green) after treatment with 60 μA/cm^2 DC using stainless steel electrodes for 6 h or 30 μA/cm^2 DC using TGON electrodes for 3 h, which were potent in killing *P. aeruginosa* and *S. aureus*.

3.5 Discussion

Different levels of direct currents (DC) and alternative currents (AC) have been demonstrated to kill biofilm cells in the presence or absence of antibiotics [28, 31, 32, 43]. Our group recently reported synergetic effects between low-level DC and the antibiotic tobramycin in killing *P. aeruginosa* biofilm and dormant persister cells [29, 30]. These data suggest that new treatment may be possible to better combat antibiotic-resistant infections. However, all those systems require a physical connection between the electrodes and a power source. Such setup needs skin piecing or battery if applied to implanted medical devices, which presents challenges such as limited device lifetime, pain, discomfort associated with the treatment, and risk of secondary infections. To address this challenge, we generated electric currents wirelessly by induction coupling and achieved effective killing of bacteria (both planktonic and biofilm cells); and synergy with antibiotics was also observed. Our results showed that the viability of *P. aeruginosa* and *S. aureus* biofilm cells could be reduced by 3.4 and 2.2 logs, respectively, with 6 h treatment of 60 or 120 μA/cm^2 DC conducted with stainless steel electrodes in saline solution compared to the untreated controls. Extremely low levels of DC (0.06 – 0.6 μA/cm^2) also exhibited a significant killing effect on planktonic cells, although not biofilms (Supplementary data, Figure S1). Synergetic effect was observed for concurrent treatment of *P. aeruginosa* biofilm with 12 μA/cm^2 DC and 4.5 μg/mL Tob for 6 h, which led to 1.8 logs of killing, and the viability of *S. aureus* biofilm was reduced by 2.2 logs by

concurrent treatment with 6 μA/cm^2 DC and 10 μg/mL CHX for 6 h. Similar killing effect to biofilm cells was also observed by the treatment with 30 μA/cm^2 DC using graphite electrodes (TGON) for 3 h. Furthermore, the same treatment conditions were found safe to human epithelial cells.

To our best knowledge, this is the first application of wirelessly induced current for bacterial control. We believe it has promising *in vivo* applications because wireless power technology has been successfully for charging implanted devices in human [47], such as pacemakers, deep brain stimulators, and cochlear implants. These systems have two coils located inside and outside of the human body respectively [48-50]. The electric power is delivered by inductive coupling between the two coils. Electromagnetic inductive coupling could power the implanted devices wirelessly through the skin and tissues without any skin piercing, indicating the safety of such delivery methods. Typical power supply for wireless electronic implants is approximately 40 - 80mW [51], which is much higher than the power requirement for DC treatment under our experimental setup. Since our effective current level (30 - 120 μA/cm^2) is lower than those of wired systems demonstrated to be safe *in vivo* [52, 53], we expect that it is practical to integrate DC treatment unit for treating biofilm infections associated implanted devices. In this study, we demonstrated that DC can be delivered through a distance of 10 mm, which exceeds the maximum thickness of skin [54]. This indicates the feasibility as some other wireless electronic implants (e.g. pacemaker and hearing aids) that are usually placed under the dermis tissue [3, 41, 55, 56]. For some devices such as cochlear implants and pacemakers, it is possible to keep the original wireless charging module and rewire the system to provide both original charging function and added infection control. It is also possible to monitor biofilm formation by measuring impedance changes of the implanted device and apply therapeutic DC on demand. The maximum current density of DC that can be safely

applied in the human brain is 2 mA/cm^2 [57-59]. The DC density used in this study is much lower than that (<120 μA/cm^2) and thus is expected to be safe with room to achieve even higher efficiency in biofilm control. In our study, we reduced the viability of *P. aeruginosa* planktonic cells by 2 logs with only 0.06 μA/cm^2 DC in 6 h, although the biofilm cells required longer treatment time or higher DC level (still less than the mA/cm^2 level of safe limit [60]).

The working distance between the transmitter coil and receiver coil is approximately 10 mm that is enough for several types of implants, such as implanted hearing aids devices and pacemaker, which are typically implanted under the skin [3, 38, 41, 55, 56]. If a device is implanted at a deeper position, e.g. gastrointestinal stimulator, the size of charging coil can be enlarged or amended by adding a resonant coil to achieve deeper penetration for DC delivery, e.g. 5-15 cm [38, 61].

The coupling induction technology that utilizes a time-varying magnetic field as the carrier is applicable to implanted medical devices since it can deliver electric power and signals wirelessly without skin piecing wires [47]. The safety limitation for the time-varying magnetic field contains two parameters: magnetic field strength (Tesla) and frequency (Hz). The magnetic field's strength in our experiment is less than 0.02 mT with the frequency of 100-200 kHz, which is much lower than the magnetic field (0.1 – 2 mT, 200 kHz) applied for healing bone fractures and this expected to be safe [62]. The application in bone nails and other orthopedic devices are more complex but can be archived by adding a receiver coil and electronic rectifier prior to implantation to generate desired DC on demand. Many orthopedic devices are implanted in the arms and legs that are far from the critical nervous system; thus, the applied DC level can be even higher to better antibacterial effects including that on antibiotic-resistant strains. The DC generation unit can also be implanted away from the device to minimize the change to devise design. Further *in vivo* studies are needed to identify the best treatment condition, e.g., relatively high current and short time or

low current but long treatment time given enough room of safe DC level that can be adjusted. This is part of our ongoing effort.

3.6 Conclusion

In summary, we demonstrated the feasibility to integrate the wireless delivery of DC and electrochemical control of biofilm cells. DC generated using wireless coupling induction was found effective in killing the model organisms *P. aeruginosa* and *S. aureus* biofilms, and synergy in bacterial killing was observed between DC and antimicrobials (tobramycin and chlorhexidine). The killing effect of low-level current was time- and current level-dependent. Wireless delivery of DC can avoid skin piercing, which eases its future application in non-invasive control of biofilm infections. The prototype device with the function of wirelessly delivered DC treatment showed the potent killing of biofilm cells in both *in vitro* and *ex vivo* models, which provide a new platform technology for future device engineering.

3.7 Acknowledgments

The authors are grateful to the Gerber Endowment funds for support. We thank Dr. Sauer at Binghamton University for sharing *S. aureus* ALC2085 (strain RN6390 containing pALC2084). The human epithelial lung cancer cell line (CLR-5803) was generously provided by Dr. Jing An at SUNY Upstate Medical University. The mouse fibroblast cell line (C3H/10T1/2) was generously provided by Dr. Pranav Soman at Syracuse University. We also thank Dr. Jianshun Zhang at Syracuse University for helping COMSOL simulation.

3.8 Reference

1. Vinh, D.C. & Embil, J.M. Device-related infections: a review. *Journal of long-term effects of medical implants* **15**, 467-488 (2005).
2. Campoccia, D., Montanaro, L. & Arciola, C.R. A review of the biomaterials technologies for infection-resistant surfaces. *Biomaterials* **34**, 8533-8554 (2013).
3. Darouiche, R.O. Treatment of infections associated with surgical implants. *The New England journal of medicine* **350**, 1422-1429 (2004).
4. Germiller, J.A., El-Kashlan, H.K. & Shah, U.K. Chronic Pseudomonas infections of cochlear implants. *Otology & neurotology : official publication of the American Otological Society, American Neurotology Society [and] European Academy of Otology and Neurotology* **26**, 196-201 (2005).
5. Granstrom, G., Bergstrom, K., Odersjo, M. & Tjellstrom, A. Osseointegrated implants in children: experience from our first 100 patients. *Otolaryngology--head and neck surgery : official journal of American Academy of Otolaryngology-Head and Neck Surgery* **125**, 85-92 (2001).
6. Cunningham, C.D., 3rd, Slattery, W.H., 3rd & Luxford, W.M. Postoperative infection in cochlear implant patients. *Otolaryngology--head and neck surgery : official journal of American Academy of Otolaryngology-Head and Neck Surgery* **131**, 109-114 (2004).
7. Skrivan, J. & Drevinek, P. A case report of a cochlear implant infection - A reason to explant the device? *Cochlear implants international* **17**, 246-249 (2016).
8. Cochlear implants and bacterial meningitis. *FDA Consum* **37**, 35 (2003).
9. Bluestone, C.D. Bacterial meningitis in children with cochlear implants. *N Engl J Med* **349**, 1772-1773; author reply 1772-1773 (2003).

10. Cohen, N.L., Roland, J.T. & Marrinan, M. Meningitis in cochlear implant recipients: the North American experience. *Otol Neurotol* **25**, 275-281 (2004).

11. An, Y.H. & Friedman, R.J. Prevention of sepsis in total joint arthroplasty. *The Journal of hospital infection* **33**, 93-108 (1996).

12. Hetrick, E.M. & Schoenfisch, M.H. Reducing implant-related infections: active release strategies. *Chemical Society Reviews* **35**, 780-789 (2006).

13. Schierholz, J.M. & Beuth, J. Implant infections: a haven for opportunistic bacteria. *The Journal of hospital infection* **49**, 87-93 (2001).

14. Glikman, D., Luntz, M., Shihada, R., Zonis, Z. & Even, L. Group B streptococcus meningitis in a child with cochlear implant. *Emerging infectious diseases* **15**, 1695-1696 (2009).

15. Gristina, A.G. Biomaterial-centered infection: microbial adhesion versus tissue integration. *Science (New York, N.Y.)* **237**, 1588-1595 (1987).

16. Harris, L.G. & Richards, R.G. Staphylococci and implant surfaces: a review. *Injury* **37 Suppl 2**, S3-14 (2006).

17. Brouqui, P., Rousseau, M.C., Stein, A., Drancourt, M. & Raoult, D. Treatment of Pseudomonas aeruginosa-infected orthopedic prostheses with ceftazidime-ciprofloxacin antibiotic combination. *Antimicrobial Agents and Chemotherapy* **39**, 2423-2425 (1995).

18. Im, G.J. et al. Analysis of Bacterial Biofilms on a Cochlear Implant Following Methicillin-Resistant Staphylococcus Aureus Infection. *Journal of audiology & otology* **19**, 172-177 (2015).

19. Norowski, P.A., Jr. & Bumgardner, J.D. Biomaterial and antibiotic strategies for peri-implantitis: a review. *Journal of biomedical materials research.Part B, Applied biomaterials* **88**, 530-543 (2009).

20. Bosetti, M., Masse, A., Tobin, E. & Cannas, M. Silver coated materials for external fixation devices: in vitro biocompatibility and genotoxicity. *Biomaterials* **23**, 887-892 (2002).

21. Xu, D. et al. Antibacterial and antifouling properties of a polyurethane surface modified with perfluoroalkyl and silver nanoparticles. *Journal of biomedical materials research.Part A* **105**, 531-538 (2017).

22. Hasan, J., Crawford, R.J. & Ivanova, E.P. Antibacterial surfaces: the quest for a new generation of biomaterials. *Trends in biotechnology* **31**, 295-304 (2013).

23. Chen, N. et al. Polymer Thin Films and Surface Modification by Chemical Vapor Deposition: Recent Progress. *Annual review of chemical and biomolecular engineering* **7**, 373-393 (2016).

24. Song, F., Koo, H. & Ren, D. Effects of Material Properties on Bacterial Adhesion and Biofilm Formation. *Journal of dental research* **94**, 1027-1034 (2015).

25. Costerton, J.W., Ellis, B., Lam, K., Johnson, F. & Khoury, A.E. Mechanism of electrical enhancement of efficacy of antibiotics in killing biofilm bacteria. *Antimicrobial Agents and Chemotherapy* **38**, 2803-2809 (1994).

26. del Pozo, J.L., Rouse, M.S., Mandrekar, J.N., Steckelberg, J.M. & Patel, R. The electricidal effect: reduction of Staphylococcus and pseudomonas biofilms by prolonged exposure to low-intensity electrical current. *Antimicrobial Agents and Chemotherapy* **53**, 41-45 (2009).

27. Spadaro, J.A. Electrically stimulated bone growth in animals and man. Review of the literature. *Clinical orthopaedics and related research* **(122)**, 325-332 (1977).

28. Schmidt-Malan, S.M. et al. Antibiofilm Activity of Low-Amperage Continuous and Intermittent Direct Electrical Current. *Antimicrobial Agents and Chemotherapy* **59**, 4610-4615 (2015).

29. Niepa, T.H., Gilbert, J.L. & Ren, D. Controlling Pseudomonas aeruginosa persister cells by weak electrochemical currents and synergistic effects with tobramycin. *Biomaterials* **33**, 7356-7365 (2012).

30. Niepa, T.H. et al. Sensitizing Pseudomonas aeruginosa to antibiotics by electrochemical disruption of membrane functions. *Biomaterials* **74**, 267-279 (2016).

31. Voegele, P. et al. Antibiofilm Activity of Electrical Current in a Catheter Model. *Antimicrobial Agents and Chemotherapy* **60**, 1476-1480 (2015).

32. Brinkman, C.L. et al. Exposure of Bacterial Biofilms to Electrical Current Leads to Cell Death Mediated in Part by Reactive Oxygen Species. *PloS one* **11**, e0168595 (2016).

33. J. Sambrook, D.W.R. Molecular cloning: a laboratory manual. (Cold Spring Harbor Laboratory Press, Cold Spring Harbor, NY, USA; 2001).

34. Zhang, H. & Chiao, M. Anti-fouling Coatings of Poly(dimethylsiloxane) Devices for Biological and Biomedical Applications. *Journal of medical and biological engineering* **35**, 143-155 (2015).

35. Abbasi, F., Mirzadeh, H. & Simjoo, M. Hydrophilic interpenetrating polymer networks of poly(dimethyl siloxane) (PDMS) as biomaterial for cochlear implants. *Journal of biomaterials science.Polymer edition* **17**, 341-355 (2006).

36. Young, H.D. & Freedman, R.A. University Physics, 14th Edition. (Pearson, Upper Saddle River, NJ, USA; 2015).

37. Giaccone, G. et al. Neuromedin B is present in lung cancer cell lines. *Cancer research* **52**, 2732s-2736s (1992).

38. Abid, A. et al. Wireless Power Transfer to Millimeter-Sized Gastrointestinal Electronics Validated in a Swine Model. *Scientific reports* **7**, 46745 (2017).

39. Coleman, W.B., Grisham, J.W. & Smith, G.J. Morphologic transformation of the C3H 10T1/2 cell line is accompanied by altered expression of the p53 tumor suppressor gene. *Carcinogenesis* **15**, 145-152 (1994).

40. Smith, G.J., Bell, W.N. & Grisham, J.W. Clonal analysis of the expression of multiple transformation phenotypes and tumorigenicity by morphologically transformed 10T1/2 cells. *Cancer Res* **53**, 500-508 (1993).

41. Zeng, F.G., Rebscher, S., Harrison, W., Sun, X. & Feng, H. Cochlear implants: system design, integration, and evaluation. *IEEE reviews in biomedical engineering* **1**, 115-142 (2008).

42. Schwartzman, D. et al. An off-the-shelf plasma-based material to prevent pacemaker pocket infection. *Biomaterials* **60**, 1-8 (2015).

43. del Pozo, J.L. et al. Effect of electrical current on the activities of antimicrobial agents against Pseudomonas aeruginosa, Staphylococcus aureus, and Staphylococcus epidermidis biofilms. *Antimicrobial Agents and Chemotherapy* **53**, 35-40 (2009).

44. Hajdu, S. et al. Increased temperature enhances the antimicrobial effects of daptomycin, vancomycin, tigecycline, fosfomycin, and cefamandole on staphylococcal biofilms. *Antimicrobial Agents and Chemotherapy* **54**, 4078-4084 (2010).

45. Blazewicz, M. Carbon materials in the treatment of soft and hard tissue injuries. *Eur Cell Mater* **2**, 21-29 (2001).

46. Niepa, T.H.R., Wang, H., Gilbert, J.L. & Ren, D. Eradication of Pseudomonas aeruginosa cells by cathodic electrochemical currents delivered with graphite electrodes. *Acta Biomater* **50**, 344-352 (2017).

47. Xue Rf, C.K.W.J.M. High-Efficiency Wireless Power Transfer for Biomedical Implants by Optimal Resonant Load Transformation.

48. Van Schuylenbergh K, P.R. Inductive Powering: Basic Theory and Application to Biomedical Systems. *New York: Springer Science+ Business Media B. V* (2009).

49. Yang Z, L.W.B.E. Inductor modeling in wireless links for implantable electronics. *IEEE Trans. Magn.* **43**, 3851 (2007).

50. Harrison, R.R. Designing efficient inductive power links for implantable devices. *Proc. IEEE Int. Symp. Circuits Syst.*, 2080 (2007).

51. Baker, M.W., Vol. Dissertation/Thesis (2007).

52. Griffin, D.T., Dodd, N.J., Zhao, S., Pullan, B.R. & Moore, J.V. Low-level direct electrical current therapy for hepatic metastases. I. Preclinical studies on normal liver. *British journal of cancer* **72**, 31-34 (1995).

53. Ehrensberger, M.T. et al. Cathodic voltage-controlled electrical stimulation of titanium implants as treatment for methicillin-resistant Staphylococcus aureus periprosthetic infections. *Biomaterials* **41**, 97-105 (2015).

54. Wilkinson, P.F.M.R. Skin (Digitally printed version ed.). (Cambridge University Press, Cambridge, UK; 2009).

55. Johansen, J.B. et al. Infection after pacemaker implantation: infection rates and risk factors associated with infection in a population-based cohort study of 46299 consecutive patients. *European heart journal* **32**, 991-998 (2011).

56. Celerier, C. et al. Pain After Cochlear Implantation: An Unusual Complication? *Otology & neurotology : official publication of the American Otological Society, American Neurotology Society [and] European Academy of Otology and Neurotology* **38**, 956-961 (2017).

57. Murray, L.M. et al. Intensity dependent effects of transcranial direct current stimulation on corticospinal excitability in chronic spinal cord injury. *Archives of Physical Medicine and Rehabilitation* **96**, S114-121 (2015).

58. Neuroelectric's, W. (

59. Valic, B., Gajsek, P. & Miklavcic, D. Current density in a model of a human body with a conductive implant exposed to ELF electric and magnetic fields. *Bioelectromagnetics* **30**, 591-599 (2009).

60. Fish, R.M. & Geddes, L.A. Conduction of electrical current to and through the human body: a review. *Eplasty* **9**, e44 (2009).

61. Rao, S. et al. in 2014 Texas Symposium on Wireless and Microwave Circuits and Systems (WMCS) (IEEE, Waco, TX, USA; 2014).

62. Victoria, G., Petrisor, B., Drew, B. & Dick, D. Bone stimulation for fracture healing: What's all the fuss? *Indian journal of orthopaedics* **43**, 117-120 (2009).

3.9 Figures

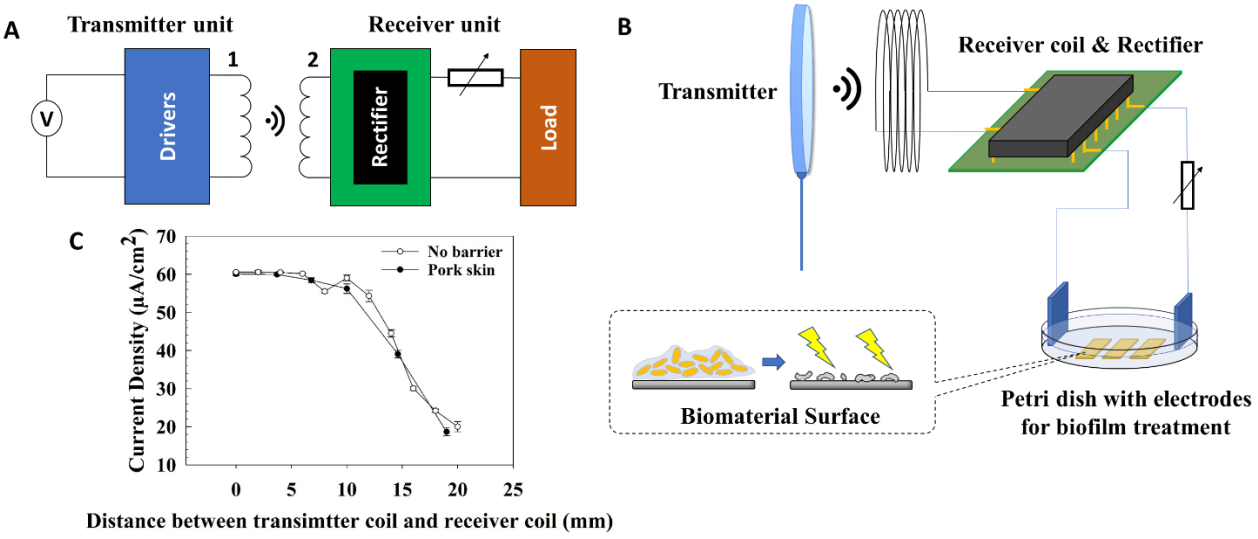

Figure 1. Engineered system for wireless delivery of DC. (A) Block diagram of wireless DC delivery system. Alternating current (AC) is generated by an AC power source, which is transferred to a changing magnetic field by coil 1. Next, coil 2 receives the magnetic field and transfers back to AC by induction coupling. The AC is converted to DC by a rectifier, followed by delivery of DC to the treatment petri dish with electrodes and attached biofilm samples. (B**)** Schematic of the DC delivery system including the power transmitter unit, receiver unit, and treatment unit. (C) The current density of the wireless DC delivery system with varying distance between the transmitter and receiver coil. The system was able to deliver DC over 10 mm under our experimental condition, which can be increased by using larger transmitter coil and higher frequency.

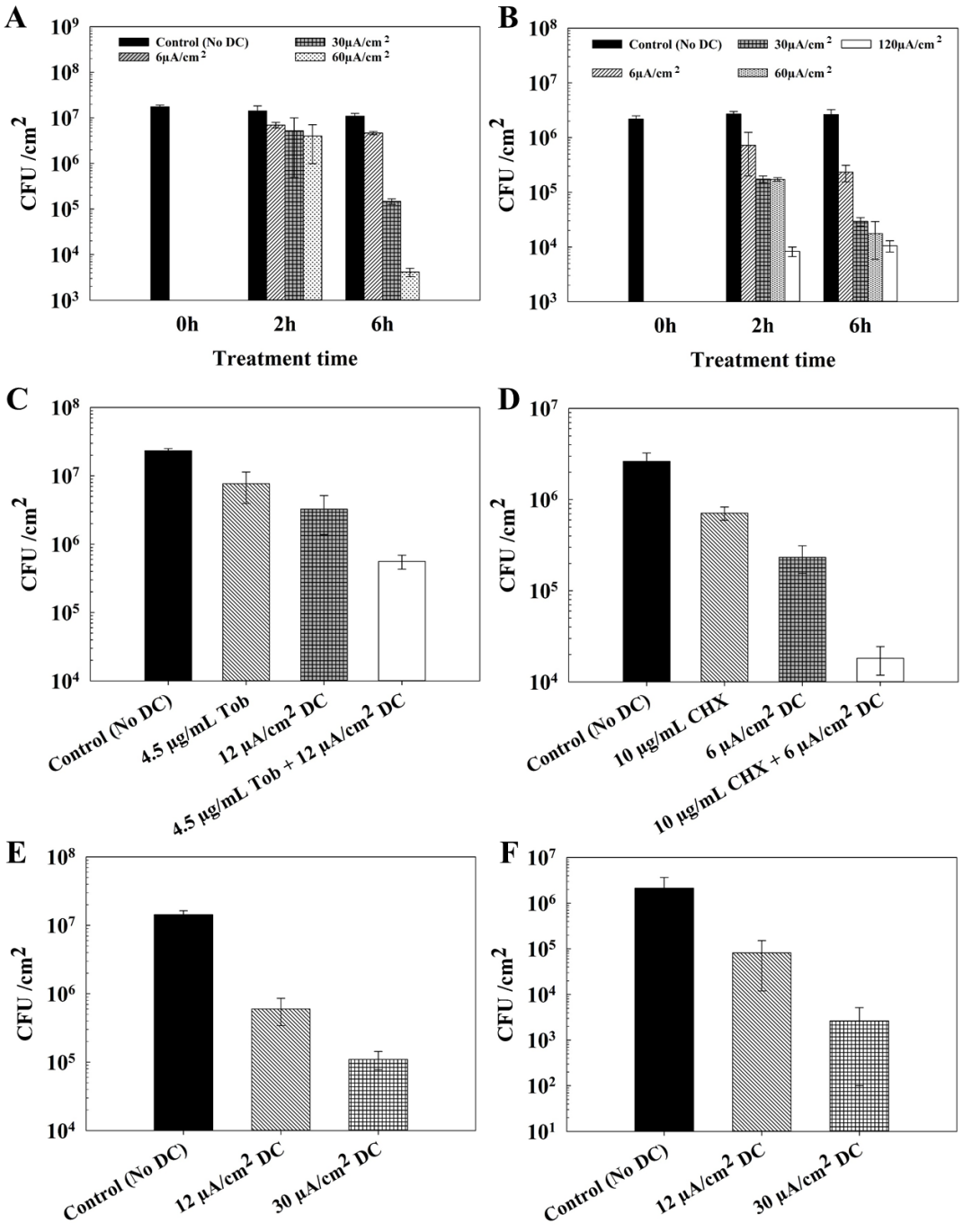

Figure 2. Viability of bacterial cells after treatment with wirelessly delivered DC in the absence or presence of antimicrobials. (A)&(B): Viability of *P. aeruginosa* (A) and *S. aureus* (B) biofilm cells after treatment with 6, 30, 60 or 120 μA/cm^2 DC in 0.85 % NaCl for 2 or 6 h. (C)&(D): Viability of *P. aeruginosa* (C) and *S. aureus* (D) biofilm cells after treatment with antimicrobials

alone (4.5 µg/mL Tob or 10 µg/mL CHX), DC (6 or 12 µA/cm^2) alone or concurrent treatment for 6 h in 0.85 % NaCl solution. (E)&(F): Viability of *P. aeruginosa* (E) and *S. aureus* (F) biofilm cells after treatment with 12 or 30 µA/cm^2 DC conducted by TGON^{TM} 805 electrodes in 0.85% NaCl for 3 h.

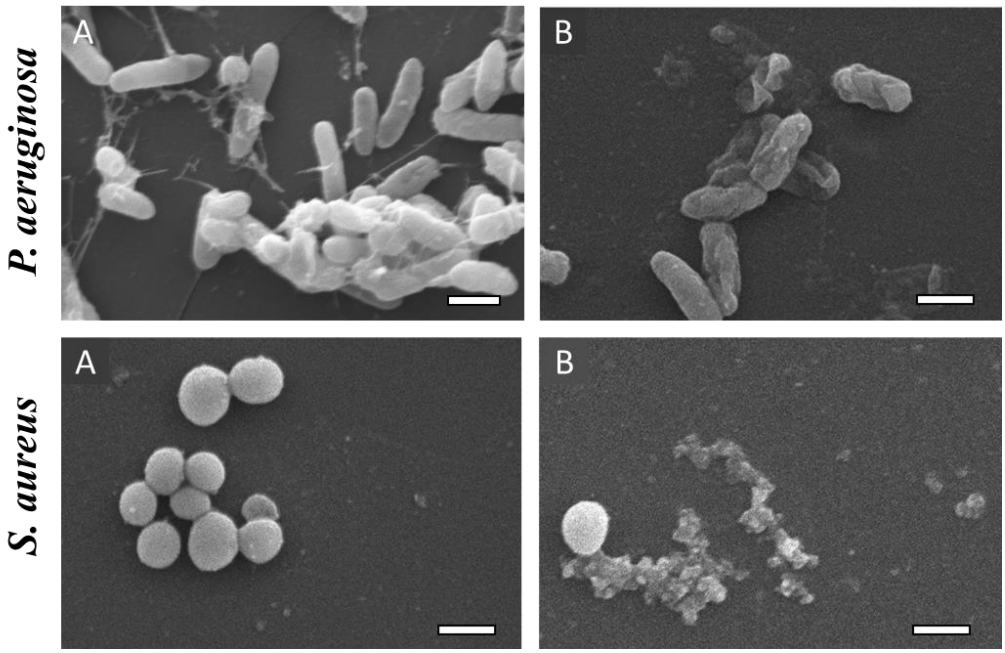

Figure 3. Representative SEM images of untreated (A) and DC treated (B) *P. aeruginosa* and *S. aureus* biofilms. Wirelessly delivered DC at 60 µA/cm^2 was used to treat biofilm cells using stainless steel electrodes. Bars = 1 µm.

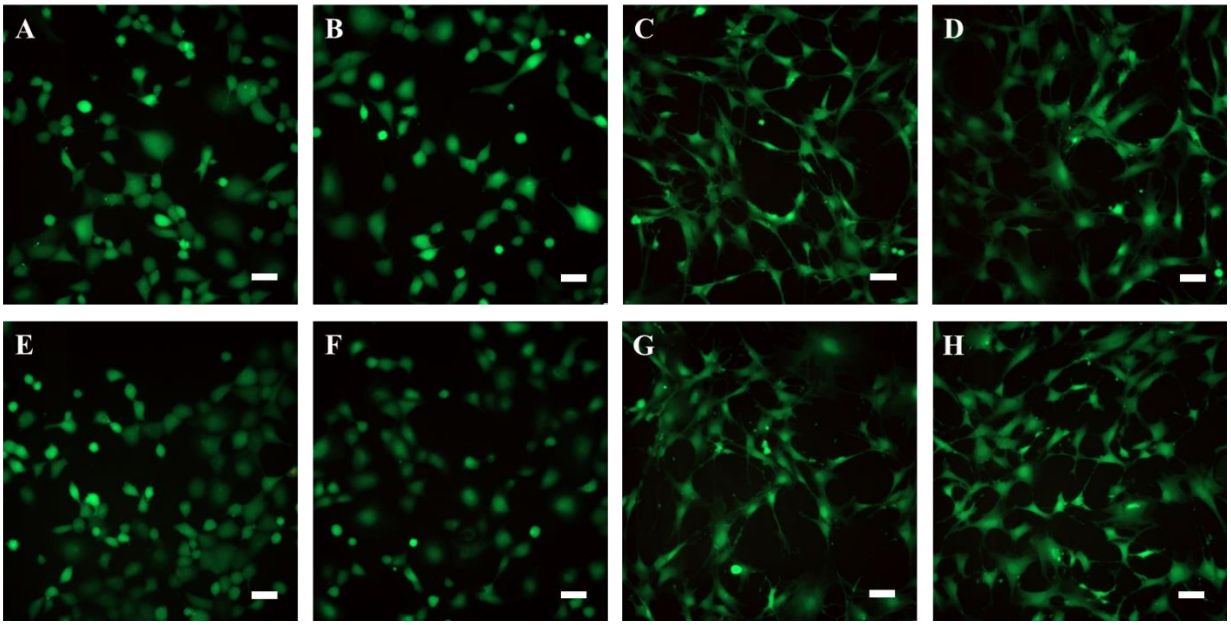

Figure 4. DC treatment of CLR-5803 epithelial cells and C3H/10T1/2 mice fibroblast cells attached on the glass bottom petri dishes in RPMI medium supplemented with 10% FBS. (A)&(B): The epithelial cells were treated without (A) or with (B) 60 μA/cm^2 DC conducted by stainless steel electrodes for 6 h. (E)&(F): The samples were treated without (E) or with 30 μA/cm^2 DC (F) using TGON^{TM} 805 electrodes for 3 h. (C)&(D): The fibroblast cells were treated without (C) or with (D) 60 μA/cm^2 DC conducted by stainless steel electrodes for 6 h. (G)&(H): The samples were treated without (G) or with 30 μA/cm^2 DC (H) using TGON^{TM} 805 electrodes for 3 h. Bar = 50 μm.

Chapter 4

Designing and engineering a prototype device of wirelessly delivered DC treatment

4.1 Abstract

In Chapter 3, we have demonstrated that the wirelessly delivered direct electric current (DC) could achieve a good killing effect on both *P. aeruginosa* and *S. aureus* biofilms. In this Chapter, we engineered a prototype device to evaluate the feasibility of integrating the system of wirelessly delivered DC treatment into the implant device. The different device designs with varying shapes, electrode layouts, and electrode materials were compared based on the results of COMSOL simulation, and the selected design contained a circular cathode on the vertical side around the round-shaped device and a small square anode in the center of the device surface. The prototype device shows the 1.0 log and 2.6 logs killing of *P. aeruginosa* and *S. aureus* biofilms, respectively, with 6 μA/cm^2 of wirelessly delivered DC using an *ex vivo* model with the porcine skin for 6 h treatment.

4.2 Introduction

Surgically implanted medical device are widely used due to their benefits in both diagnostic and therapeutic processes as well as the improvement of patient's life quality [1]. However, the events of infection associated with implants remain concerning despite the improvement in sterilization techniques during the last decades [2]. For example, approximately 4.3% of the total 2.6 million implanted orthopedic devices got infection in the United States every year [3]. The risk of cochlear implant (CI)-associated infection is also approximately 4% but higher in younger patients [4]. CI is an electronic device that provides hearing aids to patients with deafness [5]. The main components of CI are housed in a polysilicon case containing antenna coils, receiver/stimulator modulus, magnet and electrode arrays which connect to the vestibulocochlear nerve system [6 7]. The implant infection can lead to not only ulcer, swelling or inflammation of affected tissue [8], but also further surgeries for implant relocation, fixation and even explanation [9]. In some severe cases, the CI-associated infection can lead to meningitis, a life-threatening condition [8, 10].

Previous studies have shown that bacterial biofilms play an important role in medical implant-associated infections [9, 11, 12]. The major causative agents of these infections include *Staphylococcus aureus*, *Pseudomonas aeruginosa* and *Streptococcus* species [8, 13-15]. *S. aureus* is a common strain isolated from contaminated devices [8, 14] and commonly cause ulcer and swelling, while *P. aeruginosa* can form the robust biofilm on the devices' surfaces and lead to the chronic and secondary infections [4]. Recently, the *Streptococcus* species, especially *S. pneumonia* attract more attention due to the associated high risk of meningitis among children with CI implants.

Direct currents (DCs) have been shown to have bactericidal effects after either by itself or through synergy with antibiotics [16-26]. However, these systems all require a direct connection between

electrodes and power sources, which requires skin-piercing wiring for current transduction if the treatment site is inside the body [27-29].

In Chapter 3, we developed a system to deliver DC wirelessly using a magnetic field based on inductive coupling. Several implantable biomedical devices are currently in use with inductive coupling to achieve wireless communication [30], such as pacemakers, deep brain stimulators, and cochlear implants, indicating the feasibility of this approach in infection control. Our system includes two magnetic coils that are similar to the devices mentioned above. The electrical power is delivered through electromagnetic induction between the two coils, which can power the implant devices wirelessly through the skin and tissues without any skin-piercing. The DC could perform electrochemical treatment (with an additional control to obtain the appropriate current level) of biofilm infections *in vivo*. However, there are a series of issues that need to be addressed before integrating this wirelessly delivered DC system into a real medical implant for the clinical application, which includes size, current level, electrodes' layout, and sealing. The size is the primary concern since most commercial electronic implants are quite small. For example, the typical diameter of a cochlear implant is approximately 2 cm, and the volume of pacemaker ranged from 6 cm^3 to 35cm^3. Our *in vitro* wirelessly delivered DC treatment system includes a rigid receiver coil of 5 cm diameter, an adjustable rotary resistor (1 cm diameter x 3 cm height) and several wires as an internal circuit, which is very difficult to reduce the size directly. Hence, we need to re-design the new internal circuit with a simplified and smaller structure. The layout of electrodes is another important factor for designing a device since this could directly affect the treatment efficiency of the device. In our *in vitro* system, the PDMS blocks with biofilm were placed between two electrodes in a petri dish (we called "sandwich" electrode), and the biofilm was fully covered by an electric field between two electrodes (Figure 13). However, the actual

location of biofilm *in vivo* is usually on the outside shell of the implanted device, and it is impossible to install extra electrodes to cover the entire surface area of the device with the electric field *in vivo*. Therefore, we need to find new layouts of electrodes to establish a stable electrical field on the outside shell of the device. The chosen layout of the electrode is expected to not only obtain the best treatment effect to eradicate biofilms but also fit the structures of implant devices. The reliability of the system (sealing, strength, et. al) should also be considered to make the system has no leak.

To satisfy all the requirements mentioned above, we engineered a prototype device by referring to the structure of the cochlear implant and pacemaker. The device could receive the surrounding magnetic field wirelessly and then convert back to DC on its surface. This DC was expected to have a similar killing effect on the biofilms formed on the device as demonstrated *in vitro* experiments in Chapter 3. To examine the killing effects of the prototype device with different designs, we tested the function of these devices in killing *P. aeruginosa* and *S. aureus* biofilm cells both in *in vitro* and *ex vivo* model with porcine skin.

4.3 Method and materials

4.3.1 Simulation of the electric field with COMSOL

To obtain the best design of the prototype device, the distribution of electric fields in different layouts and shapes of the devices was analyzed using COMSOL Multiphysics (COMSOL Inc., Stockholm, Sweden) (Table 1). The simulations were done in the AC/DC model. Based on the results of our previous research, the potential of the electrode in the simulation was set as 1.0 and -0.9 V for anode and cathode, respectively [24]. The distribution of electric potential and current

density between electrodes are plotted as colored surface and arrows map, respectively. The boundaries of simulation were set as electrical insulation.

Table 1. The list of different shapes and layouts were simulated by COMSOL.

The shape	The layout of electrodes	The dimension
Oval	One electrode on each side	7 x 5 x 1 cm (L x W x H)
Oval	Circular electrode on side, square electrode on center	7 x 5 x 1 cm
Square	One electrode on each side	5 x 5 x 1 cm
Square	Circular electrode on side, square electrode on center	5 x 5 x 1 cm
Round	One small electrode on each side	Diameter: 4.5 cm, Height: 1 cm
Round	One large electrode on each side	Diameter: 4.5 cm, Height: 1 cm
Round	Circular electrode on side, square electrode on center	Diameter: 4.5 cm, Height: 1 cm
In vitro setup	One electrode on each side of the petri dish	Diameter of petri dish: 3.5 cm

4.3.2 Fabrication of the prototype device

The case of the prototype device was created by 3D printing. The material and working parameters of 3D printing are listed below:

Table 2. The working parameters in the 3D printing of the case.

Infilled ratio	100%
Layer thickness	0.09 mm
Resolution	Maximum ratio
Material	Polylactic acid (PLA)

The printed case contained two components: the chamber and the cover lid. The receiver module of the wirelessly delivered DC (coil and rectifier chip) was fixed in the chamber by adhesive tapes, and then covered by a lid and sealed with food-grade silicone sealant (ASI 502, American Sealants Inc, Fort Wayne, IN, USA). The electrodes were fixed on the outside of the case with the same silicone sealant. Several small holes (< 1mm of diameter) on the case were punched by a heated needle (21 gauge) to introduce copper wire to connect the inside module and outside electrodes, which were also sealed by silicone sealant.

4.3.3 Treatment of biofilms with the prototype device *in vitro*

For the *in vitro* tests, the PDMS blocks with *P. aeruginosa* or *S. aureus* biofilm were placed on top of the device case as shown in Figure 11. Then the whole device with attached biofilms was immersed in 0.85 % NaCl solution in a petri dish. The coil of the power transmitter unit was placed under the bottom of the petri dish to deliver DC wirelessly. The current density was set to be 6 $\mu A/cm^2$ (based on cathode area). The biofilm samples were treated for 6 h, and the viability of biofilm cells was determined by counting CFU.

4.3.4 Treatment of biofilms with the prototype device in an *ex vivo* model with porcine skin

The *ex vivo* model was adapted from a previous study designed for a study of the surgery site of the cochlear implant [31, 32]. It was composed of a 3D-printed PLA housing (50 mm diameter, 14 mm depth) to mimic the bone tissue that holds the cochlear implant. The prototype device was fixed into the housing by silicone sealant and immersed into a 0.85% NaCl solution (Figure 12). Before treatment, the PDMS blocks with *P. aeruginosa* or *S. aureus* biofilms were placed on top of the device as done in the *in vitro* test. Then the device was covered with a piece of porcine skin (1.0 – 1.2 mm thickness) purchased from a local grocery store and approved by Syracuse University (IACUC#: P4-18) and sterilized by UV for 2 hours on each side. The porcine skin was used to mimic the human skin that covered the cochlear device after surgery. The fat tissue of porcine skin had been prepared as described by Ackermann et al. [33] to UV sterilization. The coil of the power transmitter unit was put on the top of the porcine skin and aligned to the receiver coil in the prototype device to delivery DC wirelessly. The biofilm samples were treated for 6 h with a current level of 6 $\mu A/cm^2$, and the viability of biofilm cells was determined by counting CFU.

4.3.5 Statistical analysis

All data are presented as a mean ± standard deviation. Statistical significance was assessed with one-way or two-way ANOVA followed by Tukey test. Results with $p < 0.05$ were considered statistically significant. All analyses were performed using SAS 9.4 software (SAS Institute, Cary, NC, USA).

4.4 Results

4.4.1 Distribution of the electric field with different layouts and the shapes of the prototype device

According to the results of COMSOL simulation, the electric field distribution on the oval-shaped device was fairly uneven among the different locations with varying distances from the electrodes. For the layout of the sandwich electrodes, the higher electric potential difference located on the center of the device surface, and the little current was observed on the regions far away from the electrodes (Figure 1). When replacing the flat cathode with a circular design that can fully cover the vertical side around the device and using a small (2 x 1 cm) anode in the center of the device's surface ("circular/center" layout), the electric field on the device's surface was still uneven. For example, the region of minor ax had higher potential difference compared to the region of the major ax that was farther from the anode (Figure 2).

The case of square shape had more uniform electric field distribution on the device surface for both layouts (sandwich and circular/center). Although there was minor electric current outside the device surface within the flat side of the electrodes (Figure 3), the circular/center layout keep the entire electric current on the device surface (Figure 4). The square shape device had a challenge in sealing, especially in the corner regions, which could lead to leaking. This can cause possible issues in real manufacturing. Additionally, the square-shaped design was abnormal because the rather sharp edge may cause tissue damage or discomfort.

The round-shaped device had the most uniform distribution of electric field on the entire device surface among the three shapes simulated, especially for the round-shaped case with the circular/center layout (Figure 7). The sandwich layout had electric current going outside of the

device parameter (Figure 5&6), while the circular/center layout concentrated the electric current within radius of the device. No sealing problem was encountered.

Test of the prototype devices also showed that the circular/center layout had a more uniform killing effect on biofilm cells than the sandwich layout. For example, when treating *P. aeruginosa* PAO1 biofilm cells on the oval-shaped device with the sandwich layout, the viability of biofilm cells that were close to the anode side was reduced by approximately 3 ± 0.5 logs (p = 0.006) ; but only weaker killing was observed for two biofilm cells closed to the cathode (1.8 ± 0.4 logs, p = 0.006), while the viability of another two biofilm cells closed to the cathode had no significant change (p > 0.05) (Figure 8). The round-shaped device with sandwich layout also had varying killing effects on biofilm samples at different locations (3 – 4.3 logs, p <0.001) (Figure 9). When replacing the sandwich design with the circular/center layout, the viability of biofilm cells was reduced more evenly (Figure 11). This is consistent with the simulation results that demonstrate even distribution of the electric field across the device surface.

4.4.2 Evaluating the prototype device *in vitro* and *ex vivo* for biofilm control

Based on the results of COMSOL simulation and preliminary DC treatment, the final version of the device was selected to have contained a round-shaped case (45 mm of diameter) with a square TGON anode (1 x 1 cm) in the center and a stainless steel cathode (approximately 1 x 14 cm) around the vertical side. This layout generated a well-defined electric field and high current density on the surface of the device (Figure 10). The total volume of the device was 25 cm^3, close to that of the commercial pacemaker devices. A customized copper receiver coil with a diameter of 30 mm and thickness of 2 mm was installed in the device's chamber. The coil was connected to a

rectifier chip (3 x 1 x 0.5 cm) by soldering. Both TGON and stainless steel electrodes on the outside of the device were also connected to the chip by copper wires (26 gauge).

The prototype device was evaluated by treating *P. aeruginosa* and *S. aureus* biofilms on PDMS blocks placed on top of the device. By supplying power wirelessly to the device, we generated DC at 6 μA/cm^2. With a 6 h treatment *in vitro*, there were 1.5 ± 0.2 ($p < 0.001$) and 3.0 ± 0.1 logs ($p = 0.003$) of the reduction of the viability of *P. aeruginosa* and *S. aureus* biofilm cells, respectively (Figure 11). When the whole system was tested in the *ex vivo* model, the viability of *P. aeruginosa* and *S. aureus* biofilm cells were reduced to 1.0 ± 0.14 ($p = 0.03$) and 2.6 ± 0.8 logs ($p <0.001$), respectively (Figure 12).

4.5 Discussion

In the proof-of-concept test, a strong and uniform electric field was established between the anode and cathode, covering the entire PDMS blocks with biofilm samples (Figure 13). The viability of biofilm cells on each PDMS was reduced equally after treatment. Because the implanted devices have critical functions, the design of the prototype must promise its reliability and reusability for repeated use and consistent performance. Hence, the prototype device should not have any corrosion-sensitive material as the anode because it could decrease the lifetime of the device and release substrates that have potential impact on to surrounding tissues. Additionally, the device should be easy to seal to prevent the leakage of body fluid, which would cause short circuit and failure of the device.

The circular/central layout of the electrodes was chosen based on the results of the COMSOL simulation. Although the sandwich layout with flat electrodes is easier for fabrication, the electric

field is more dispersed which can lead to lower current density on the device surface, and consequently reduce the killing efficacy of DC treatment. The circular/central layout had a more concentrated electric field on the device surface; therefore, it could generate higher current density on the device. This should improve the efficiency of treatment and safety to the host tissues.

For the shape of the device, the square device was excluded because of poor sealing on the corners and uneven electric potential difference on the device's surface. The oval device was also abandoned from further study because of the uneven distribution of the electric field, which led to the uneven killing effects on biofilm cells. In comparison, the round-shaped device was easy to construct, and the distribution of the electric field on the round surface was more uniform than the other two designs based on the simulation result of COMSOL. The round-shaped device had equal killing effects on the biofilm cells presumably because of its uniform electric field.

The electrode's materials should also be well considered in prototype design. According to the results of the previous proof-of-concept experiments in Chapter 3, the stainless steel electrodes had stronger killing activities against *P. aeruginosa* than *S. aureus* planktonic cells, while the graphite-based TGON electrodes were more efficient in killing *S. aureus* biofilm cells. There was a large number of metal precipitates using stainless steel electrodes when the current level was more than 60 $\mu A/cm^2$. The steel anode is oxidized and produces metal ions (Fe, Cr, et al.) during DC treatment [22, 23, 34] (called Galvanic corrosion) [35]. These ions precipitated as solid particles if the solution is basic or contains certain cations. As a result, the device surface and treatment solution were both stained yellow or brown after treatment. To prevent this and keep the device and tissue clean in real applications, the TGON electrodes were chosen to replace steel as the anode because of its high resistance to electrochemical corrosion. TGON is graphite materials and thus there were no metal particles produced. The device surface was still clean after treatment [24]. In our study, we

used small TGON square as the anode and stainless steel as the cathode to ease the manufacturing and avoid corrosion of either electrode during treatment.

The final version of the prototype device had a round case that had approximately 25 mL of volume and 12 cm^2 of surface area. This size was close to commercial pacemaker implants (20-25 mL). The layout of electrodes included a circular steel electrode on the side of the device and a square TGON electrode on the center of the top surface. The wirelessly delivered DC showed 1.5 and 3 logs killing at 6 $\mu A/cm^2$ for *P. aeruginosa* and *S. aureus* biofilm, respectively, which demonstrated the potential of this platform technology for controlling infections associated with implanted medical devices. The treatment result of using the *ex vivo* model also had 2.6 logs killing effect on *S. aureus* biofilm cells on the surface of the device. This suggests that the skin tissue would not reduce the efficiency of wireless delivery of DC significantly, which is consistent with the result of the proof-of-concept experiments *in vitro*.

4.6 Conclusion

In summary, we have designed and engineered a prototype device with the function of wireless delivery of DC based on the comparison of different device designs with varying shapes, electrode layouts and electrode materials. The selected design of the device demonstrated good efficacy in killing both *P. aeruginosa* and *S. aureus* cells in *in vitro* and *ex vivo* model. The results demonstrate that this is an effective platform for investigating the *in vivo* treatment using wirelessly delivered DC in the future.

4.7 References

1. Vinh, D.C. & Embil, J.M. Device-related infections: a review. *Journal of long-term effects of medical implants* **15**, 467-488 (2005).
2. Campoccia, D., Montanaro, L. & Arciola, C.R. The significance of infection related to orthopedic devices and issues of antibiotic resistance. *Biomaterials* **27**, 2331-2339 (2006).
3. Darouiche, R.O. Treatment of infections associated with surgical implants. *The New England journal of medicine* **350**, 1422-1429 (2004).
4. Germiller, J.A., El-Kashlan, H.K. & Shah, U.K. Chronic Pseudomonas infections of cochlear implants. *Otology & neurotology : official publication of the American Otological Society, American Neurotology Society [and] European Academy of Otology and Neurotology* **26**, 196-201 (2005).
5. Celerier, C. et al. Pain After Cochlear Implantation: An Unusual Complication? *Otology & neurotology : official publication of the American Otological Society, American Neurotology Society [and] European Academy of Otology and Neurotology* **38**, 956-961 (2017).
6. Stover, T. & Lenarz, T. Biomaterials in cochlear implants. *GMS current topics in otorhinolaryngology, head and neck surgery* **8**, Doc10 (2009).
7. Zeng, F.G., Rebscher, S., Harrison, W., Sun, X. & Feng, H. Cochlear implants: system design, integration, and evaluation. *IEEE reviews in biomedical engineering* **1**, 115-142 (2008).

8. Cunningham, C.D., 3rd, Slattery, W.H., 3rd & Luxford, W.M. Postoperative infection in cochlear implant patients. *Otolaryngology--head and neck surgery : official journal of American Academy of Otolaryngology-Head and Neck Surgery* **131**, 109-114 (2004).
9. Skrivan, J. & Drevinek, P. A case report of a cochlear implant infection - A reason to explant the device? *Cochlear implants international* **17**, 246-249 (2016).
10. Bluestone, C.D. Bacterial meningitis in children with cochlear implants. *N Engl J Med* **349**, 1772-1773; author reply 1772-1773 (2003).
11. Costerton, J.W., Montanaro, L. & Arciola, C.R. Biofilm in implant infections: its production and regulation. *Int J Artif Organs* **28**, 1062-1068 (2005).
12. Arciola, C.R. et al. Strong biofilm production, antibiotic multi-resistance and high gelE expression in epidemic clones of Enterococcus faecalis from orthopaedic implant infections. *Biomaterials* **29**, 580-586 (2008).
13. Glikman, D., Luntz, M., Shihada, R., Zonis, Z. & Even, L. Group B streptococcus meningitis in a child with cochlear implant. *Emerging infectious diseases* **15**, 1695-1696 (2009).
14. Im, G.J. et al. Analysis of Bacterial Biofilms on a Cochlear Implant Following Methicillin-Resistant Staphylococcus Aureus Infection. *Journal of audiology & otology* **19**, 172-177 (2015).
15. Pettersen, G., Ovetchkine, P. & Tapiero, B. Group A streptococcal meningitis in a pediatric patient following cochlear implantation: report of the first case and review of the literature. *Journal of clinical microbiology* **43**, 5816-5818 (2005).

16. Costerton, J.W., Ellis, B., Lam, K., Johnson, F. & Khoury, A.E. Mechanism of electrical enhancement of efficacy of antibiotics in killing biofilm bacteria. *Antimicrobial Agents and Chemotherapy* **38**, 2803-2809 (1994).

17. del Pozo, J.L. et al. Effect of electrical current on the activities of antimicrobial agents against Pseudomonas aeruginosa, Staphylococcus aureus, and Staphylococcus epidermidis biofilms. *Antimicrobial Agents and Chemotherapy* **53**, 35-40 (2009).

18. Del Pozo, J.L. et al. The electricidal effect is active in an experimental model of Staphylococcus epidermidis chronic foreign body osteomyelitis. *Antimicrob Agents Chemother* **53**, 4064-4068 (2009).

19. del Pozo, J.L., Rouse, M.S., Mandrekar, J.N., Steckelberg, J.M. & Patel, R. The electricidal effect: reduction of Staphylococcus and pseudomonas biofilms by prolonged exposure to low-intensity electrical current. *Antimicrobial Agents and Chemotherapy* **53**, 41-45 (2009).

20. Schmidt-Malan, S.M. et al. Antibiofilm Activity of Low-Amperage Continuous and Intermittent Direct Electrical Current. *Antimicrobial Agents and Chemotherapy* **59**, 4610-4615 (2015).

21. Spadaro, J.A., Berger, T.J., Barranco, S.D., Chapin, S.E. & Becker, R.O. Antibacterial effects of silver electrodes with weak direct current. *Antimicrobial Agents and Chemotherapy* **6**, 637-642 (1974).

22. Niepa, T.H., Gilbert, J.L. & Ren, D. Controlling Pseudomonas aeruginosa persister cells by weak electrochemical currents and synergistic effects with tobramycin. *Biomaterials* **33**, 7356-7365 (2012).

23. Niepa, T.H. et al. Sensitizing Pseudomonas aeruginosa to antibiotics by electrochemical disruption of membrane functions. *Biomaterials* **74**, 267-279 (2016).

24. Niepa, T.H.R., Wang, H., Gilbert, J.L. & Ren, D. Eradication of Pseudomonas aeruginosa cells by cathodic electrochemical currents delivered with graphite electrodes. *Acta Biomater* **50**, 344-352 (2017).

25. Brinkman, C.L. et al. Exposure of Bacterial Biofilms to Electrical Current Leads to Cell Death Mediated in Part by Reactive Oxygen Species. *PloS one* **11**, e0168595 (2016).

26. Voegele, P. et al. Antibiofilm Activity of Electrical Current in a Catheter Model. *Antimicrobial Agents and Chemotherapy* **60**, 1476-1480 (2015).

27. Canty, M., Luke-Marshall, N., Campagnari, A. & Ehrensberger, M. Cathodic voltage-controlled electrical stimulation of titanium for prevention of methicillin-resistant Staphylococcus aureus and Acinetobacter baumannii biofilm infections. *Acta Biomater* **48**, 451-460 (2017).

28. Ehrensberger, M.T. et al. Cathodic voltage-controlled electrical stimulation of titanium implants as treatment for methicillin-resistant Staphylococcus aureus periprosthetic infections. *Biomaterials* **41**, 97-105 (2015).

29. Nodzo, S.R. et al. Cathodic Voltage-controlled Electrical Stimulation Plus Prolonged Vancomycin Reduce Bacterial Burden of a Titanium Implant-associated Infection in a Rodent Model. *Clin Orthop Relat Res* **474**, 1668-1675 (2016).

30. Xue Rf, C.K.W.J.M. High-Efficiency Wireless Power Transfer for Biomedical Implants by Optimal Resonant Load Transformation.

31. Darlong, V. et al. Perioperative complications of cochlear implant surgery in children. *J Anesth* **29**, 126-130 (2015).

32. Gheorghe, D.C. & Zamfir-Chiru-Anton, A. Complications in cochlear implant surgery. *J Med Life* **8**, 329-332 (2015).

33. Ackermann, D.M., Smith, B., Wang, X.F., Kilgore, K.L. & Peckham, P.H. Designing the optical interface of a transcutaneous optical telemetry link. *IEEE Trans Biomed Eng* **55**, 1365-1373 (2008).

34. Niepa, T.H., Wang, H., Dabrowiak, J.C., Gilbert, J.L. & Ren, D. Synergy between tobramycin and trivalent chromium ion in electrochemical control of Pseudomonas aeruginosa. *Acta Biomater* **36**, 286-295 (2016).

35. Ju, H. et al. Mapping the Galvanic Corrosion of Three Metals Coupled with a Wire Beam Electrode: The Influence of Temperature and Relative Geometrical Position. *Materials (Basel)* **11** (2018).

4.8 Figures

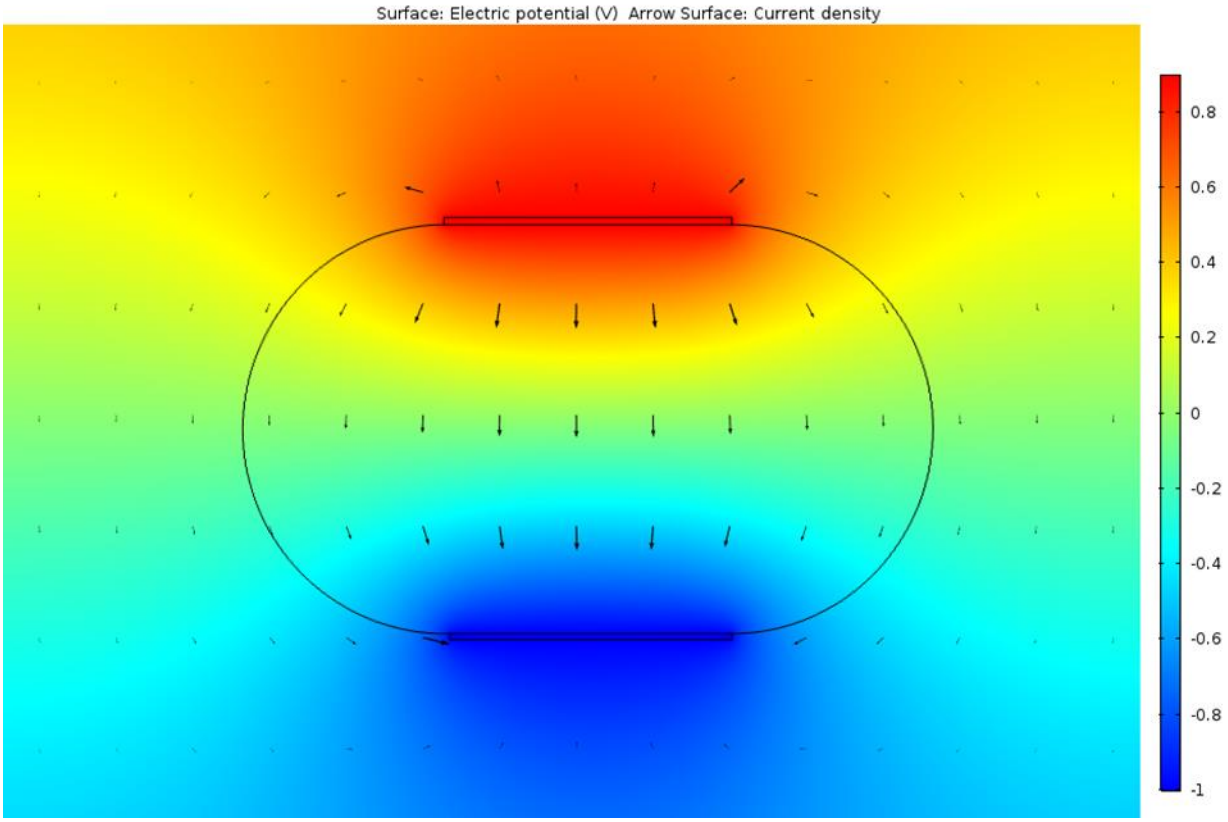

Figure 1. Overhead view of distribution of electric potential (color surface) and current density (arrows map) on the surface of the oval-shaped device with the sandwich layout of electrodes.

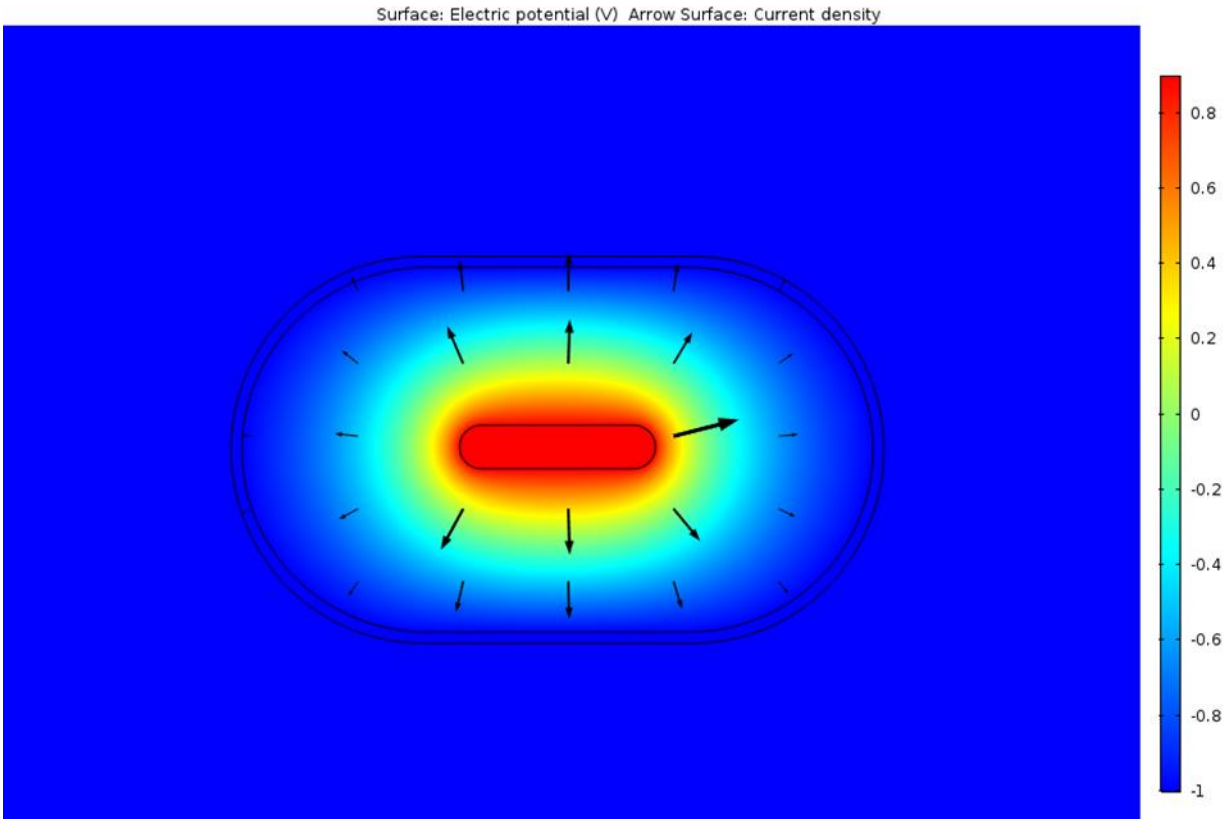

Figure 2. Overhead view of distribution of electric potential (color surface) and current density (arrows map) on the surface of the oval-shaped device with the circular/center layout of electrodes.

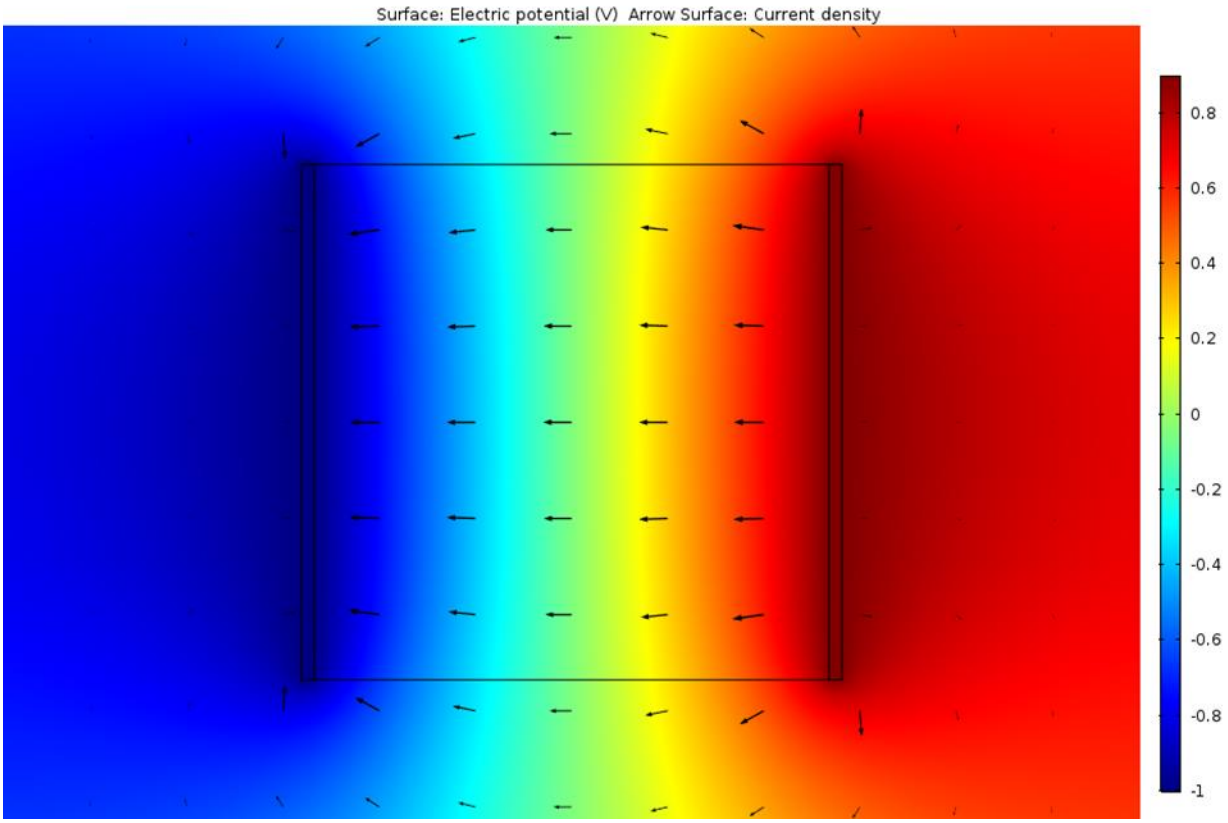

Figure 3. Overhead view of distribution of electric potential (color surface) and current density (arrows map) on the surface of the square-shaped device with the sandwich layout of electrodes.

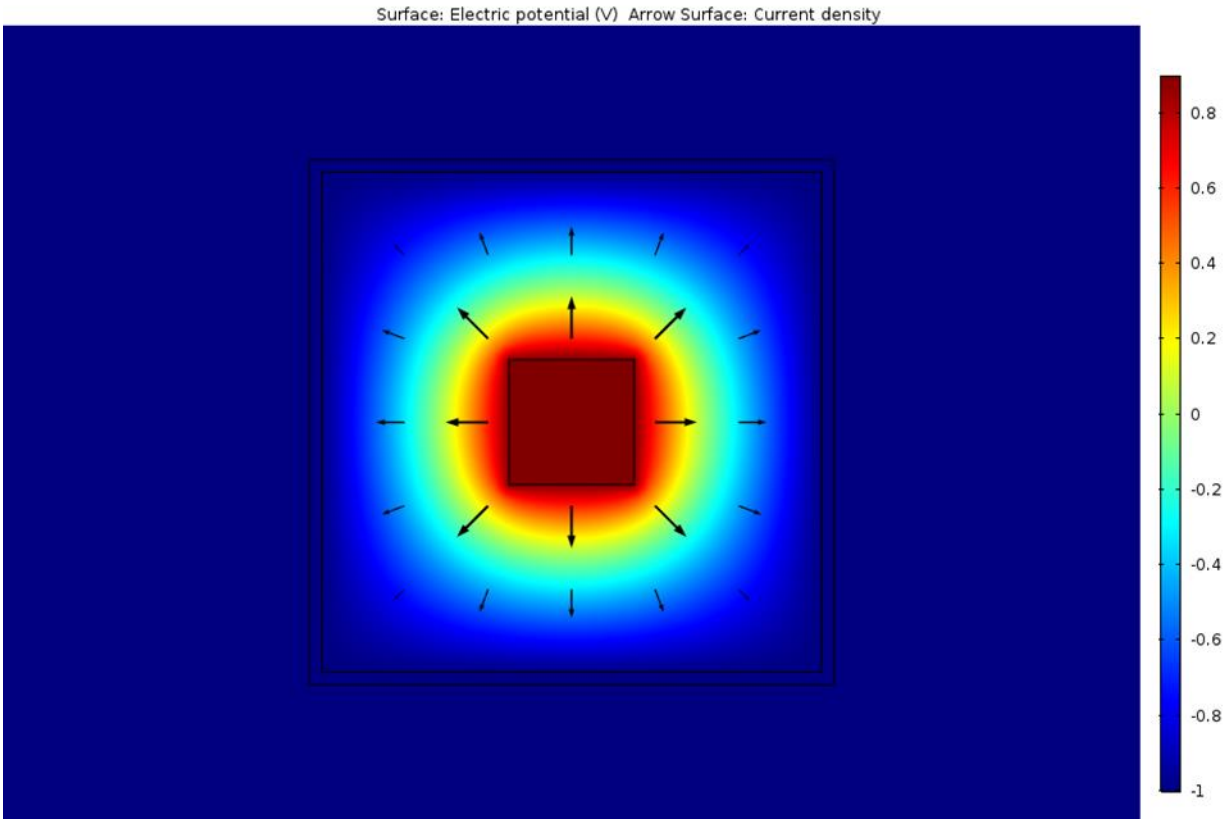

Figure 4. Overhead view of distribution of electric potential (color surface) and current density (arrows map) on the surface of the square-shaped device with the circular/center layout of electrodes.

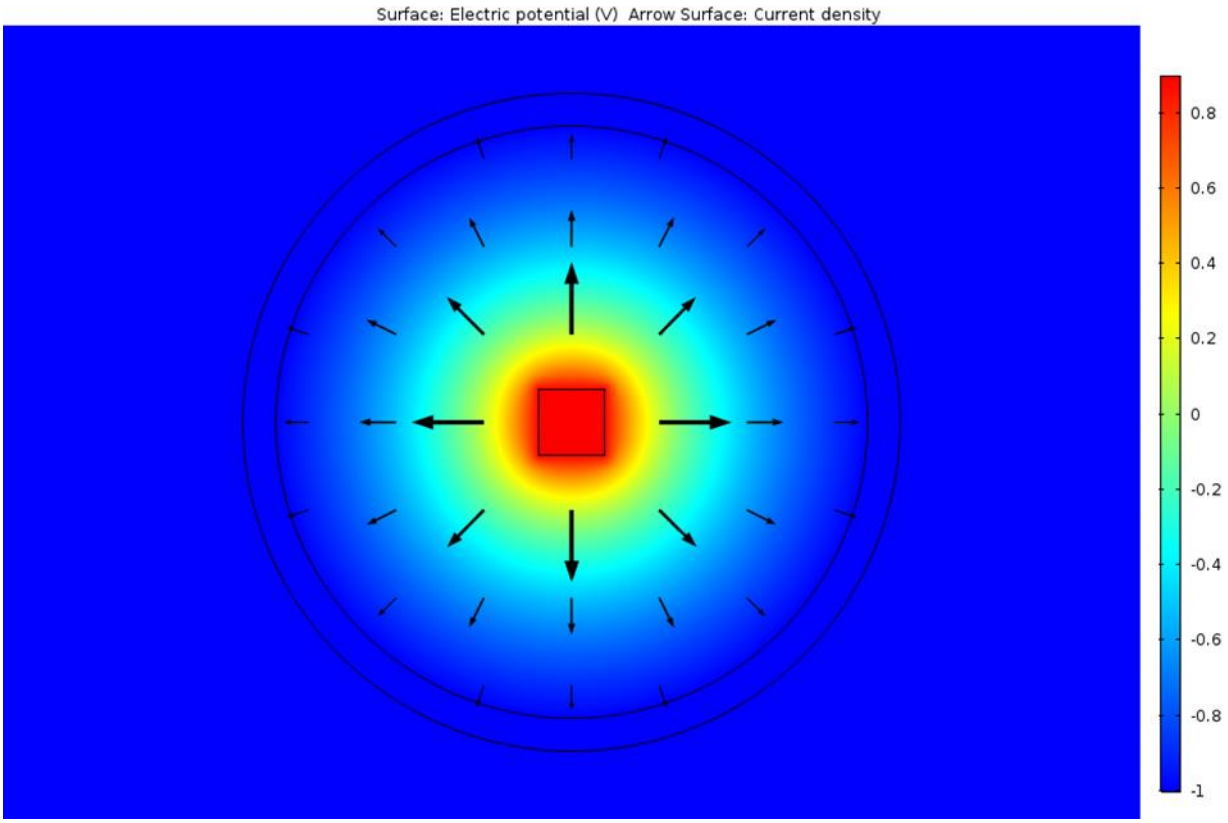

Figure 5. Overhead view of distribution of electric potential (color surface) and current density (arrows map) on the surface of the round-shaped device with the circular/center layout of electrodes.

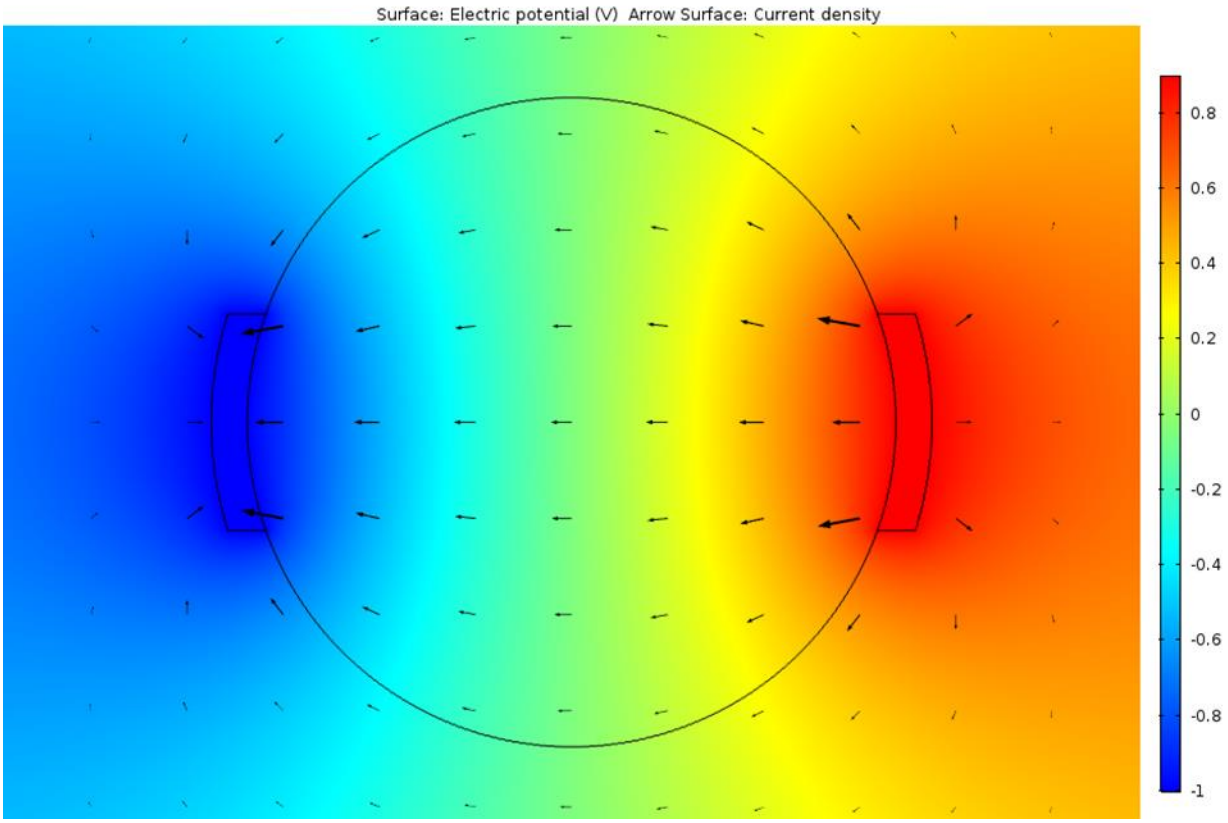

Figure 6. Overhead view of distribution of electric potential (color surface) and current density (arrows map) on the surface of the round-shaped device with the small sandwich layout of electrodes.

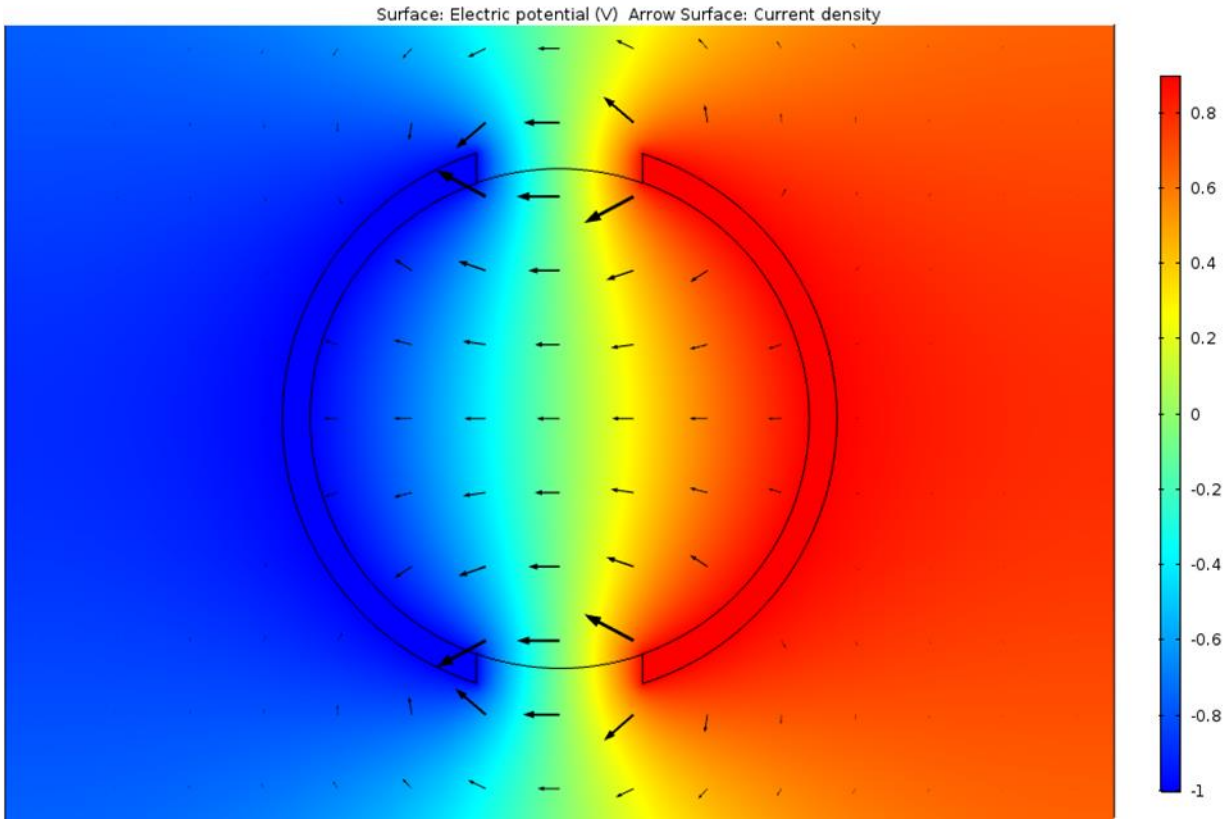

Figure 7. Overhead view of distribution of electric potential (color surface) and current density (arrows map) on the surface of the round-shaped device with the large sandwich layout of electrodes.

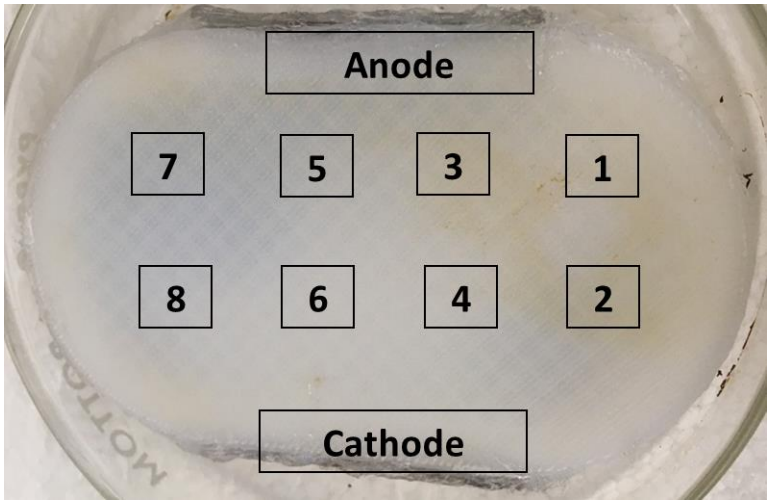

(A)

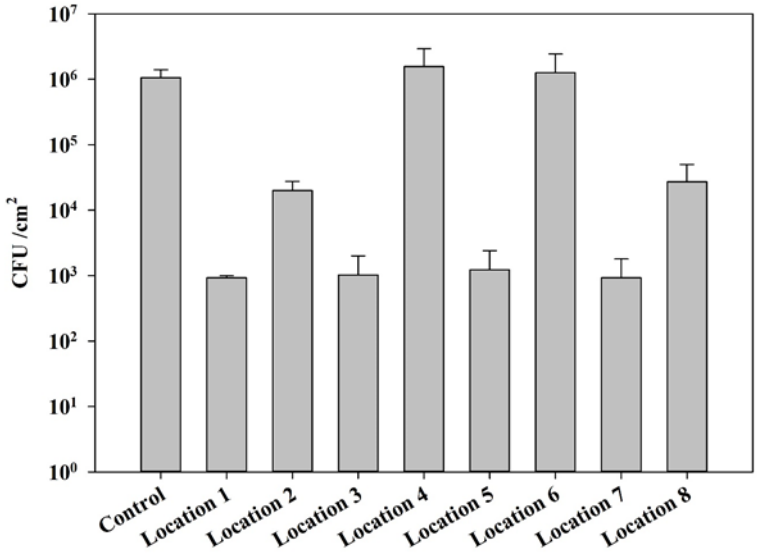

(B)

Figure 8. Experimental setup and killing effects of *S. aureus* biofilms at different locations of the oval-shaped device with the sandwich layout of electrodes. (A): The experimental setup of *S. aureus* biofilm samples on the surface of a prototype device. (B): Viability of *S. aureus* biofilm cells on the surface of the prototype device after treatment with wirelessly delivered DC (12 $\mu A/cm^2$) for 6 h.

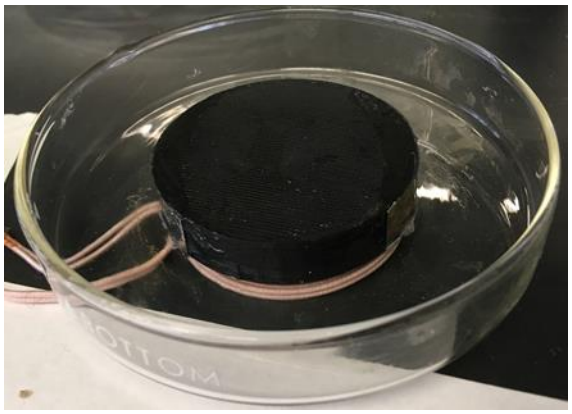

(A)

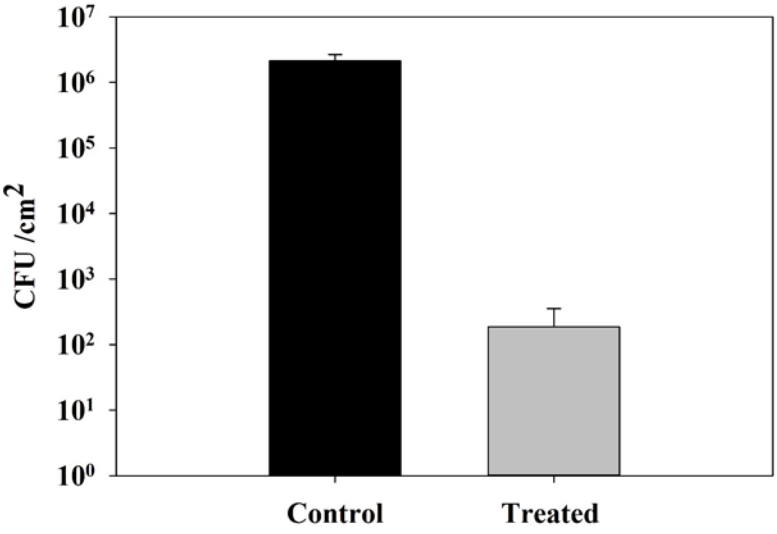

(B)

Figure 9. Experimental setup and killing effects of *S. aureus* biofilm on different locations of the round-shaped device with flat-side electrodes. (A): The experimental setup of prototype device. (B): The viability of *S. aureus* biofilm on the surface of the prototype device after treatment with wirelessly delivered DC (170 µA/cm^2) for 6 h.

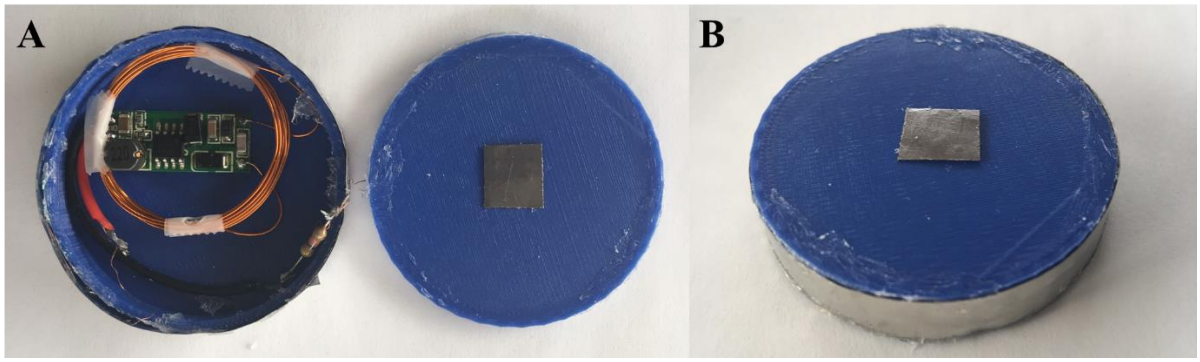

Figure 10. The final design of the round-shaped prototype device with a circular cathode and center anode. (A): The internal circuit including receiver coil, rectifier chip, and internal resistor. (B) The layout of electrodes on the surface of the prototype device.

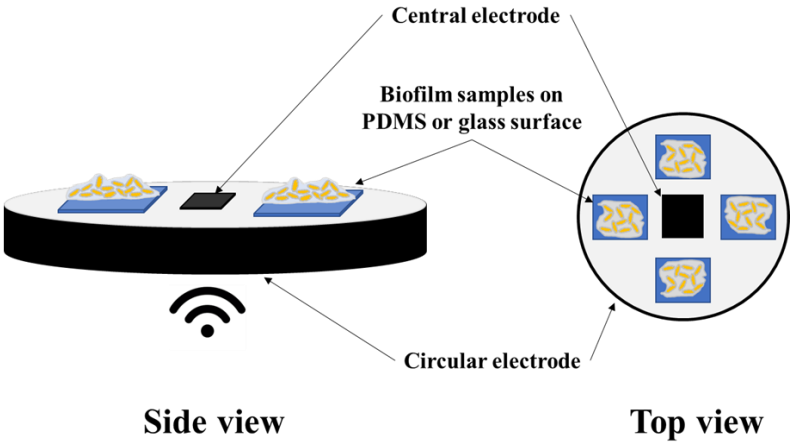

(A)

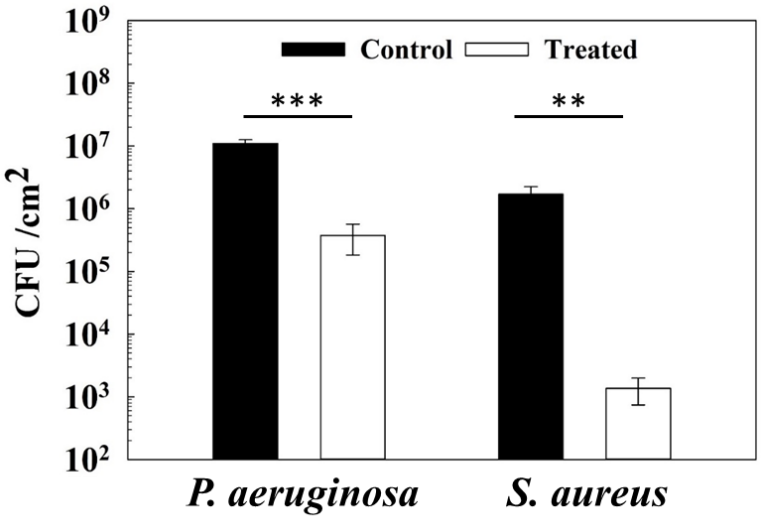

(B)

Figure 11. *In vitro* test of the selected prototype device. (A): Schematic of the experimental setup. The PDMS blocks with biofilm were placed on the top of the device and around the central electrode for DC treatment. (B): Viability of *P. aeruginosa* and *S. aureus* biofilm cells after treatment with 6 µA/cm^2 for 6 h *in vitro*. (***, $p < 0.001$; **, $p = 0.01$)

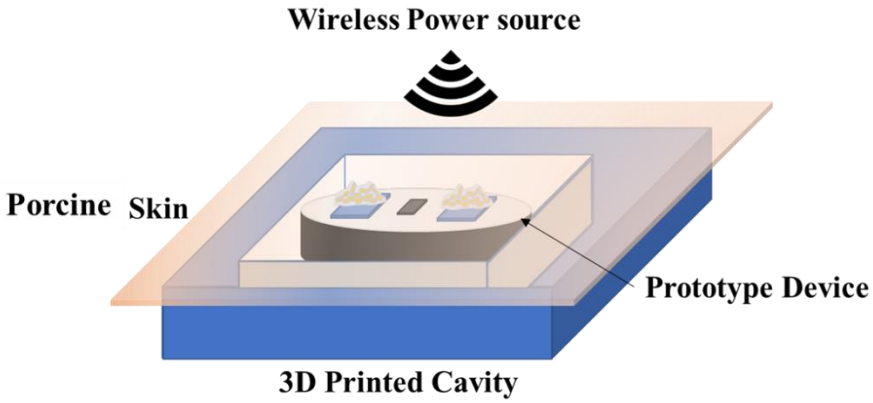

(A)

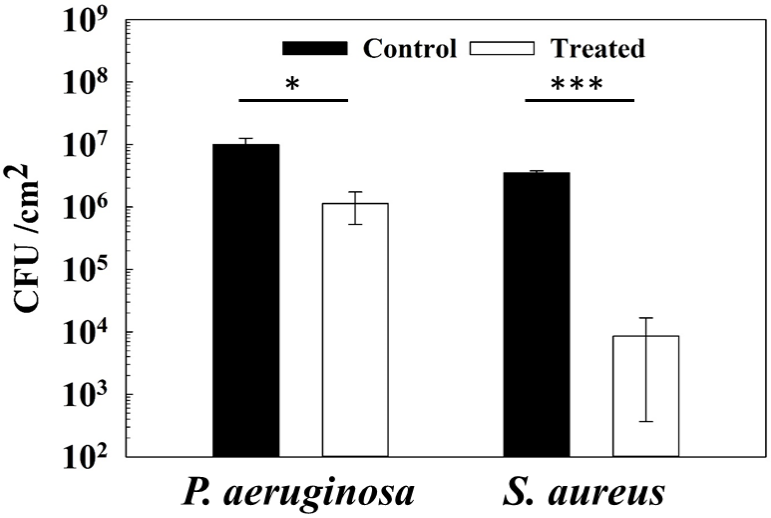

(B)

Figure 12. *Ex vivo* test of the selected prototype device. (A): Schematic of the experimental setup in model. The device was fixed into the 3D-printed cavity and covered with porcine skin. The wireless power transmitter was placed on the top of the skin. (B): Viability of P. aeruginosa and S. aureus biofilm cells after treatment with 6 µA/cm2 for 6 h in ex vivo model. (***, $p < 0.001$; *, $p < 0.05$)

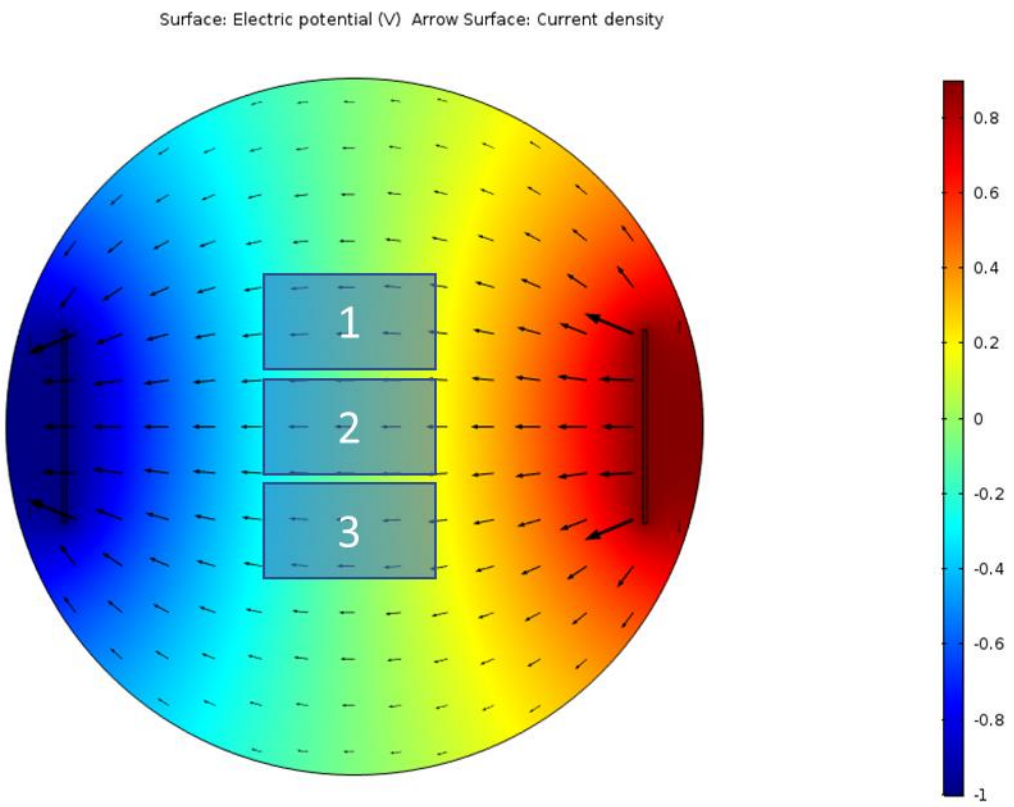

Figure 13. COMSOL simulation of electric potential (color surface) and current density (arrows map) distribution in a petri dish with the flat stainless steel electrode (0.5 cm width, 0.01 cm thickness) positioned on opposite side. Three PDMS coupons with biofilm were placed in the electric field between two electrodes. The total DC level was approximately 100 µA.

Chapter 5

Killing mechanism of DC treatment

5.1 Abstract

Direct electric current (DC) has been reported in many studies for its biocidal effects on pathogenic microorganisms in the presence or absence of antimicrobials. The reactive oxygen species (ROS) and metal ions produced by the electrochemical reaction during DC treatment are believed to contribute the killing effects, although only the bactericidal effect of hydrogen peroxide has been reported in the previous studies. In this Chapter, the killing mechanism of DC treatment was investigated by comparing the killing effects of different electrochemical products, such as hypochlorite, hydrogen peroxide, iron, and chromium ions. According to the results, we find that the DC treatment using TGON electrodes killed biofilm cells by generating hypochlorite from the anode, which depended on the concentration of sodium chloride in the solution. The DC treatment using stainless steel electrodes could induce Fenton reaction by the metal ions from anode and hydrogen peroxide from the cathode to produce free radicals that have the potent bactericidal effect. By understanding the killing mechanism of DC treatment, it will be helpful for improving the device design and assessment of cytotoxicity to host tissues.

5.2 Introduction

The first study of bacterial control by electric current was reported in 1915 by Beattie [1], who applied alternating current (AC) at 3000 – 4000 V to eradicate microorganisms from milk. Later, Rosenberg [2] found that *E. coli* could be killed with 2 A of AC using platinum electrodes. The biocidal effects of low-level AC to bacteria were also reported by Pareilleux et al. [3] that the viability of *E. coli* was reduced after treatment from 10 to 200 mA of AC using stainless-steel electrodes.

Compared to AC, direct current (DC) received more attention as an alternative antimicrobial method. Rowley [4] first showed the biocidal effects on *E. coil* using 1- 140 mA DC conducted with platinum electrodes in the 1970s. Then Baranco [5] reported the reduction of the viability of *S. aureus* cells after treatment with 400 µA DC using silver, platinum, gold or stainless steel electrodes. In general, DC requires lower levels than AC to achieve significant biocidal effects, and this is more suitable for application *in vivo*, although *in vivo* treatment may require higher current levels. For example, Ehrensberger et al. [6, 7] reported that the number of viable *S. aureus* cells were reduced by 90% after treatment with 1 mA DC in the rabbit model although they obtained more than 2 logs of killing effect on *S. aureus* cells with lower DC level *in vitro*. In addition to the effects of DC alone, the synergy between DC and antibiotics has also been reported. For example, more than 2 additional logs of killing effects were observed in the concurrent treatment of *E. coli* cells with 6 mA/cm^2 of DC and gentamicin and oxytetracycline compared to DC treatment alone [8]. Costerton [9] et al. also reported that 100 $\mu A/cm^2$ DC could promote killing efficiency of tobramycin to *P. aeruginosa* biofilm.

The killing mechanism of electric current treatment is still not well understood although several theories have been proposed. In 1962, Brandt et al. [3, 10] first speculated that the free radicals generated by electric treatment have a bactericidal effect. For the treatment with high-level electric currents, cell membranes are believed to be permanently damaged by current-associated high energy, leading to cells' death [11]. Lower level DC may cause bacterial killing with electrochemical products [12, 13]. A number of possible redox reactions could occur at the interface between electrode and electrolyte solution during electrolysis:

Oxidation reactions on anode: [14]

$$2H_2O \rightarrow 4H^+ + O_2 + 2e^-$$

$$Fe \rightarrow Fe^{2+} + 2e^-$$

$$Fe^{2+} \rightarrow Fe^{3+} + e^-$$

$Cr \rightarrow Cr^{3+} + 3e^-$ (Trace in steel anode)

$$2Cl^- \rightarrow Cl_2 + 2e^-$$

$$Cl^- + H_2O \rightarrow HClO + 2e^- + H^+$$

$$Cl_2 + 2H_2O \rightarrow 2HClO + 2e^- + 2H^+$$

Reduction reactions on cathode:

$$H_2O + 2e^- \rightarrow H_2 + 2OH^-$$

$$O_2 + 2H^+ + 2e^- \rightarrow H_2O_2$$

$$O_2 + H_2O + e^- \rightarrow HO_2 \cdot + OH^-$$

$$O_2 + 2H_2O + 2e^- \rightarrow H_2O_2 + 2OH^-$$

Redox reactions in electrolyte solution: [15]

$$Fe^{2+} + H_2O_2 \rightarrow Fe^{3+} + OH\cdot + OH^-$$

$$Fe^{3+} + H_2O_2 \rightarrow Fe^{2+} + OOH\cdot + H^+$$

$$2Fe^{3+} + 2H_2O \rightarrow 2Fe^{2+} + H_2O_2 + 2H^+$$

The metal anode, especially silver, copper, and steel, are oxidized to release metal ions (Ag^+, Cu^{2+}/Cu^+, Cr^{3+}, Fe^{2+}/Fe^{3+}, et al.) during DC treatment [13]. These ions could accumulate and interrupt cell metabolism. Moreover, the metal ions could move ion flow in an electric field, which was found disrupt the integrity of the cell membrane [12, 13]. Based on electrochemistry, radical oxygen species and free radicals could be generated from the redox reactions at the electrodes. However, it is difficult to directly prove since many of those species have a short life and can react with cells immediately. Hydrogen peroxide (H_2O_2) is one of the few radical oxygen species that have been verified as generated during electric treatment. H_2O_2 could disrupt the structure and permeability of the cell wall and membrane [16]. The concentration of H_2O_2 close to the electrode surface range from 0.2 μM to more than 20 μM when the current density increases from 5 to 40 μA/cm^2 [17]; however, this concentration decreases quickly towards zero over the distance from the electrode [18]. Another reported radical oxygen species generated in DC treatment is hypochlorite when the electrolyte solution contains chloride ions. The chloride ions are oxidized on the anode to produce chlorine and hypochlorite [19]. Hypochlorite could disrupt many activities of bacteria, such as oxidative phosphorylation and sulfhydration, as well as DNA synthesis [20]. To evaluate how those electrochemical products could affect the killing results of wireless DC treatment of biofilm cells, we conducted a series of experiments using DC and different electrochemical products in this study

to mimic the actual electrochemical reactions during DC treatment and evaluate the killing effects of these reactions.

We reported that the activities of some antibiotics (e.g. tobramycin) could be enhanced in the presence of an electric field conducted by stainless steel electrodes, but not graphite electrodes [12]. We speculated that this may result from synergistic interactions between metal ions from stainless steel and antibiotic molecules. For example, tobramycin could bind to ribosome RNA and interrupt protein synthesis in *P. aeruginosa* [21]. We suspected the metal ions may form a complex with tobramycin molecules to increase its affinity to RNA, leading to the enhanced killing effect on *P. aeruginosa* cells. The hammerhead ribozyme cleavage reaction is an ideal model to study the interactions between RNA molecules and antimicrobial agents since the hammerhead ribozyme has a small, well-defined structure [22 23]. In this study, we utilize the hammerhead ribozyme system to investigate the interaction between Cr (III) (Tobramycin) complex and RNA *in vitro*.

5.3 Methods and materials

5.3.1 Killing assay of *P. aeruginosa* biofilm with metal ions, sodium hypochlorite and hydrogen peroxide

The *P. aeruginosa* biofilm samples on PDMS were cultured in LB medium for 24 hours followed by washing with 0.85% NaCl solution twice. Then, the biofilm samples were placed in a petri dish and soaked in 3 mL of 0.85% NaCl solution mixed with different chemicals including sodium hypochlorite (5%, Fisher Scientific, Hampton, NH, U.S.), hydrogen peroxide (30%, Fisher Scientific, Hampton, NH, U.S.) and ferric chloride (1%, Fisher Scientific, Hampton, NH, U.S.). The concentration of chemicals is listed in Table 1. The biofilms were treated with these chemicals

at room temperature for 3h. After treatment, the biofilm cells were harvested by following the same methods described in Chapter 3 and the viability was determined by counting CFU.

5.3.2 DC treatment of *P. aeruginosa* biofilms in different concentrations of NaCl solution

P. aeruginosa biofilm samples on PDMS were prepared and washed as described previously. Then they were placed between two TGON or stainless-steel electrodes in a petri dish. The electrodes were connected to a potentiostat (Potentiostat WaveNow, Pine Research Instrumentation, Raleigh, NC, U.S.) that applied 30 μA/cm^2 DC to a treatment facility for 3 h. During DC treatment, the biofilm samples were soaked in the electrolysis solutions with different concentrations of sodium chloride (Table 1). Fe (III) ions were also added into electrolysis to explore the possible synergistic effect. After treatment, the biofilm cells were harvested following the same methods and cell viability was determined by counting CFU. The control was biofilm cells without DC treatment.

Table 1. Conditions tested for treatment of *P. aeruginosa* biofilms in single chamber system

Condition No.	NaCl %	Electrodes	DC level μA/cm^2	Other chemicals in solution
1	0.85	TGON	30	-
2	0.01	TGON	30	-
3	0.001	TGON	30	-
4	0.001	Stainless steel	30	-
5	0.85	Stainless steel	30	
6	0.85	-	-	0.1% NaOCl
7	0.85	-	-	0.01% NaOCl
8	0.85	-	-	0.001% NaOCl
9	0.85	-	-	2 mg/L H_2O_2
10	0.85	-	-	20 mg/L H_2O_2
11	0.85	-	-	200 mg/L H_2O_2

5.3.3 DC treatment of *P. aeruginosa* biofilms in the dual chamber system

To prevent the interference between anode and cathode during DC treatment, a similar test of *P. aeruginosa* biofilms was also conducted in a dual chamber system that was used in previous research [13, 24]. This system contained two chambers with the only one single electrode in each chamber filled with 0.85% NaCl solution. A capillary tubing containing 0.85% NaCl solution was used as a salt bridge between the two chambers and complete the electric circuit. The *P. aeruginosa* biofilm samples were placed both in anode and cathode chambers. Then 30 $\mu A/cm^2$ of DC was applied to the system using a potentiostat in 3 h. After treatment, the viability of biofilm cells was determined by counting CFU.

5.3.4 DC treatment of *P. aeruginosa* planktonic cells in the presence of chromium (III)

To investigate if chromium ions have bactericidal effects in the electric field, *P. aeruginosa* PAO1 planktonic cells were treated with chromium (III) ions in the presence and absence of DC. The overnight planktonic cells culture was washed with DI water twice to remove chloride and dissolved organic components. Then the cells were resuspended in 3 mL 0.001% NaCl solution to a final cell density of 10^8 per mL in the petri dish. Two TGON electrodes were inserted into the petri dish and connected with a potentiostat to apply 60 $\mu A/cm^2$ DC to the treatment chamber for 1 hour. After treatment, the viability of planktonic cells was determined by counting CFU.

The similar test was also conducted in the dual chamber system mentioned above. The washed *P. aeruginosa* cells were resuspended in two chambers followed by adding 10 μM $CrCl_3$ (Acros Organics, NJ, USA). Then 20 $\mu A/cm^2$ of DC was applied to the system using a potentiostat in 1 h. After treatment, the viability of planktonic cells was determined by counting CFU.

5.3.5 DC treatment of *S. aureus* planktonic cells in agarose gel

The agar matrix could limit the motility of bacterial cells allowing one to observe which area between anode and cathode has strong killing effects on the cells. In this study, the overnight planktonic cells culture was washed with 0.85% sodium chloride solution twice followed by mixing with sterilized 1.0% agarose solution containing 0.85% sodium chloride (Fisher Scientific, Hampton, NH, U.S.) at approximately 40 °C. Then the mixture was added into a 3 mL cuvette with a stainless steel electrode placed on each side. After the gel was set, the electrodes were connected to a potentiostat to apply 60 $\mu A/cm^2$ DC for 1 hour. After treatment, the agarose gel with cells was stained by the Live/Dead staining kit (Thermofisher, Waltham, MA, USA) for 15 min. The cell viability was determined using fluorescence microscopy.

5.3.6 Hammerhead ribozyme-catalyzed cleavage reaction

To investigate the mechanism of synergy between chromium ions and antibiotics in bacterial killing, we conducted a hammerhead ribozyme-catalyzed cleavage test using Cr (III) ion and tobramycin. The experiment materials and procedure are similar to that described in C. S. Chow's report [23]. Briefly, the hammerhead ribozyme and fluorescein-labeled RNA substrate, which shared the same sequence as Chow's experiment, were obtained from Integrated DNA Technologies (Coralville, IA, USA). Other reagents involved included 0.4 M $MgCl_2$ (Amresco, Solon, OH, USA), 6.4 mM tobramycin (Tokyo Chemical Industry, Japan), 6.4 mM $CrCl_3$ (Acros Organics, NJ, USA), and 1 M Tris-HCl buffer (pH 7.5). The gel was made with 20% 37.5:1 acrylamide–bisacrylamide solution, 10% (w/v) ammonium persulfate in H_2O, and TEMED (N, N, N', N'-tetramethyl ethylenediamine). The gel running buffer was 10X TBE (900 mM Tris base, 90 mM

boric acid, 25 mM EDTA, pH 8.3). The loading buffer consisted of 16 M urea, 30% glycerol and 1X TBE.

First, the hammerhead ribozyme (30 pmol) was mixed with RNase free water and 1 µl Tris-HCl buffer in 1.5 mL centrifuge tubes, followed by boiling for 90 seconds. After the mixture cooled down to room temperature (in 10 minutes), a mixture of 1 µL tobramycin (final concentration 320 µM) and 1 µL $CrCl_3$ (final concentration ranged from 320 µM to 32 µM) were added into each tube. Next, the fluorescein-labeled RNA substrates (100 pmol) were added into mixture solution followed by 1 µL 0.4 M $MgCl_2$. There were one negative control without hammerhead ribozyme and one positive control with neither tobramycin nor $CrCl_3$. Besides, to compare with inhibitory effects of tobramycin or Cr^{3+} alone, another four control samples with the same concentration of tobramycin or $CrCl_3$ alone were set up. The final volume of the mixture in each tube was 20 µL. The mixtures were incubated at 37°C for 1 h. The loading buffer was added to mixtures after reaction completion, and then they were stored at -80°C immediately after boiling for 90 seconds.

The 20% polyacrylamide (37.5:1 acrylamide–bisacrylamide) gel was prepared following Chow's protocol [23]. The gel was run at 100 V in 1X TBE buffer for approximately 2 h (Mini-PROTEAN® Tetra Cell system, Bio-Rad Laboratories, Hercules, CA, USA). Then the gel was imaged using a Bio-Rad Gel Doc XR+ system with Image-lab software (Bio-Rad Laboratories, Hercules, CA, USA).

The relative quantity of RNA in each band was calculated based on the strength of fluorescence using the negative control as a reference. The ratio of cleavage was calculated by the equation below:

$$Ratio\ of\ cleavage = \frac{relative\ quantity\ of\ products\ (lower\ bands)}{relative\ quantity\ of\ substrates\ (upper\ bands)}$$

The ratio is inversely correlated with the inhibitory.

5.3.7 Statistical analysis

All data are presented as a mean ± standard deviation. Statistical significance was assessed with one-way or two-way ANOVA followed by Tukey test. Results with $p < 0.05$ were considered statistically significant. All analyses were performed using SAS 9.4 software (SAS Institute, Cary, NC, USA).

5.4 Results

5.4.1 Killing effect of DC in solutions with different concentrations of sodium chloride

According to the results of killing assay under different conditions, TGON electrodes showed dosage-dependent killing effects based on the concentration of sodium chloride in the solution. For example, the viability of *P. aeruginosa* biofilm was reduced by 1.8 ± 0.1, 1.4 ± 0.07 and 0.8 ± 0.09 logs ($p = 0.01$) with 0.85%, 0.1%, 0.01% and 0.001% NaCl, respectively. However, the treatments using a stainless steel electrode did not show a significant difference (1.1 ± 0.04 and 1.3 ± 0.3 logs, $p > 0.05$) between 0.85% and 0.001% NaCl solution (Figure 1&2).

5.4.2 Killing effect of chlorite and hydron peroxide on *P. aeruginosa* biofilm

The killing effect of sodium hypochlorite on *P. aeruginosa* biofilm cells was dosage-dependent, which was 6.0 ± 0.2, 1.4 ± 0.8 and 0.6 ± 0.2 logs ($p < 0.001$) in 0.01%, 0.001% and 0.0001% NaOCl for 6 h treatment (Figure 1). In comparison, H_2O_2 at 100 mg/L showed only 0.9 ± 0.05 logs ($p < 0.001$) killing of *P. aeruginosa* biofilm cells, while the H_2O_2 solution of lower concentrations didn't show the significant killing effect (Figure 2).

5.4.3 Killing effect of DC treatment on *P. aeruginosa* biofilm in dual chamber system

In the dual chamber system, the DC treatment using TGON electrodes showed 2.6 ± 0.2 logs (p = 0.002) killing effect on biofilm cells in anode chamber, while there was no significant killing in cathode chamber (0.4 log, p >0.05) (Figure 3). The DC treatment using stainless steel electrodes demonstrated 0.6 ± 0.3 (p = 0.03) and 0.7 ± 0.01 (p = 0.004) logs killing effect on biofilm cells in anode and cathode chamber, respectively (Figure 4).

5.4.4 The role of chromium ions in the killing mechanism of DC

In previous research, we reported that the stainless-steel electrode could release metal ions during DC treatment. These ions were found to have bactericidal effects on the cells under an electric field. To understand if wirelessly induced DC also show similar effects, chromium (III) and Ferric (III) were tested on *P. aeruginosa* PAO1 planktonic cells. When *P. aeruginosa* planktonic cells were treated with wirelessly induced DC and chromium (III) ions for 1 h, 2.4 ± 0.3 logs of killing was observed under the condition of concurrent treatment with 60 μA DC/cm^2 and 10 μM chromium (III) ions. In comparison, treatment with 60 μA/cm^2 DC or 10 μM chromium (III) ions alone only showed 0.4 ± 0.2 logs and 0.9 ± 0.2 logs of killing (p = 0.005), respectively (Figure 5). When the concentration of chromium (III) ions increased to 100 μM, the viability of planktonic cells was reduced by 6.1 ± 0.2 logs (p = 0.014) with concurrent treatment with 60 μA DC/cm^2. But the chromium (III) ions only exhibited 0.9 ± 0.3 logs of killing (Figure 6).

Similar results of synergetic effects between DC and chromium (III) ions were observed in concurrent treatment in the dual chamber system. For example, the number of viable *P. aeruginosa* planktonic cells was reduced by 2.8 ± 0.05 logs after concurrent treatment with 20 μA/cm^2 DC and 10 μM chromium (III) ions in the cathode chamber (p = 0.002). In comparison, concurrent

treatment with DC and chromium (III) in anode only showed a 1.0 ± 0.01 log of killing (Figure 7). Meanwhile, the planktonic cells in anode and cathode chamber were reduced by less than 0.1 logs, respectively.

5.4.5 The killing effects of DC on *S. aureus* planktonic cells in agarose gel

Multiple brown bands of precipitate were observed in the middle region of agarose gel between anode and cathode after DC treatment (Figure 8). The color and density of bands were found dependent on the duration of treatment. The precipitates could dissolve in the diluted hydrogen chloride solution. According to the Live/Dead staining images in Figure 9A&B, there were also several dark bands in *S. aureus* planktonic cells culture in the agarose gel. In these bands, the number of live (green) cells dramatically decreased to almost nothing while the dead (red) cells were more compared to surrounding areas (Figure 9C&D). Furthermore, the locations of dark bands and precipitate bands overlapped in the agarose gel. These precipitates didn't show the bactericidal effect on *S. aureus* cells in the absence of the electric field when mixed with planktonic cells and precipitates from the electrolysis solution after DC treatment (Figure 9E).

5.4.6 The enhanced affinity between RNA and tobramycin-chromium (III) complex

The samples with the mixture of 320 μM tobramycin and 320 μM Cr (III) had the lowest ratio of cleavage (4.2 ± 2.1, $p = 0.002$), and it raised to 9.3 ± 1.3 and 11.8 ± 3.7 when the concentrations of Cr (III) reduced to 160 μM and 32 μM, respectively. The sample with tobramycin alone had the ratio of 14.1 ± 1.7, and the three samples with Cr (III) alone (without tobramycin, concentration ranged from 320 μM to 32 μM) had a nearly constant ratio of cleavage (15.0 ± 3.2, 15.1 ± 1.0 and 15.2 ± 2.4). Apart from this, the cleavage ratio of the positive control was the highest (21 ± 3.3) and the negative control was zero (Figure 10&11).

5.5 Discussion

Hydrogen peroxide generation from both metal and nonmetal electrodes has been well studied. The killing effect of other electrolysis products from the electrode is still unknown. Compared to the results of stainless steel electrodes, our study shows that the graphite-based TGON electrodes may have a different killing mechanism against biofilm cells. We found the killing effect of TGON electrodes reduced dramatically when replacing 0.85% sodium chloride solution with 0.01% or 0.001% solution during treatment, which was consistent to the killing results of different concentrations of sodium hypochlorite in the absence of DC. This finding suggests that the hypochlorite may play an important role in killing bacterial cells with TGON conducted DC because electrolysis of saline solution can produce chlorine and hypochlorite by anode oxidation reaction in the presence of chloride ions. The killing effect of stainless steel electrodes wasn't affected by the concentration of chloride ions, which may result from different electrochemical products of metal electrodes during DC treatment. The stainless steel anode could release metal ions (Fe, Cr, Ni et al.) during the DC treatment due to the oxidation of anode metal, while the stainless steel cathode could reduce dissolved oxygen to produce hydrogen peroxide. When treated bacteria cells with stainless steel electrodes in a two-chamber system that could separate the anodic and cathodic electrolytic products [24], no significant killing effect was observed. This supports our hypothesis that the killing effect of DC conducted by steel electrodes results from the secondary products of reactions between electrochemical products of anode and cathode. Interestingly, hydrogen peroxide also did not show the significant killing effect on biofilm cells in our research even with a high concentration of 200 mg/L. The measurable level of hydrogen peroxide ranged from 5 to 40 μM near the electrode surface during DC treatment. However, the concentration in

bulk solution decreased towards zero over distance [17]. This helps explain our finding because the biofilm samples were approximate 2-3 mm away from both anode and cathode in the treatment facility.

Chloride is the most abundant anion in humans and an essential element for maintaining cell homeostasis and transmitting action potentials [25]. It is also required for the immune response mediated by phagocytes and neutrophils [26]. In the 1960s, the antivirus activity of 150 mmol sodium chloride against mengovirus was reported based on treatment at 37 °C for 2 hours [27]. Similar killing effects were also seen with other chloride compounds, such as potassium chloride, magnesium chloride. This suggests that the biocidal effects to the microorganism of chloride compounds came from chlorite anion, not cations. Recently Ramalingam et al. [27] reported that the viral inhibition was not from sodium chloride directly when treated virus with epithelial, fibroblast and hepatic cells although the increasing concentration of sodium chloride promoted the effects. Adding myeloperoxidase inhibitor could reverse the inhibition, which showed that chloride anions could be converted to other forms of molecules during inhibition procedure. Wang [26] found that chloride anions could be converted to hypochlorous acid by myeloperoxidase (MPO) in phagosomes. This reaction needs hydrogen peroxide as the reactant. Both hydrogen peroxide and hypochlorite have antimicrobial activities as oxidants that target electron transport chain, DNA replication, adenine nucleotides, metabolic enzymes and unsaturated fatty acids in cells' membranes [28]. Hypochlorous acid has even more potent effects. Chensey et al. [28] showed that hypochlorous acid had 500 to 1,000 folds higher toxicity to *E. coli* cells than hydrogen peroxide. In our study, the treatment of *P. aeruginosa* biofilms with hydrogen peroxide and hypochlorite showed dosage-dependent killing effects, although the minimal biofilm killing concentration of hypochlorite was much lower than hydrogen peroxide. As mentioned in Chapter 2, the major electrochemical products with

possible biocidal effect during DC treatment using TGON electrodes were hypochlorous acid and hydrogen peroxide. Reducing the concentration of sodium chloride in the electrolyte solution can reduce the generation of hypochlorous acid. According to the result, we found decreasing killing effect in DC treatment with the same current level conducted by TGON electrodes. All of these findings suggest that the hypochlorous acid generated by TGON anode is the primary bactericidal agent during DC treatment using TGON electrodes.

The bactericidal mechanism of DC treatment using stainless steel electrodes is more complex than TGON since there are more electrochemical reactions involved. Because steel is not a corrosion resistant material, the anode itself is easily oxidized and metal ions are released when applied with positive potential. Appropriate metal ions are essential elements required for cell metabolism; however, an excess amount of metal ions could also be toxic to bacterial cells, since they could interfere with normal metabolic process by improper metalation of metalloproteins with the unwanted metal [29]. Besides, the negative-charged bacterial membrane has high affinity to those metal cations. Although binding to metal cations on the membrane may not directly kill cells, these ions alter the normal net charge across the cell membrane and interfere the membrane functions [30]. Based on our test, treating biofilm cells with metal ions (such as chromium (III)) alone only showed a slight reduction in cell viability. This suggests that other more potent biocidal agents may exist during DC treatment, or the movement of ions may be essential for DC-mediated killing. Hydrogen peroxide is produced during DC treatment despite stainless steel or TGON electrodes, but it couldn't eradicate biofilm effectively if the concentration was lower than 100 mg/L, which is much higher than the concentration (5 – 40 μM) measured in hydrolysis process with 40 $\mu A/cm^2$ DC [17]. However, if metal ions and hydrogen peroxide are mixed, they could induce the Fenton reaction that could produce free radicals, such as hydroxyl and carboxylic radicals. These free

radicals are powerful oxidant with the ability to mineralize most organics, which could kill bacterial cells quickly by disrupting cell membrane and causing cell lysis [13]. Anfruns-Estrada et al. [15] had reported that by treating with 20 mA/cm^2 in a cylindrical tank reactor in presence of 0.25 mM $FeSO_4$, the viability of *E. coli* cells in wastewater could be reduced by 5 logs. They contributed the killing effect to the electro-Fenton reaction that occurred between added ferric ions and hydrogen peroxide produced by the electrodes. In our study, DC treatment can also generate metal ions and hydrogen peroxide from anode and cathode, respectively. When contacting with each other in the solution, the Fenton's reaction could occur. Although it's difficult to detect Fenton reaction products directly due to a short life and rapid reactions of these species, we obtained indirect evidence supporting the presence of Fenton reaction. For example, DC treatment with the dual chamber system using stainless steel electrodes didn't show the significant killing effect on bacterial cells. The products of anode and cathode in the dual chamber system are still the same as the single chamber, but they are isolated in different chambers and can't contact each other to initiate Fenton reaction. And neither metal ions nor hydrogen peroxide is a potent biocidal agent alone against biofilms. As a result, the killing effect decreased in the dual chamber system. Moreover, when we replaced 0.85% sodium chloride electrolyte solution with 0.85% sodium chloride agar, we observed be a precipitate band in the middle region of agar between anode and cathode after DC treatment. We speculated this resulted from the diffusion of anode and cathode products. Once they meet each other in the middle region of agarose, the Fenton reaction occurred and left precipitate products trapped in the agarose. Interestingly, if the planktonic cells were added into ager and carried on the same treatment, a dark zone without any live cells was seen at the same location with the precipitate band in the agar. This region may have Fenton reaction during

DC treatment so that the bacterial cells in the same location were effectively killed by free radicals immediately after being produced.

Another interesting finding was the killing effects of chromium (III) ions in the presence of DC. The stainless steel contains approximately 16-18 % of chromium. The chromium is the essential element to protect steel from corrosion since it could be oxidized earlier than ferric ions and form a protective coating on the steel surface. Hence, chromium ions should be produced earlier than ferric during DC treatment. Chromium (III) is also a well-known nutrient element for human, which is essential for insulin synthesis. However, chromium (III) is toxic to bacteria cells. Fathima et al. [31] reported chromium (III) could damage cell membrane and DNA by generating ROS, although we didn't find the significant biocidal effect when mixed chromium (III) with planktonic cells. Chromium could induce a Fenton-like reaction in presence of hydrogen peroxide [32] and produce hydroxyl radicals. Our study shows the evidence that Fenton-like reaction may happen during DC treatment. If we added chromium into the electrolyte solution, the significant increase in the killing effect was observed, which suggests that there should be a large number of bactericidal agents produced in the solution. Besides, when the anode and cathode chamber were separated, adding chromium only increased the killing effects in the cathode chamber. All of these findings support the existence of the Fenton-like reaction induced by chromium (III) during DC treatment, and it may have a significant role in the bactericidal effect of DC treatment using stainless steel electrodes.

Like hydrogen peroxide, hypochlorite can react with ferric ions to produce hydroxyl and chlorine radicals [33]. These products from Fenton-like reaction may also contribute to the killing effect of hypochlorite from the DC treatment. Furthermore, the concentration of intercellular labile iron in

mammalian cells (1μM) [34] are 10 – 100 times lower than bacterial cells (10 - 100 μM) [35, 36], which could promote the selectivity of the DC treatment to biofilm cell over host mammalian cells.

Our results showed that Chromium not only kills bacterial cells by itself in presence of DC but also form the complex with antibiotic and increase the affinity to target molecules. Compared to tobramycin alone, a lower cleavage ratio of the reaction was observed when combining chromium (III) with tobramycin. This effect was also related to the molar ratio of tobramycin to chromium (III). The samples with the mixtures of tobramycin and chromium (III) at 1:1 ratio had the lowest cleavage ratio, which increased to 2:1 and 10:1. This is consistent with our previous finding that the chromium (III) (tobramycin) complex was more stable when tobramycin and chromium (III) were mixed at 1:1 ratio. The cleavage ratios of chromium (III) alone were slightly higher than tobramycin alone and did not show any obvious changes despite the concentration of chromium (III). This suggested that chromium (III) had a potential inhibitory effect since it can also bind to RNA molecules by Coulomb force, and then interfere with the interaction between ribozymes and substrate RNAs. Generally, chromium (III) had an enchanting effect for tobramycin at 1:1 mole ratio in hammerhead ribozyme cleavage reaction, which could reduce the ratio of cleavage to 25% of the positive control. Chromium (III) alone also showed the inhibitory effect in the reaction, which was slightly weaker than tobramycin alone. The concentration of tobramycin and chromium (III) were 10 to 100 folds higher than the amount used in our previous studies [12, 13]. These concentrations were also used in other research with hammerhead ribozyme-catalyzed cleavage systems, which suggests that higher concentration of antimicrobial agents is necessary to obtain "observable" results.

5.6 Conclusion

In summary, we tested the killing effect of different treatment conditions to *P. aeruginosa* cells and explored the affinity of tobramycin-chromium (III) complex to RNA molecules in this study. According to the results, we found that the bactericidal effect came from the hypochlorous acid generated when using TGON electrodes during DC treatment, while stainless steel electrodes generate the free radicals as Fenton reaction products between metal ions and hydrogen peroxide to eradicate biofilm cells. Moreover, chromium ions may play the more important role than ferric ions during DC treatment since it only initiates Fenton reaction with hydrogen peroxide but also forms a complex with some antibiotic molecules and enhance its affinity to the target, e.g. RNA. These findings provide more information for designing better devices in the future.

5.7 Reference

1. Beattie, J.M. & Lewis, F.C. The Electric Current (apart from the Heat Generated): A Bateriological Agent in the Sterilization of Milk and other Fluids. *J Hyg (Lond)* **24**, 123-137 (1925).
2. ROSENBERG, B., VANCAMP, L. & KRIGAS, T. INHIBITION OF CELL DIVISION IN ESCHERICHIA COLI BY ELECTROLYSIS PRODUCTS FROM A PLATINUM ELECTRODE. *Nature* **205**, 698-699 (1965).
3. Pareilleux, A. & Sicard, N. Lethal effects of electric current on Escherichia coli. *Appl Microbiol* **19**, 421-424 (1970).
4. Rowley, B.A. Electrical Current Effects on E. coil Growth Rates. *Experimental Biology and Medicine* **139** (1972).
5. Barranco, S.D., Spadaro, J.A., Berger, T.J. & Becker, R.O. In vitro effect of weak direct current on Staphylococcus aureus. *Clin Orthop Relat Res*, 250-255 (1974).
6. Canty, M., Luke-Marshall, N., Campagnari, A. & Ehrensberger, M. Cathodic voltage-controlled electrical stimulation of titanium for prevention of methicillin-resistant Staphylococcus aureus and Acinetobacter baumannii biofilm infections. *Acta Biomater* **48**, 451-460 (2017).
7. Ehrensberger, M.T. et al. Cathodic voltage-controlled electrical stimulation of titanium implants as treatment for methicillin-resistant Staphylococcus aureus periprosthetic infections. *Biomaterials* **41**, 97-105 (2015).
8. Caubet, R. et al. A radio frequency electric current enhances antibiotic efficacy against bacterial biofilms. *Antimicrob Agents Chemother* **48**, 4662-4664 (2004).

9. Costerton, J.W., Ellis, B., Lam, K., Johnson, F. & Khoury, A.E. Mechanism of electrical enhancement of efficacy of antibiotics in killing biofilm bacteria. *Antimicrobial Agents and Chemotherapy* **38**, 2803-2809 (1994).

10. Edebo, L. & Selin, I. The effect of the pressure shock wave and some electrical quantities in the microbicidal effect of transient electric arcs in aqueous systems. *J Gen Microbiol* **50**, 253-259 (1968).

11. Aronsson, K., Rönner, U. & Borch, E. Inactivation of Escherichia coli, Listeria innocua and Saccharomyces cerevisiae in relation to membrane permeabilization and subsequent leakage of intracellular compounds due to pulsed electric field processing. *Int J Food Microbiol* **99**, 19-32 (2005).

12. Niepa, T.H., Gilbert, J.L. & Ren, D. Controlling Pseudomonas aeruginosa persister cells by weak electrochemical currents and synergistic effects with tobramycin. *Biomaterials* **33**, 7356-7365 (2012).

13. Niepa, T.H. et al. Sensitizing Pseudomonas aeruginosa to antibiotics by electrochemical disruption of membrane functions. *Biomaterials* **74**, 267-279 (2016).

14. Kalbacova, M. et al. The effect of electrochemically simulated titanium cathodic corrosion products on ROS production and metabolic activity of osteoblasts and monocytes/macrophages. *Biomaterials* **28**, 3263-3272 (2007).

15. Anfruns-Estrada, E. et al. Inactivation of microbiota from urban wastewater by single and sequential electrocoagulation and electro-Fenton treatments. *Water Res* **126**, 450-459 (2017).

16. Samoĭlenko, I.I., Vasil'eva, E.I., Pavlova, I.B. & Tumanian, M.A. [Mechanisms of the bactericidal action of hydrogen peroxide]. *Zh Mikrobiol Epidemiol Immunobiol*, 30-33 (1983).

17. Sultana, S.T. et al. Electrochemical scaffold generates localized, low concentration of hydrogen peroxide that inhibits bacterial pathogens and biofilms. *Sci Rep* **5**, 14908 (2015).

18. Drogui, P., Elmaleh, S., Rumeau, M., Bernard, C. & Rambaud, A. Oxidising and disinfecting by hydrogen peroxide produced in a two-electrode cell. *Water Res* **35**, 3235-3241 (2001).

19. Sahrmann, P. et al. Effect of low direct current on anaerobic multispecies biofilm adhering to a titanium implant surface. *Clin Implant Dent Relat Res* **16**, 552-556 (2014).

20. Fukuzaki, S. Mechanisms of actions of sodium hypochlorite in cleaning and disinfection processes. *Biocontrol Sci* **11**, 147-157 (2006).

21. Yang, G., Trylska, J., Tor, Y. & McCammon, J.A. Binding of aminoglycosidic antibiotics to the oligonucleotide A-site model and 30S ribosomal subunit: Poisson-Boltzmann model, thermal denaturation, and fluorescence studies. *J Med Chem* **49**, 5478-5490 (2006).

22. Stage, T.K., Hertel, K.J. & Uhlenbeck, O.C. Inhibition of the hammerhead ribozyme by neomycin. *RNA* **1**, 95-101 (1995).

23. Chow, C.S., Somne, Smita & Llano-Sotelo, B. Monitoring Hammerhead Ribozyme-Catalyzed Cleavage with a Fluorescein-Labeled Substrate: Effects of Magnesium Ions and Antibiotic Inhibitors. A Biochemistry Laboratory: Part 2. *J. Chem. Educ.* **76**, 651 (1999).

24. Niepa, T.H.R., Wang, H., Gilbert, J.L. & Ren, D. Eradication of Pseudomonas aeruginosa cells by cathodic electrochemical currents delivered with graphite electrodes. *Acta Biomater* **50**, 344-352 (2017).

25. Jentsch, T.J., Stein, V., Weinreich, F. & Zdebik, A.A. Molecular structure and physiological function of chloride channels. *Physiol Rev* **82**, 503-568 (2002).

26. Wang, G. Chloride flux in phagocytes. *Immunol Rev* **273**, 219-231 (2016).

27. Ramalingam, S. et al. Antiviral innate immune response in non-myeloid cells is augmented by chloride ions via an increase in intracellular hypochlorous acid levels. *Sci Rep* **8**, 13630 (2018).

28. Chesney, J.A., Eaton, J.W. & Mahoney, J.R. Bacterial glutathione: a sacrificial defense against chlorine compounds. *J Bacteriol* **178**, 2131-2135 (1996).

29. Capdevila, D.A., Edmonds, K.A. & Giedroc, D.P. Metallochaperones and metalloregulation in bacteria. *Essays Biochem* **61**, 177-200 (2017).

30. Urrutia Mera, M., Kemper, M., Doyle, R. & Beveridge, T.J. The membrane-induced proton motive force influences the metal binding ability of Bacillus subtilis cell walls. *Appl Environ Microbiol* **58**, 3837-3844 (1992).

31. Fathima, A. & Rao, J.R. Is Cr(III) toxic to bacteria: toxicity studies using Bacillus subtilis and Escherichia coli as model organism. *Arch Microbiol* **200**, 453-462 (2018).

32. Luo, H., Lu, Y., Shi, X., Mao, Y. & Dalal, N.S. Chromium (IV)-mediated fenton-like reaction causes DNA damage: implication to genotoxicity of chromate. *Ann Clin Lab Sci* **26**, 185-191 (1996).

33. Folkes, L.K., Candeias, L.P. & Wardman, P. Kinetics and mechanisms of hypochlorous acid reactions. *Arch Biochem Biophys* **323**, 120-126 (1995).

34. Kakhlon, O. & Cabantchik, Z.I. The labile iron pool: characterization, measurement, and participation in cellular processes(1). *Free Radic Biol Med* **33**, 1037-1046 (2002).

35. Yan, Y., Waite-Cusic, J.G., Kuppusamy, P. & Yousef, A.E. Intracellular free iron and its potential role in ultrahigh-pressure-induced inactivation of Escherichia coli. *Appl Environ Microbiol* **79**, 722-724 (2013).

36. Yamamoto, Y. et al. Regulation of the intracellular free iron pool by Dpr provides oxygen tolerance to Streptococcus mutans. *J Bacteriol* **186**, 5997-6002 (2004).

5.8 Figures

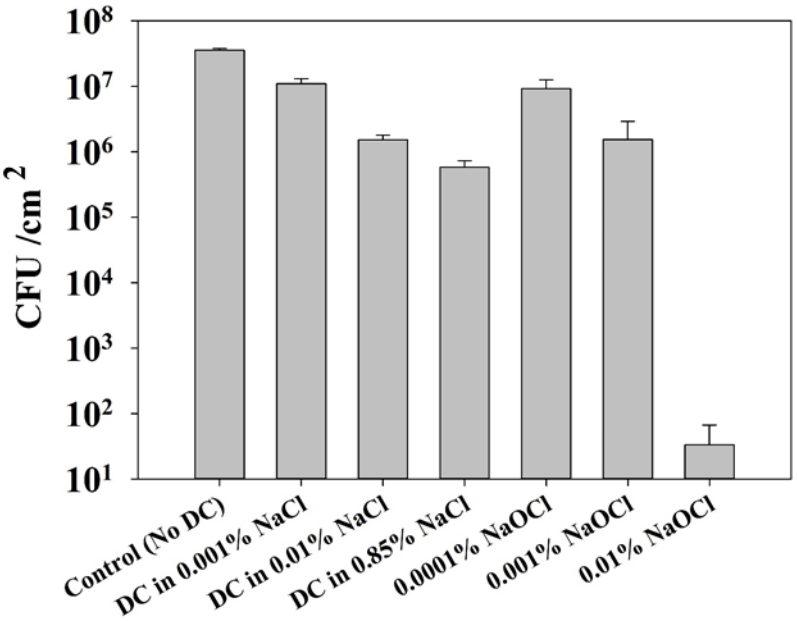

Figure 1. Viability of *P. aeruginosa* biofilm cells after treatment in saline solutions with different concentrations of NaCl (with 30 µA/cm^2 DC, TGON electrodes) and NaOCl solution (without DC).

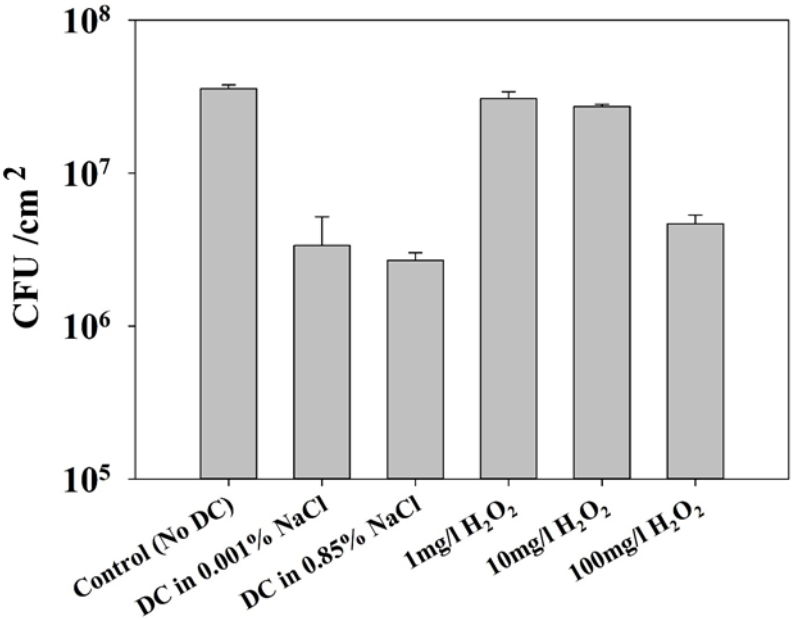

Figure 2. Viability of *P. aeruginosa* biofilm cells after treatment in saline solutions with different concentrations of NaCl (with 30 µA/cm^2 DC, TGON electrodes) and H_2O_2 solution (without DC).

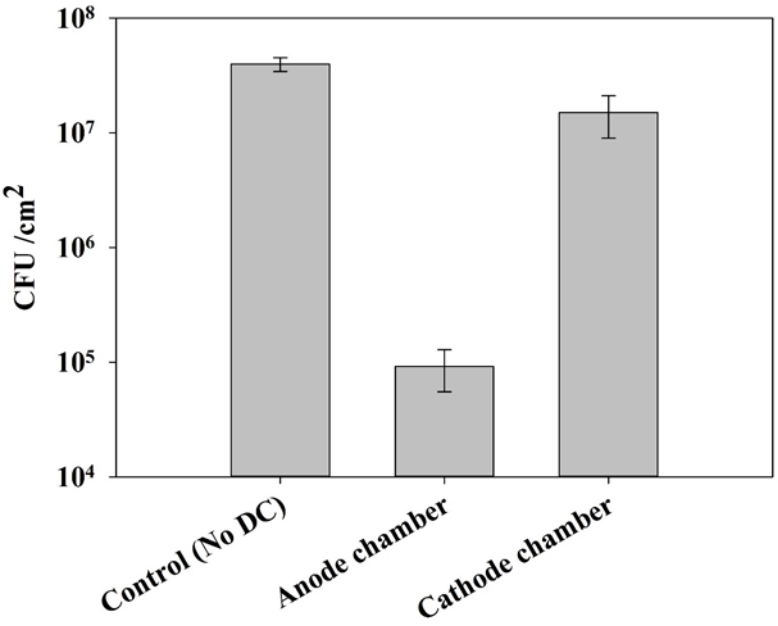

Figure 3. Viability of *P. aeruginosa* biofilm cells after treatment with 30 µA/cm^2 DC in 0.85 % NaCl solution in dual chamber system with TGON electrodes.

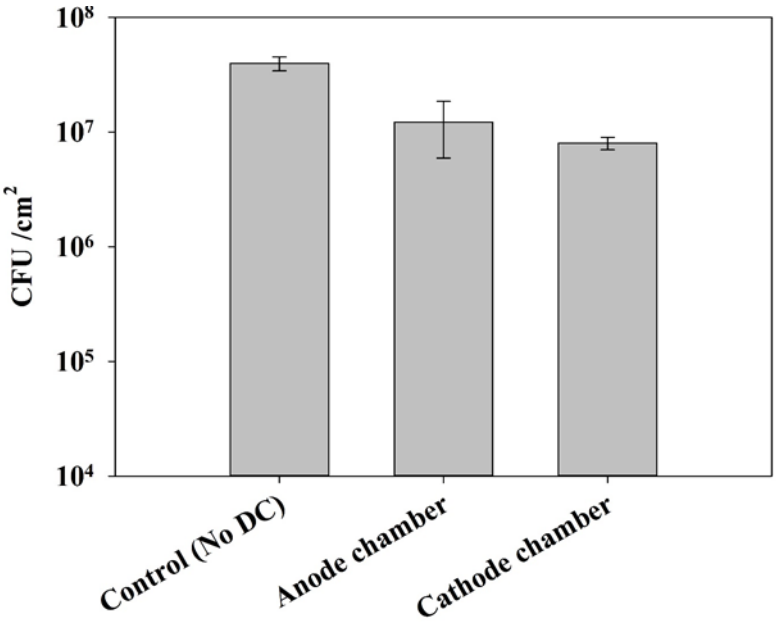

Figure 4. Viability of *P. aeruginosa* biofilm cells after treatment with 30 µA/cm^2 DC in 0.85 % NaCl solution in dual chamber system with stainless steel electrodes.

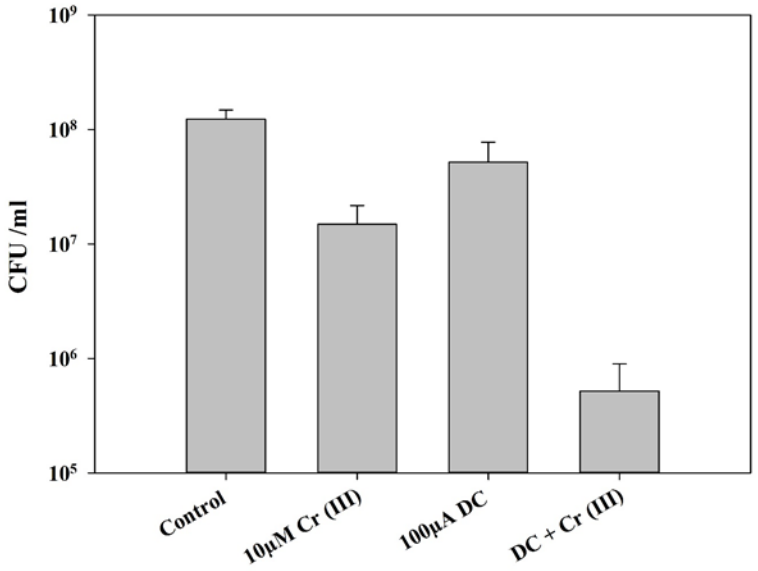

Figure 5. Viability of P. aeruginosa planktonic cells after treatment with Cr (III) alone (10 μM), DC (60 μA/cm^2) alone or concurrent treatment for 1 h in 0.001% NaCl solution

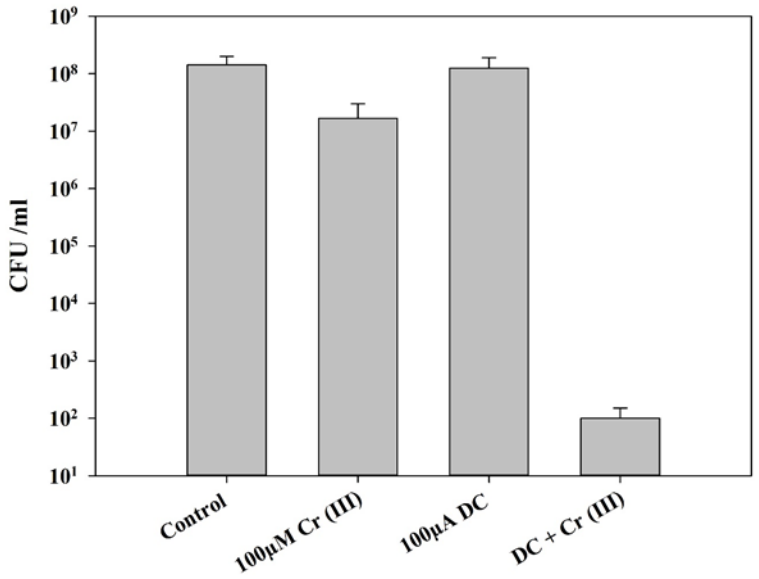

Figure 6. Viability of *P. aeruginosa* planktonic cells after treatment with Cr (III) alone (100 μM), DC (60 μA/cm^2) alone or concurrent treatment for 1 h in 0.001% NaCl solution.

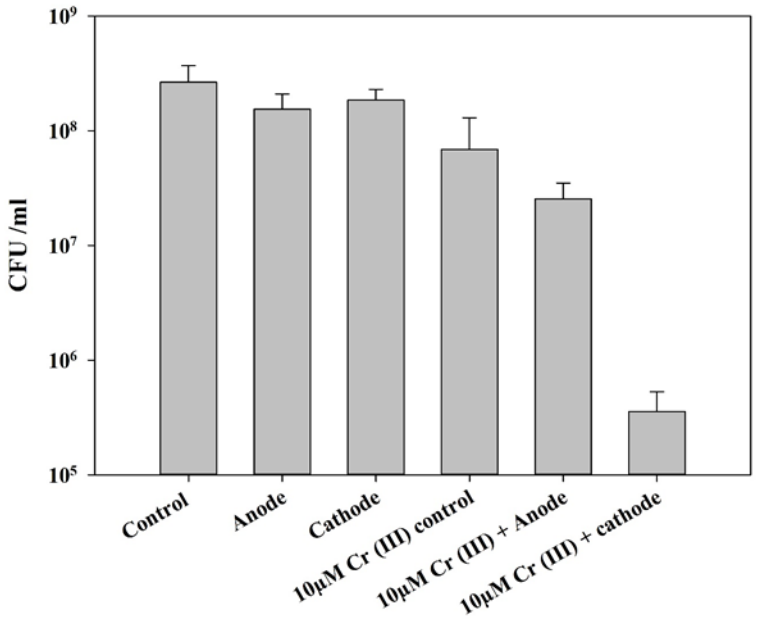

Figure 7. Viability of *P. aeruginosa* planktonic cells after treatment with Cr (III) alone (10 µM), DC (20 µA/cm^2) alone or concurrent treatment for 1 h in 0.1 % NaCl solution in dual chamber system.

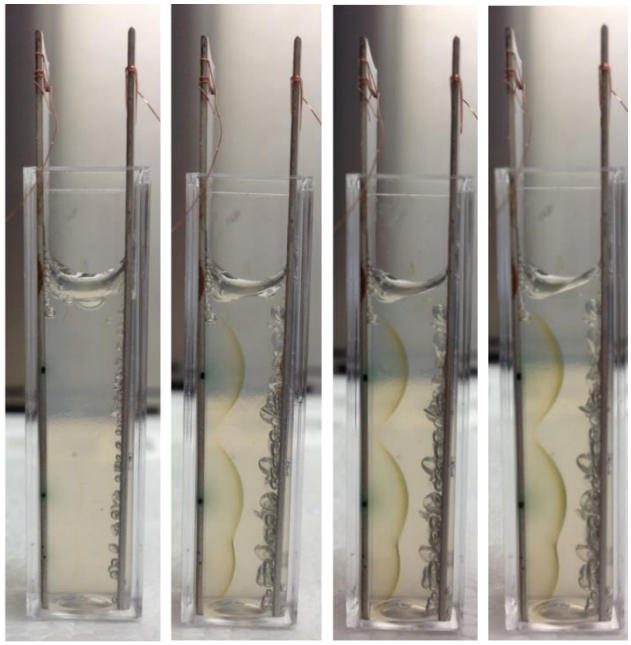

Figure 8. Representative images of agarose gel with embedded *S. aureus* planktonic cells after being treated with 60 µA/cm^2 DC for varying duration of time.

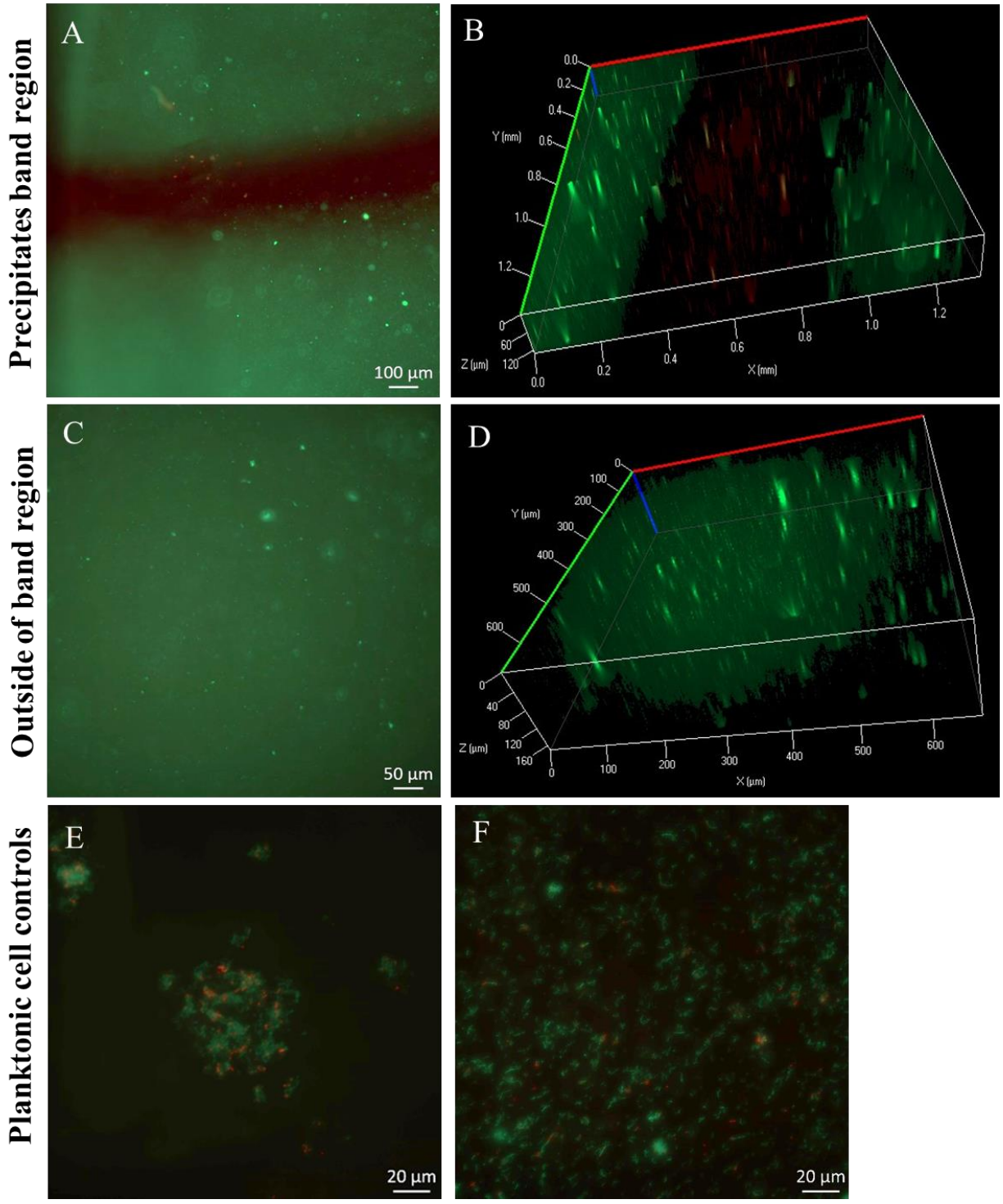

Figure 9. Living/Dead images of *S. aureus* planktonic cells in the agarose after DC treatment. (A)&(B): The cells in the precipitation band region. (C)&(D): The cells outside of the precipitation band region. (E): The untreated planktonic cells mixed with the precipitates produced by DC treatment. (F): The untreated planktonic cells.

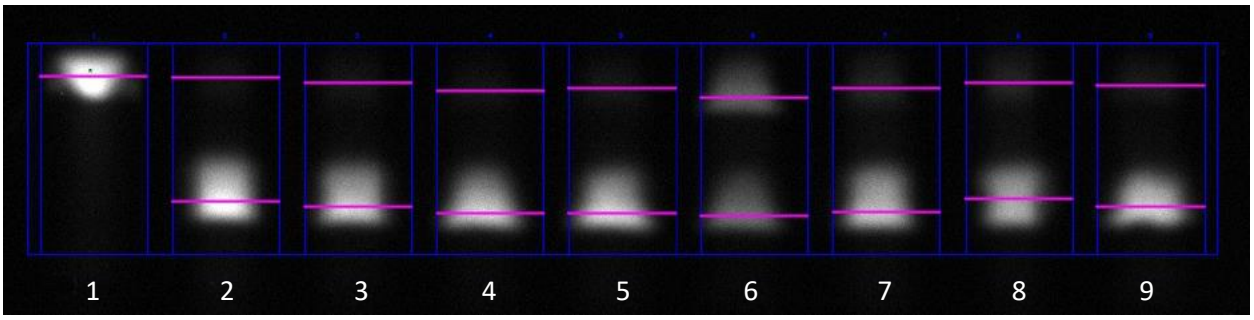

Figure 10. Cleavage of substrate RNA by the hammerhead ribozyme. Only the fluorescently labeled RNA was visible. The upper bands were un-cleavage substrates and lower bands were cleavage products. From left: 1) Negative control (reference band); 2) Positive control; 3-5) Cr^{3+} alone (320 µM, 160 µM, 32 µM); 6-8) Mixture of Cr^{3+} and tobramycin (Cr^{3+}: 320 µM, 160 µM, 32 µM, Tobramycin: 320 µM); 9) Tobramycin alone (320 µM).

This figure has been published in Acta Biomaterialia. Volume 36, May 2016, Pages 286-295.

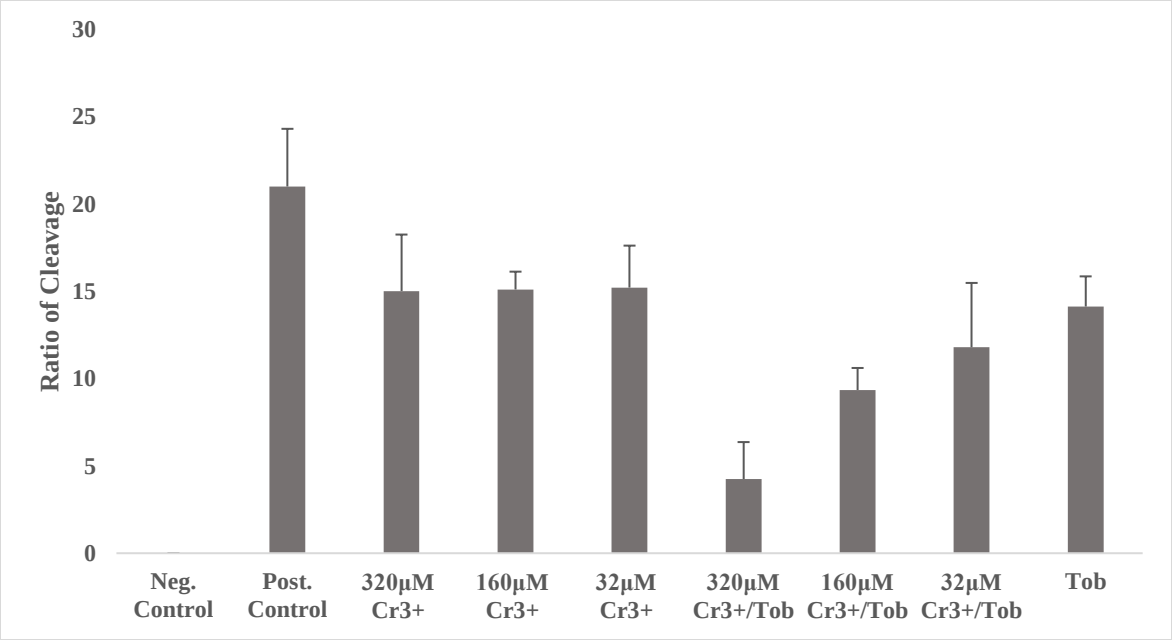

Figure 11. The ratio of cleavage in samples of negative control, positive control, Cr^{3+} alone (320 µM, 160 µM and 32 µM), a mixture of Cr^{3+} (320 µM, 160 µM and 32 µM) & tobramycin (320 µM) and tobramycin alone (320 µM).

This figure has been published in Acta Biomaterialia. Volume 36, May 2016, Pages 286-295.

Chapter 6

Controlling dental plaque with direct current and chlorhexidine

This work has been published in **AMB EXPRESS**. 7 pp 204 (2017)

6.1 Abstract

Microbial biofilms formed on biomaterials are major causes of chronic infections. Among them, Gram-positive bacteria *Streptococcus mutans* and *Staphylococcus aureus* are important pathogens causing infections associated with dental caries (tooth decay) and other medical implants. Unfortunately, current antimicrobial approaches are ineffective in disrupting established biofilms and new methods are needed to improve the efficacy. In this study, we report that the biofilm cells of *S. mutans* and *S. aureus* can be effectively killed by low-level direct current (DC) and through synergy in concurrent treatment with DC and chlorhexidine (CHX) at low concentrations. For example, after treatment with 28 μA/cm^2 DC and 50 μg/mL CHX for 1 h, the viability of biofilm cells was reduced by approximately 4 and 5 logs for *S. mutans* and *S. aureus*, respectively. These results are useful for developing more effective approaches to control pathogenic biofilms.

6.2 Introduction

Biofilms are characterized by microbial cells embedded in a matrix comprised of extracellular polymeric substance (EPS) containing polysaccharide, proteins, and DNA. The presence of this extracellular matrix provides protection to microbial pathogens from certain antimicrobials and host immune cells/factors [1, 2]. Biofilms can form on both biotic and abiotic surfaces and are common causes of chronic infections on implant devices. The protection of EPS plus the dormancy of biofilm cells render these multicellular structures extremely difficult to eradicate [3-5].

In the previous chapters, we have demonstrated the wireless delivered electric current (DC) could eradicate pathogen biofilm on polysiloxane surface *in vitro* and *ex vivo*, which provides a new approach to control biofilm-associated infection for electronic medical implants, such as cochlear device, pacemaker, brain stimulator, et al. As mentioned in Chapter 2, the dental biofilm or dental plaque) is another serious and common biofilm-associated infections that has bothered people for thousand years. In this chapter, we investigated if we could also reduce the viability of oral pathogenic biofilm cells on denture materials with a similar level of DC. The substrate for biofilm growth in this study was acrylate that is very common denture materials and suitable adhesive surface for dental pathogens.

Streptococcus mutans is a Gram-positive bacterium commonly found in human dental biofilms. It is a dominant species with higher biomass in dental biofilms than other *Streptococcus* species, including *S. sanguinis, S. mitis,* and *S. salivarius,* due to its acid tolerance and thus the capability to live in low pH environment of oral cavities [6-9]. *S. mutans* expresses multiple exoenzymes (glucosyltransferases) that make it the primary EPS producer in oral cavity [9], while it is also highly acidogenic and aciduric. *S. mutans* can rapidly colonize tooth surface and establish cariogenic

biofilms with EPS. This acidifies the local microenvironment and promotes the growth of an acidogenic microbiota, facilitating the development of dental caries [9, 10].

Staphylococcus aureus is also an abundant Gram-positive bacterium, which usually harbors in the nasal passages and ears of patients [4]. Previous studies have shown that *S. aureus* is not only the significant cause of many localized and systemic infections such as osteomyelitis [11], chronic wound infection [12], and chronic rhinosinusitis [13] but also has a strong connection to dental implant infections [14, 15]. The established biofilms of *S. aureus*, especially the methicillin-resistant *S. aureus* (MRSA), are highly tolerant to common antimicrobial treatments [16-18].

Few approaches are currently available for controlling cariogenic biofilms [1]. Chlorhexidine (CHX) is considered the "gold standard" for oral antimicrobial therapy [19]. However, use of high dose CHX has adverse side effects such as tooth staining and calculus formation. Also, CHX is not recommended for long-term daily therapeutic use [20]. In 1994, Costerton et al. (1994) reported bacterial killing by synergistic effects between low-level electric currents and antibiotics, a phenomenon named "bioelectric effects". Since 1990s, direct currents (DCs) ranging from μA to mA were reported for their bactericidal effects after a relatively long period (from several hours to days) of treatment [21-24] either by DC alone or with antibiotics together [25-28]. Recent studies reported the mA level DC could enhance the killing effect of 0.2% (200 μg/mL) chlorhexidine on biofilms of Gram-negative *Porphyromonas gingivalis* [29] though there was no bactericidal effect by DC alone. To explore the potential of lower levels of DC and CHX in killing dental biofilms of Gram-positive bacteria, we conducted this study with using *S. mutans* and *S. aureus* as model species. We demonstrate that stainless steel electrode derived DC and CHX have strong synergy in killing *S. mutans* and *S. aureus* biofilms, and the levels of DC and CHX are lower than other reported systems.

6.3 Materials and methods

6.3.1 Bacteria strains and growth media

S. mutans Clarke strain (ATCC 25175) was cultured in brain heart infusion (BHI) broth (ATCC medium 44). The *S. aureus* ALC2085 (strain RN6390 containing pALC2084) was obtained from the Sauer lab at Binghamton University and cultured in Luria-Bertani (LB) medium [26] containing 10 g/L tryptone, 5 g/L Yeast extract and 10 g/L NaCl, supplemented with 10 µg/mL chloramphenicol (Sigma-Aldrich, St. Louis, MO, U.S.) [30]. Both strains were routinely cultured overnight at 37 °C with shaking at 200 rpm.

6.3.2 Biofilm formation

Biofilms were formed on acrylic coupons (3.5 cm x 0.5 cm x 0.1 cm; McMaster-Carr, Aurora, OH, U.S.). Briefly, 25 µL of an overnight culture of *S. mutans* was used to inoculate a petri dish containing 25 mL of BHI medium and acrylic coupons. The culture was incubated at 37°C for 48 h without shaking. Then the coupons with biofilms were removed from petri dish and washed gently with 0.85% NaCl solution for treatment. The *S. aureus* biofilm samples were prepared in the same way except that the medium was LB plus 10 µg/mL chloramphenicol and the incubation time was reduced to 24 h due to a higher growth rate of *S. aureus*.

6.3.3 Electrochemical treatment

The experimental system for DC treatment was the same as we described previously (Niepa, et al. 2012; Niepa, et al. 2016). Briefly, an electrochemical cell was constructed with two electrodes on the opposite sides of a plastic cuvette (Thermo Fisher Scientific, Pittsburg, PA, U.S.). DC was generated using a potentiostat (Potentiostat WaveNow, Pine Research Instrumentation, Raleigh, NC, U.S.) in the three electrodes' configuration system with a silver wire (0.015" diameter, A-M

Systems, Sequim, WA, U.S.) placed in bleach for 30 min to create Ag/AgCl reference electrode. The DC level and voltage across the electric field were monitored and recorded using the AfterMath software (Potentiostat WaveNow, Pine Research Instrumentation, Raleigh, NC, U.S.) in the galvanostatic mode during the treatment.

6.3.4 DC treatment of biofilms

Each DC treatment was carried out in 3 mL 0.85% NaCl solution. First, one sterile SS304 electrode (3.5 cm x 0.95 cm x 0.05 cm) was inserted into a cuvette, followed by an acrylic coupon with *S. mutans* or *S. aureus* biofilm attached. Another sterile SS304 electrode was then inserted on the opposite side. The biofilm was treated galvanostatically with direct current (DC) for 1 h in the absence or presence of CHX (MP Biomedicals, Solon, OH, U.S.). Samples treated with DC or CHX alone and untreated samples were used as controls. After treatment, each acrylic coupon was transferred to a 10 mL tube containing 5 mL 0.85% NaCl solution. The biofilm cells were removed from the surface by sonication for 1 min. The number of viable cells detached from acrylic coupons was quantified by counting colony forming units (CFUs) in the solution.

To evaluate the effects in an environment similar to that of oral cavity, the test medium was replaced with artificial saliva medium or a mixture of 0.85% NaCl and artificial saliva medium (2:1). The recipe for artificial saliva from Pratten et al. (1998) was followed. It contains 2 g/L yeast extract, 5 g/L peptone, 2.5g/L type III hog gastric mucin, 0.2g/L NaCl, 0.2 g/L KCl and 0.3 g/L $CaCl_2$, supplemental with 1.25 mL of sterile 40% urea. The CHX was tested at 50 µg/mL to 500 µg/mL. The treatment process was the same as described above for NaCl solution.

6.3.5 Live/Dead staining

To corroborate the CFU results, another set of acrylic coupons with biofilms treated with DC and CHX in the same way were stained with Live/Dead staining kit (Life Technologies Inc., Carlsbad, CA, U.S.) for 10 min. Then the biofilm samples were imaged using a fluorescence microscope (Axio Imager M1, Carl Zeiss Inc., Berlin, Germany).

6.3.6 Statistical analysis

Statistical significance was assessed with two-way ANOVA followed by Tukey test. Statistical significance was set as $p < 0.05$. All the analyses were performed using SAS 9.4 software (SAS Institute, Cary, NC, USA).

6.4 Results

6.4.1 Effects of DC and CHX on *S. mutans* and *S. aureus* biofilms in 0.85% NaCl solution

As shown in Figure 1, treatment with either CHX (at 5, 10, 20 and 50 μg/mL, Figure 1 A) or DC (at 7, 14 and 28 μA/cm^2, Figure 1 B) showed moderate but significant killing. For example, up to 1.2 logs and 0.7 logs of killing was obtained with 28 μA/cm^2 DC and 50 μg/mL CHX, respectively. In comparison, synergy was observed between DC and CHX in killing *S. mutans* biofilms dose-dependently. Among the tested conditions, the maximum killing effect (4 logs) was observed under the condition of 28 μA/cm^2 DC and 50 μg/mL CHX (Figure 1 C & 2 A, $p = 0.02$, two-way ANOVA with Tukey test).

Similar synergistic effects were also observed for *S. aureus* biofilms under the same treatment conditions. The number of viable *S. aureus* biofilm cells was reduced by more than 5 logs (Figure

3 A, $p<0.0001$, two-way ANOVA with Tukey test) after treatment with 28 μA/cm^2 DC and 50 μg/mL CHX for 1 h in 0.85% NaCl solution. In comparison, treatment with the same level of DC or CHX alone only reduced the number of viable biofilm cells by 60.0 ± 7.9% and 74.3 ± 2.5% (less than 1 log for both conditions), respectively.

The CFU results were corroborated with fluorescence microscopy. According to the images from Live/Dead staining of *S. mutans* and *S. aureus* biofilms, the number of live cells (green) decreased when treated with DC and CHX even at low doses (7 μA/cm^2 DC and 5 μg/mL CHX for *S. mutans*, 28 μA/cm^2 DC and 20 μg/mL CHX for *S. aureus*); and almost no live cells (only dead cells show) were found on the surface of acrylic coupons after concurrent treatment with DC and CHX together (Figure 4 & 5). Compared with sample treated with DC alone, samples treated with both CHX and DC concurrently only have patches of cell debris in red, suggesting that substantial cell lysis might have occurred.

6.4.2 Effects in the presence of artificial saliva

Since the dental surfaces are commonly covered with saliva, we also tested the effects of DC and CHX in the presence of artificial saliva. When artificial saliva was added to 0.85% NaCl solution as treatment medium, the killing effects were reduced but still significant. For example, the reduction of biofilm cell viability was 98.0 ± 0.4% (~1.7 log) when *S. aureus* biofilm was treated with 50 μg/ml CHX and 28 μA/cm^2 DC in a mixture of artificial saliva and 0.85 % NaCl solution (1:2 v/v) (Figure S2). No significant killing effect was observed when biofilms were treated in pure artificial saliva medium under the same dosage of CHX or DC level (data not shown). However, when the concentration of CHX increased to 500 μg/mL (0.05 w/v %, the dosage used in commercial oral rising products is 0.12 w/v %) while keeping the DC level at 28 μA/cm^2, the

number of viable *S. aureus* cells in biofilm was reduced by 2.5 logs compared to untreated control (Figure 3 B, $p = 0.005$, two-way ANOVA with Tukey test). The viability of biofilm cells treated with CHX alone was reduced by approximately 1 log and no significant killing effect was observed for 28 μA/cm^2 DC treatment alone (Figure 3 B). Similar results were observed for *S. mutans* biofilms (Figure 2 B and S1), although the killing of *S. mutans* biofilm cells in artificial saliva medium was lower than *S. aureus*. The number of viable cells was reduced by 0.54 log, 0.17 log, and 1.63 logs when treated with CHX alone, DC alone and concurrent treatment with CHX and DC, receptively (Figure 2 B, $p = 0.02$, two-way ANOVA with Tukey test).

6.5 Discussion

Direct currents (DC) and alternative currents (AC) are known to kill biofilm cells in the presence or absence of antibiotics, and treatment time-tested to date varies from hours to days [22-24]. Our group recently found synergetic effect between low-level DC and the antibiotic tobramycin in killing *Pseudomonas aeruginosa* biofilm and persister cells [26, 27]. However, most of the previous studies focus on biofilms formed on the surface of electrodes.

To mimic real application, it is important to test biofilms that are not in direct contact with electrodes. In this study, we set a sandwich structure with biofilms formed on acrylic coupons in the middle of the electric field and about 1.5 mm from each electrode. Our results show that the viability of *S. mutans* and *S. aureus* biofilm cells (placed in between two electrodes) on the surface of denture material can be reduced by low-level DC and CHX through concurrent treatment in 1 h; and the effect was approximately 1-3 logs stronger than that obtained with the same level of DC or CHX alone indicating synergistic effects between DC and CHX in killing biofilm cells of these

two dental bacteria. The effect was more profound in 0.85% NaCl solution than in the artificial saliva medium. The images of Live/Dead staining also confirmed that there was profound killing by concurrent treatment.

We speculated that this synergy primarily resulted from the interaction between the products of DC treatment and CHX. In a recent study, we showed that a large amount of hydrogen peroxide was generated from electrode surface during DC treatment [26], which had been reported for its synergetic antibacterial effect with CHX against *Streptococcus* and *Staphylococcus* species [31]. Furthermore, some metal ions (Zn^{2+}, Cu^{2+}) were shown for their capabilities to enhance the effect of CHX on different oral pathogens [31, 32]. The stainless-steel electrodes used in this study have a larger surface area and can release multiple types of metal ions including Fe^{2+}, Fe^{3+}, Cr^{2+}, Cr^{3+} and Cr^{6+} during DC treatment [26]. Fe^{2+} and Fe^{3+} ions were found to kill *P. aeruginosa* persister cells in the presence of antibiotics in an electric field [28]. We also found that Cr^{3+} and Cr^{6+} can form ion complex with antibiotic compounds, and thus increase the affinity between antibiotics and intracellular targets [28]. It is possible that some released ions interact with CHX molecules and result in the observed synergy in killing *S. mutan*s and *S. aureus*. This is also part of our ongoing study.

Recently, Lasserre et al. [29] reported that the viability of *P. gingivalis* biofilm could be reduced by 81.1% and 98.9% in 10 min when treated with 2000 μg/mL (0.2 w/v %) CHX alone and concurrent treatment with same dosage of CHX and 5882 μA/cm^2 DC, receptively; while the treatment with DC itself did not kill *P. gingivalis* cells. The biofilms were cultured on the discs of a Modified Robbins Device (MRD), which were placed between two electrodes of platinum wires in the MRD's chamber. This is an exciting discovery, but the DC level appears high and may not be suitable for *in vivo* therapy, especially for the implants closed to nervous systems that do not

tolerate more than a maximum current density of 30 μA/cm^2 [33-35]. Hence, it is necessary to reduce DC to μA level for future *in vivo* application. In this study, we treated *S. aureus* and *S. mutans* biofilm without direct contact to electrodes by placing the acrylic coupon in the middle of the low-level electric field and parallel to the electrode surfaces. By using stainless steel as electrode material, the level of DC and CHX in our study are much lower (28 μA/cm^2 DC and 50 μg/mL CHX), and strong killing effects (3-4 logs) were obtained.

Compared to the 6-7 log killing of *P. aeruginosa* after 1 h of treatment with DC alone as we reported previously [26], both *S. mutans* and *S. aureus* showed stronger tolerance to a similar level of DC. Although better killing effect may be archived with longer treatment and higher current levels, we believe it is better to keep DC treatment duration as 1 h and current level lower than 30 μA/cm^2 to minimize the generation of ferric oxide and to avoid the formation of mass hydrogen or oxygen bubbles.

CHX is bacteriostatic at low concentrations by affecting the integrity of bacterial cell wall and bactericidal at high concentrations by disrupting the cell [36]. *S. mutans* and *S. aureus* appear to be quite susceptible to CHX according to MIC data (< 8 μg/mL) [37]. We found that 50 μg/mL CHX was enough to inhibit planktonic growth completely (data not shown); however, the maximum killing of preformed biofilms by CHX alone in our experimental system was only less than 1.5 logs even with a dosage up to 500 μg/mL.

Through synergy with DC, CHX was found to be more effective in killing biofilm cells. The doses of CHX we used were only 50 μg/mL (0.005 w/v %) in 0.85% NaCl solution and 500 μg/mL (0.05 w/v %) in artificial saliva medium, which are much lower than that of commercial products but still exhibited killing effects with DC. This CHX level is expected to be safe because the

commercial products for oral wash have approximately 1200 µg/mL (0.12 w/v %) – 2000 µg/mL (0.2 w/v %) of CHX. The exact mechanism for such synergistic killing is unknown and is part of our ongoing research.

This study demonstrated that the DC delivered by wire to treatment facility could eradicate the dental plaque on the surface of denture material in presence of CHX. This system could also be modified to satisfy the requirements of wireless DC delivering without any reduction to power output. The size of receiver coil and controller chip need to be redesigned to fit the narrow space of oral cavity; however, people have invented the new generation of pacemaker device with a tiny antenna and an electronic controller for wireless communication. We can utilize a similar design to integrate the wireless DC treatment facility into the single denture. After being implanted into the oral cavity, the denture could become a mini DC treatment facility once it receives suitable magnetic fields.

6.6 Conclusion

In this study, we demonstrated that the biofilm cells of two Gram-positive pathogenic bacteria, *S. mutans*, and *S. aureus*, could be efficiently killed by concurrent treatment with low-level DC and CHX in 1 h. This electrochemical control is effective against the biofilms formed on the acrylic materials. The synergistic effect between DC and CHX can help design new devices and strategies for controlling pathogenic biofilm. The interaction between electrochemical products and CHX may play a significant role in the observed synergy in biofilm killing, which deserves further study.

6.7 Acknowledgements

This work was partially supported by the U.S. National Science Foundation (EFRI-1137186).

6.8 References

1. Liu, Y. et al. Topical delivery of low-cost protein drug candidates made in chloroplasts for biofilm disruption and uptake by oral epithelial cells. *Biomaterials* **105**, 156-166 (2016).
2. Hall, C.W. & Mah, T.F. Molecular mechanisms of biofilm-based antibiotic resistance and tolerance in pathogenic bacteria. *FEMS Microbiol Rev* **41**, 276-301 (2017).
3. Kouidhi, B., Al Qurashi, Y.M. & Chaieb, K. Drug resistance of bacterial dental biofilm and the potential use of natural compounds as alternative for prevention and treatment. *Microbial pathogenesis* **80**, 39-49 (2015).
4. Smith, A., Buchinsky, F.J. & Post, J.C. Eradicating chronic ear, nose, and throat infections: a systematically conducted literature review of advances in biofilm treatment. *Otolaryngol Head Neck Surg* **144**, 338-347 (2011).
5. Song, F., Koo, H. & Ren, D. Effects of Material Properties on Bacterial Adhesion and Biofilm Formation. *Journal of dental research* **94**, 1027-1034 (2015).
6. Bender, G.R., Sutton, S.V. & Marquis, R.E. Acid tolerance, proton permeabilities, and membrane ATPases of oral streptococci. *Infection and immunity* **53**, 331-338 (1986).
7. Harper, D.S. & Loesche, W.J. Growth and acid tolerance of human dental plaque bacteria. *Archives of Oral Biology* **29**, 843-848 (1984).
8. Kreth, J., Merritt, J., Shi, W. & Qi, F. Competition and coexistence between Streptococcus mutans and Streptococcus sanguinis in the dental biofilm. *Journal of Bacteriology* **187**, 7193-7203 (2005).
9. Falsetta, M.L. et al. Symbiotic relationship between Streptococcus mutans and Candida albicans synergizes virulence of plaque biofilms in vivo. *Infect Immun* **82**, 1968-1981 (2014).

10. Falsetta, M.L. et al. Novel antibiofilm chemotherapy targets exopolysaccharide synthesis and stress tolerance in Streptococcus mutans to modulate virulence expression in vivo. *Antimicrobial Agents and Chemotherapy* **56**, 6201-6211 (2012).
11. Lew, D.P. & Waldvogel, F.A. Osteomyelitis. *Lancet* **364**, 369-379 (2004).
12. Hansson, C., Hoborn, J., Möller, A. & Swanbeck, G. The microbial flora in venous leg ulcers without clinical signs of infection. Repeated culture using a validated standardised microbiological technique. *Acta Derm Venereol* **75**, 24-30 (1995).
13. Stephenson, M.F. et al. Molecular characterization of the polymicrobial flora in chronic rhinosinusitis. *J Otolaryngol Head Neck Surg* **39**, 182-187 (2010).
14. Salvi, G.E., Fürst, M.M., Lang, N.P. & Persson, G.R. One-year bacterial colonization patterns of Staphylococcus aureus and other bacteria at implants and adjacent teeth. *Clin Oral Implants Res* **19**, 242-248 (2008).
15. Harris, L.G. & Richards, R.G. Staphylococcus aureus adhesion to different treated titanium surfaces. *J Mater Sci Mater Med* **15**, 311-314 (2004).
16. Jones, S.M., Morgan, M., Humphrey, T.J. & Lappin-Scott, H. Effect of vancomycin and rifampicin on meticillin-resistant Staphylococcus aureus biofilms. *Lancet* **357**, 40-41 (2001).
17. O'Donnell, L.E. et al. Dentures are a Reservoir for Respiratory Pathogens. *Journal of prosthodontics : official journal of the American College of Prosthodontists* (2015).
18. Lewis, N. et al. Colonisation of dentures by Staphylococcus aureus and MRSA in out-patient and in-patient populations. *European journal of clinical microbiology & infectious diseases : official publication of the European Society of Clinical Microbiology* **34**, 1823-1826 (2015).

19. Jones, C.G. Chlorhexidine: is it still the gold standard? *Periodontol 2000* **15**, 55-62 (1997).

20. Flotra, L., Gjermo, P., Rolla, G. & Waerhaug, J. Side effects of chlorhexidine mouth washes. *Scandinavian journal of dental research* **79**, 119-125 (1971).

21. Costerton, J.W., Ellis, B., Lam, K., Johnson, F. & Khoury, A.E. Mechanism of electrical enhancement of efficacy of antibiotics in killing biofilm bacteria. *Antimicrobial Agents and Chemotherapy* **38**, 2803-2809 (1994).

22. del Pozo, J.L., Rouse, M.S., Mandrekar, J.N., Steckelberg, J.M. & Patel, R. The electricidal effect: reduction of Staphylococcus and pseudomonas biofilms by prolonged exposure to low-intensity electrical current. *Antimicrobial Agents and Chemotherapy* **53**, 41-45 (2009).

23. Schmidt-Malan, S.M. et al. Antibiofilm Activity of Low-Amperage Continuous and Intermittent Direct Electrical Current. *Antimicrobial Agents and Chemotherapy* **59**, 4610-4615 (2015).

24. Spadaro, J.A., Berger, T.J., Barranco, S.D., Chapin, S.E. & Becker, R.O. Antibacterial effects of silver electrodes with weak direct current. *Antimicrobial Agents and Chemotherapy* **6**, 637-642 (1974).

25. Wattanakaroon, W. & Stewart, P.S. Electrical enhancement of Streptococcus gordonii biofilm killing by gentamicin. *Arch Oral Biol* **45**, 167-171 (2000).

26. Niepa, T.H., Gilbert, J.L. & Ren, D. Controlling Pseudomonas aeruginosa persister cells by weak electrochemical currents and synergistic effects with tobramycin. *Biomaterials* **33**, 7356-7365 (2012).

27. Niepa, T.H. et al. Sensitizing Pseudomonas aeruginosa to antibiotics by electrochemical disruption of membrane functions. *Biomaterials* **74**, 267-279 (2016).

28. Niepa, T.H., Wang, H., Dabrowiak, J.C., Gilbert, J.L. & Ren, D. Synergy between tobramycin and trivalent chromium ion in electrochemical control of Pseudomonas aeruginosa. *Acta Biomater* **36**, 286-295 (2016).

29. Lasserre, J.F., Leprince, J.G., Toma, S. & Brecx, M.C. Electrical enhancement of chlorhexidine efficacy against the periodontal pathogen Porphyromonas gingivalis within a biofilm. *The new microbiologica* **38**, 511-519 (2015).

30. Sauer, K., Steczko, J. & Ash, S.R. Effect of a solution containing citrate/Methylene Blue/parabens on Staphylococcus aureus bacteria and biofilm, and comparison with various heparin solutions. *The Journal of antimicrobial chemotherapy* **63**, 937-945 (2009).

31. Steinberg, D., Heling, I., Daniel, I. & Ginsburg, I. Antibacterial synergistic effect of chlorhexidine and hydrogen peroxide against Streptococcus sobrinus, Streptococcus faecalis and Staphylococcus aureus. *J Oral Rehabil* **26**, 151-156 (1999).

32. Drake, D.R., Grigsby, W., Cardenzana, A. & Dunkerson, D. Synergistic, growth-inhibitory effects of chlorhexidine and copper combinations on Streptococcus mutans, Actinomyces viscosus, and Actinomyces naeslundii. *J Dent Res* **72**, 524-528 (1993).

33. McCreery, D.B., Agnew, W.F., Yuen, T.G. & Bullara, L. Charge density and charge per phase as cofactors in neural injury induced by electrical stimulation. *IEEE Trans Biomed Eng* **37**, 996-1001 (1990).

34. Shannon, R.V. A model of safe levels for electrical stimulation. *IEEE Trans Biomed Eng* **39**, 424-426 (1992).

35. **Clark** , G. Cochlear Implants: Fundamentals and Applications. (Springer, 2003).

36. McDonnell, G. & Russell, A.D. Antiseptics and disinfectants: activity, action, and resistance. *Clinical microbiology reviews* **12**, 147-179 (1999).

37. Chung, J.Y., Choo, J.H., Lee, M.H. & Hwang, J.K. Anticariogenic activity of macelignan isolated from Myristica fragrans (nutmeg) against Streptococcus mutans. *Phytomedicine : International Journal of Phytotherapy and Phytopharmacology* **13**, 261-266 (2006).

6.9 Figures

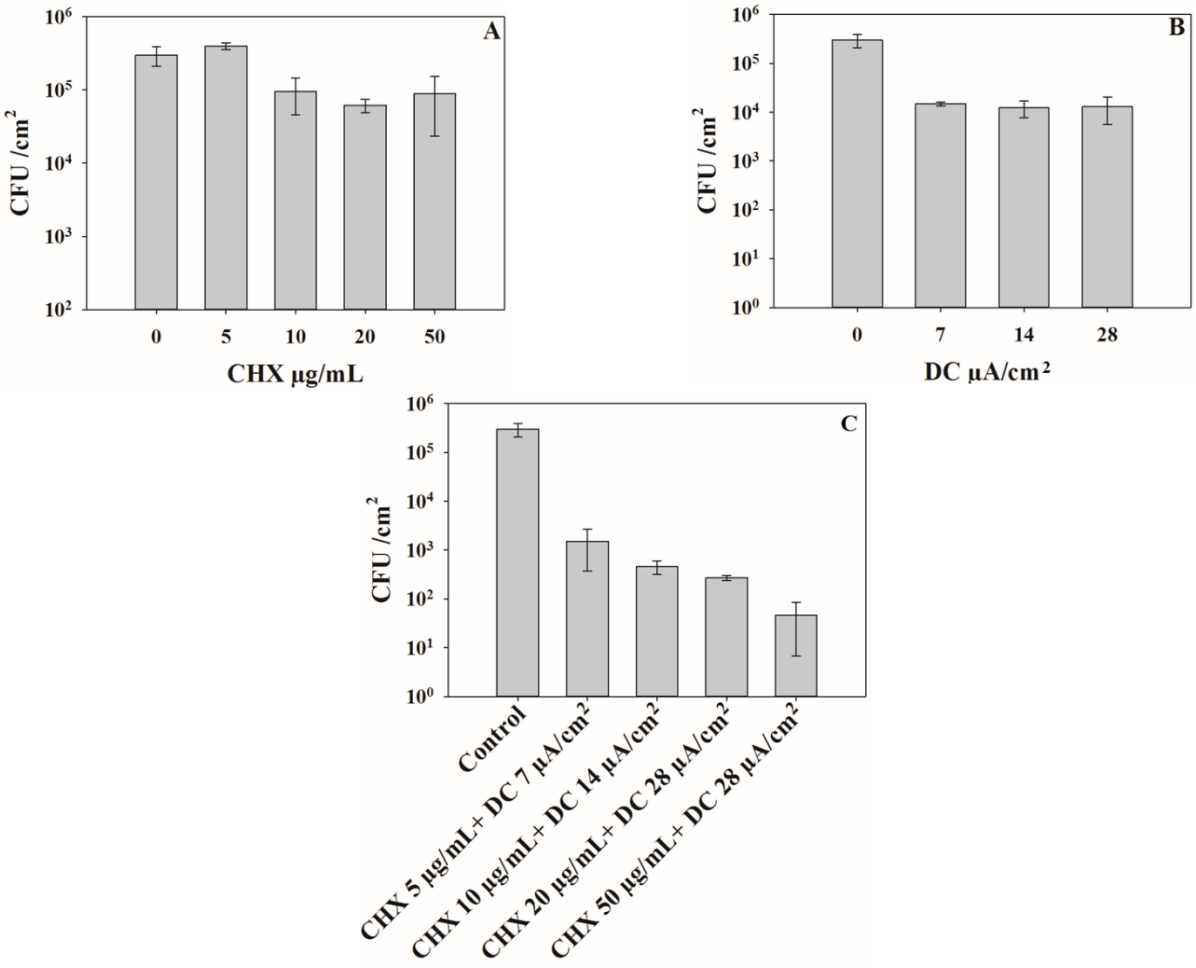

Figure 1. Viability of *S. mutans* biofilm cells after 1 h treatment with CHX alone (A), DC alone (B) or concurrent treatment with CHX and DC (C). All treatments were tested in 0.85 % NaCl solution.

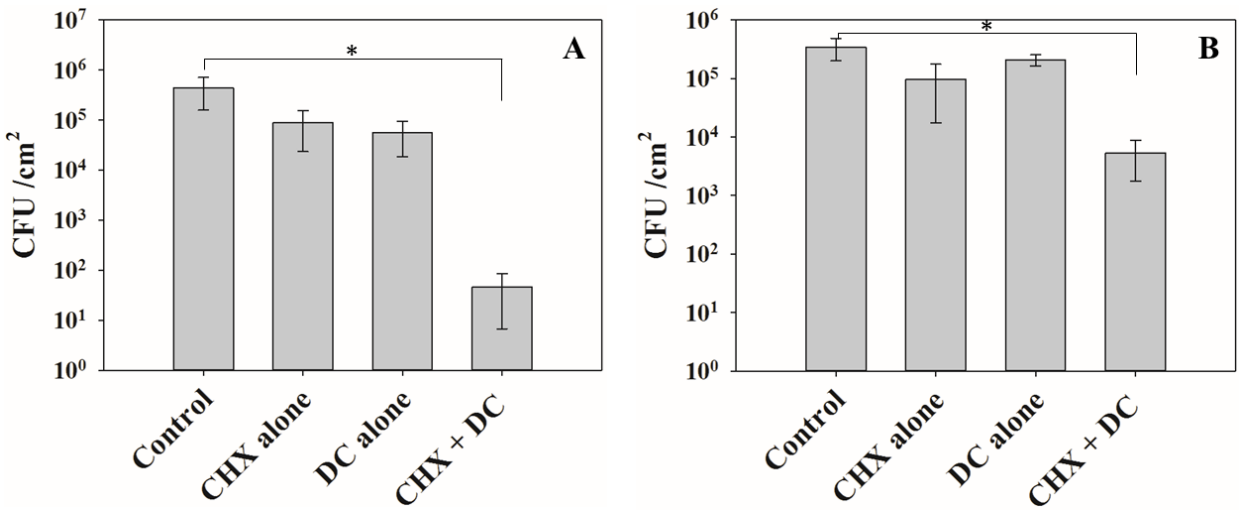

Figure 2. Viability of S. mutans biofilm cells after treatment with CHX alone, DC alone or concurrent treatment with CHX and DC. A: treatment medium: 0.85 % NaCl, DC level: 28 µA/cm^2, CHX dosage: 50 µg/mL. B: treatment medium: artificial saliva, DC level: 28 µA/cm^2, CHX dosage: 500 µg/mL.

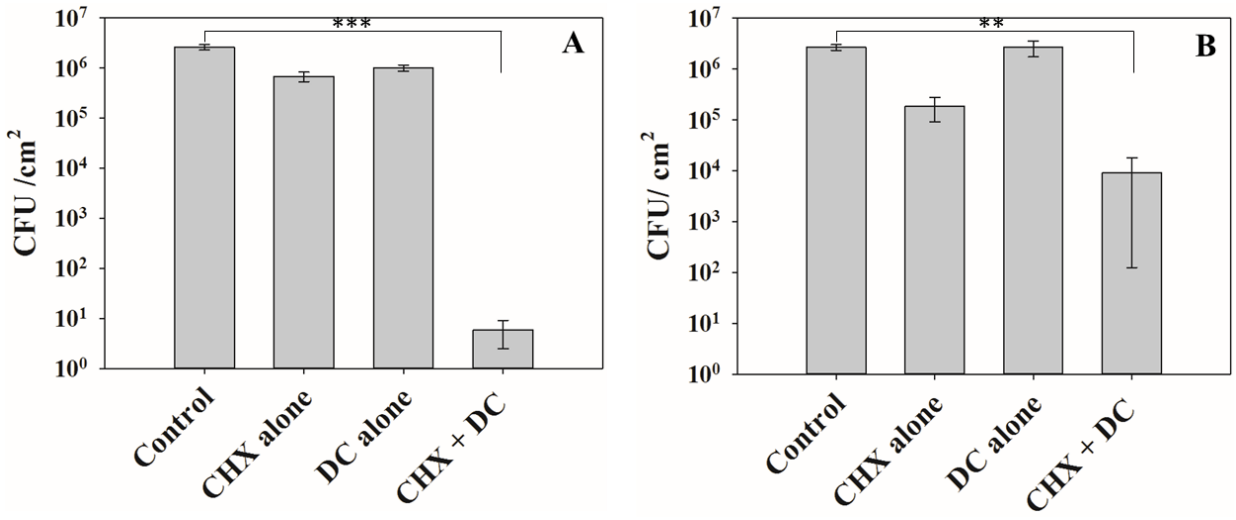

Figure 3. Viability of S. aureus biofilm cells after treatment with CHX alone, DC alone or concurrent treatment with CHX and DC. A: treatment medium: 0.85 % NaCl, DC level: 28 µA/cm2, CHX dosage: 50 µg/mL. B: treatment medium: artificial saliva, DC level: 28 µA/cm2, CHX dosage: 500 µg/mL.

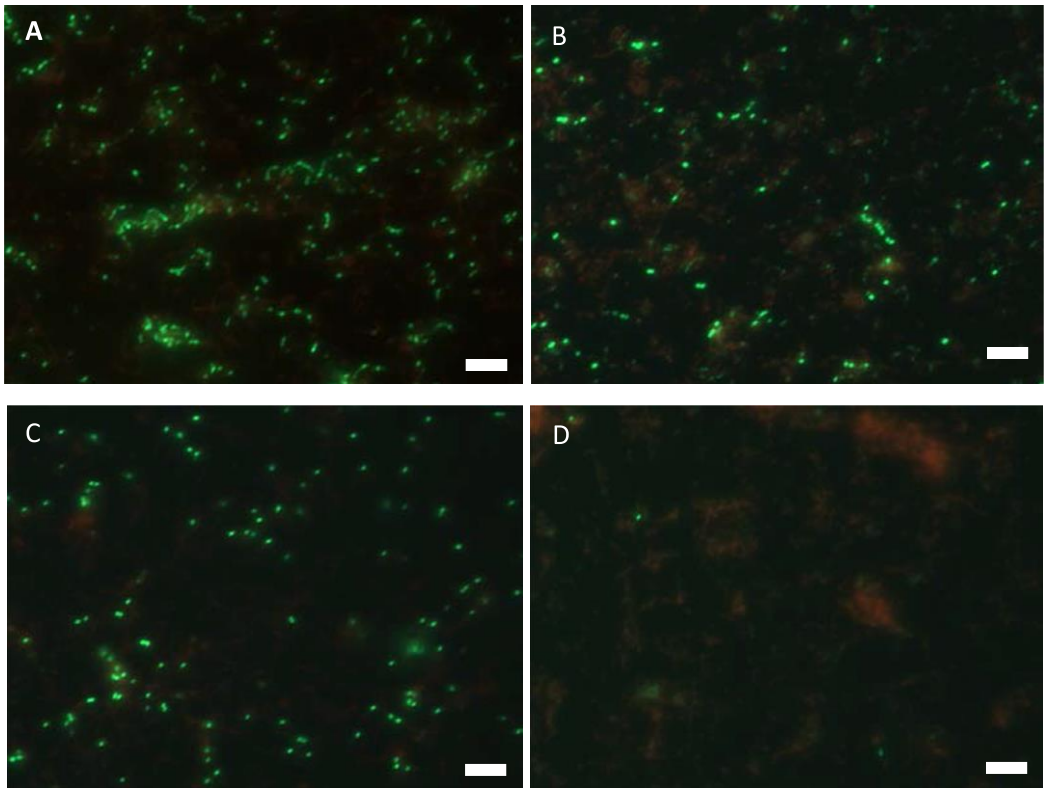

Figure 4. Living/dead staining of *S. mutans* biofilms treated with 5 μg/mL CHX (B), 7 μA/cm^2 DC (C), 5 μg/mL CHX plus 7 μA/cm^2 DC (D) and no treatment (A). Bar = 20 μm.

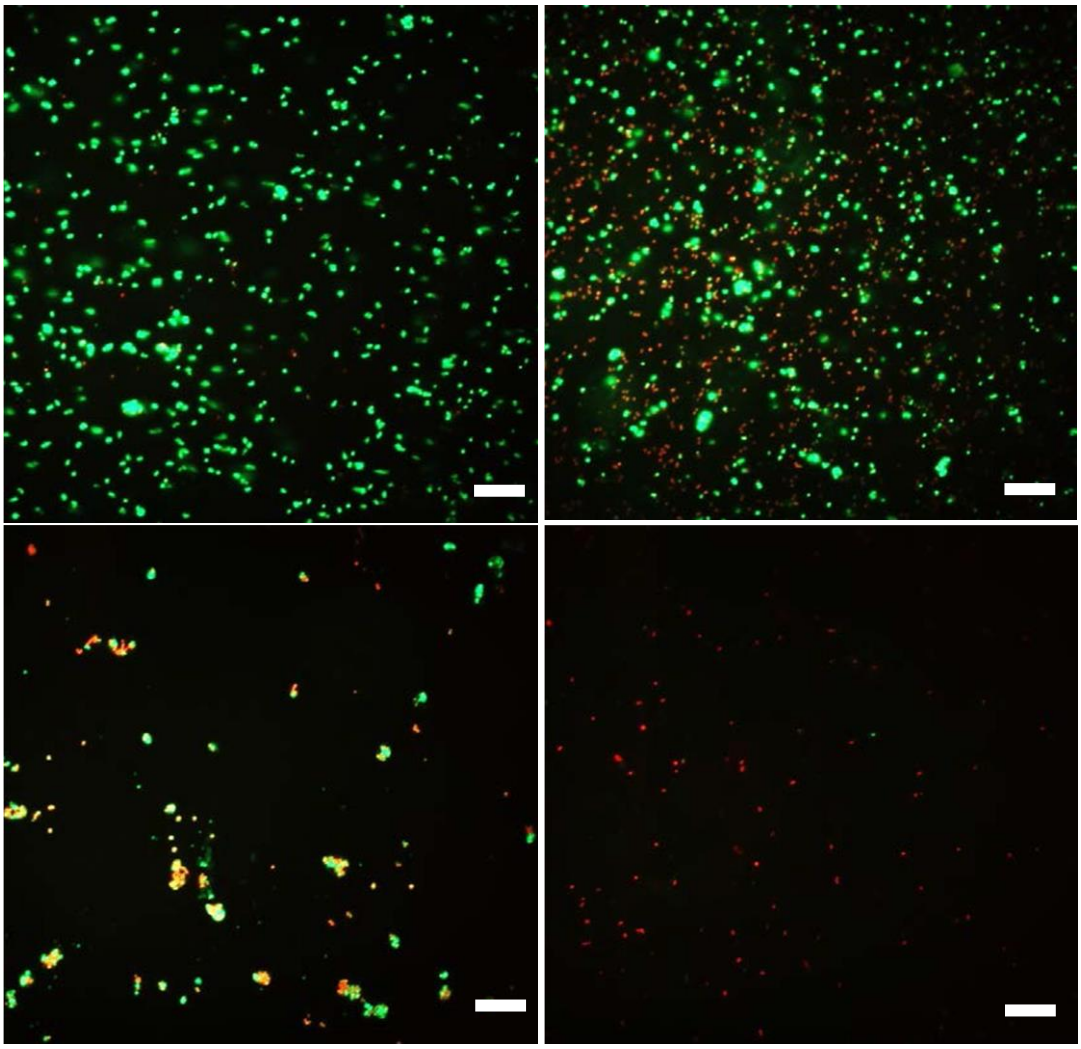

Figure 5. Living/dead staining of *S. aureus* biofilms treated with 20 μg/mL CHX (B), 28 μA/cm^2 DC (C), 20 μg/mL CHX plus 28 μA/cm^2 DC (D) and no treatment (A). Bar = 20 μm.

Chapter 7

Wirelessly delivered DC treatment of *S. aureus* biofilms in a rabbit model

7.1 Abstract

Device-associated infection is a serious risk for patients with implant devices, and this risk becomes more and more significant because of the increasing application of medical devices. The biofilm on the contaminated device after surgery is reported as a leading cause of infection. The potent bactericidal activities of direct current (DC) have attracted increasing interest recently. In Chapter 3, we have demonstrated that the wirelessly delivered direct electric current (DC) could achieve a good killing effect on *Staphylococcus aureus* biofilms on the PDMS surface. In this Chapter, the bactericidal effects of wirelessly delivered DC were further tested on an *in vivo* model. The contaminated prototype devices with *S. aureus* biofilms under the dermis tissue of rabbits and the biofilms were treated for 6 h with 12 $\mu A/cm^2$ wirelessly delivered DC. Compared to untreated controls, treatment with DC reduced the total number of *S. aureus* within the rabbit by 65 %. In addition, histological analysis of the dermis and muscle tissues confirmed the safety of wirelessly delivered DC treatments in the rabbit model.

7.2 Introduction

From the 1990s, many studies have shown that the potent killing effects of DC on biofilms [1-9]. These studies demonstrated that the number of viable biofilm cells on the surface of the electrode or other biomaterials could be reduced by several logs with DC treatment at 10 μA to 100 mA levels for 1 – 24 h. Furthermore, there have been several successful *in vivo* anti-biofilm studies carried in the mice, rodent, rabbit and goat models; however, all of them used wires to deliver electric current, which had to pierce animals' skins (Table 1).

Table 1. Bactericidal effects of electric current *in vivo*

Current/potential level	Strain	Bactericidal effect	Animal model	Antibiotics	Duration	Ref.
-1.8 V vs AgCl	*S. aureus*	87% reduction (Tissue) 98% Reduction (Implant)	Rodent	Vancomycin	1 h	[10]
-1.8 V vs AgCl	*S. aureus*	2 log reduction (Implant)	Rodent	Vancomycin	1 h twice	[12]
1 mA	*P. aeruginosa*	58% reduction	Rabbit	Tobramycin	1 h	[13]
100 μA	*Staphylococcus epidermidis*	80% reduction	Goat	-	21 days	[14]
10 MHz low level AC	*P. aeruginosa*	1.5 log reduction	Mice	-	48 h	[15]

As mentioned in Chapters 3 and 4, we have demonstrated that wirelessly delivered DC can effectively kill *S. aureus* biofilm cells on PDMS surfaces For example, the viability of *S. aureus* biofilm cells was reduced by 3.0 and 2.6 logs using a prototype device to wirelessly delivered DC

treatment of 6 μA/cm^2 *in vitro* and *ex vivo*, respectively. These findings motivated us to further apply this technique *in vivo*.

To evaluate the safety and efficacy of wirelessly delivered DC *in vivo*, we conducted an animal test using a rabbit model. The design was adapted from a previous study of pacemaker material in a rabbit model, which compared the efficiency of different anti-biofilm coatings pacemaker models [16].

7.3 Materials and methods

7.3.1 Experimental setup of wirelessly delivered DC treatment in a rabbit model

A total of 8 rabbits were used to compared DC treatment and DC-free control. The control devices also carried all components in the case, but the electrodes and control modules were discontinued. Four 1 cm by 0.5 cm *S. aureus* biofilm samples on PDMS cultured for 24 h in LB medium were positioned on each device. Each rabbit was implanted with one control and one treatment sample. Another rabbit was included as biofilm free control, which was also inserted with a DC-free control and DC-delivering device. This rabbit provided a baseline for histology.

7.3.2 Rabbit model

A total of 9 female adult rabbits (New Zealand, >2 kg each) were involved to investigate the antibiofilm efficiency of wirelessly delivered DC on *S. aureus* biofilms formed on implant devices as well as safety to host tissues. To form the biofilm on the surface of a device, *S. aureus* cells were grown overnight in LB medium at 37 °C with shaking at 200 rpm. On the following day, the overnight culture was used to inoculate 25 ml fresh LB medium with a 1,000 times dilution. Then

sterilized PDMS coupons (1 x 0.5 cm each) were immersed in the medium and incubated at 37 °C without shaking for 24 hours. On the following day, PDMS coupons with biofilms were washed with 0.9% sodium chloride solution twice and then attached on the top the prototype device surface (around the center anode) in the same way as *in vitro* setup. The devices with biofilm samples were kept in petri dishes to ensure moisture.

Before surgery, each rabbit underwent general anesthesia using inhaled 3-5% isoflurane for induction and 2-4% isoflurane for maintenance. Isoflurane anesthesia was maintained for the duration of the entire experiment including the implantation of the prototype, wirelessly delivered DC treatment, and implant removal. A warm blanket was used to help maintain body temperature. The surgical sites (just a few centimeters lateral to the spine on each side) were identified and shaved to remove hair. The shaved areas were scrubbed with betadine followed by 75% alcohol three times. Sterile drapes were placed over the surgical sites. One lidocaine (1%) and 1:100,000 epinephrine was injected to rabbits. An incision on the subcutaneous layer of the skin was made using a #15 blade, and then the adjacent skin was undermined by scissors to make a pocket cavity. The prototype device was placed into the pocket and the skin was closed with sutures. The process was repeated on the contralateral side. Then 30 mL saline solution was injected into each packet cavity (Figure 1A).

7.3.3 Treatment with wirelessly delivered DC

An electromagnetic transmitter coil connected to the controller chips and USB power cable was placed over the implant site of prototypes for 6 h of treatment (Figure 1B&C). The DC level was approximately 200 μA. To minimize the variation among different rabbits, each rabbit was inserted with two devices including one control (without DC) and one for DC treatment corresponding to

a current density of 12 μA/cm^2 (total 200 μA). During treatment, 30 mL saline solution was injected into each pocket every 2 hours to keep cavity wet.

7.3.4 Sample collection

After treatment, the incision was opened, and the prototype devices were harvested. Tissue that had directly contacted with the prototype device was harvested and placed in 10% buffered formalin, saline solution or frozen directly for future evaluation (Figure 2). After completion of tissue harvest, the animals were euthanized by an intraperitoneal injection of pentobarbital 150 mg/kg. The PDMS coupons with biofilm were placed in the 0.9% saline solution to determine the viability of *S. aureus*.

7.3.5 Histological analysis

To evaluate the cytotoxicity of the wirelessly delivered DC treatment on the dermis layer and muscle tissue in contact with the device, approximately 20% of the collected skin and muscle specimens were frozen immediately by ice bath upon harvesting. The specimens underwent cryosection to obtain the thin film (5 -15 μm of thickness). Then the samples were mounted on glass slides and Hematoxylin and Eosin staining were performed. Finally, the stained samples were observed under microscopy to determine if there was any histological change. Another 20% of collected specimens were kept in 10% buffer formalin solution and sent to IDEXX company to perform a thorough pathology analysis.

7.3.6 Viability of biofilm cells

About half of the skin tissue that had directly contacted the device and PDMS coupons were collected after treatment and kept in 0.9% saline solution. Then they were subjected to sonication

for 1 minute followed by 30s of vortexing. The viability of *S. aureus* biofilm cells on PDMS coupons and skin tissue was determined by counting CFU and by Live/Dead staining.

7.3.7 Statistical analysis

Statistical significance was assessed with Wilcoxon Signed Rank Sum Test. Results with $p < 0.05$ were considered statistically significant.

7.4 Results

7.4.1 Experimental design of the treatment by wirelessly delivered DC *in vivo*

Previous electrochemical studies using animal models aimed to eradicate the biofilm on the surface of an electrode[10, 11]. During those experiments, the electrodes were implanted into deep tissue that contained abundant body fluid (e.g. blood, serum, et al.). The body fluid offers good conductivity between the anode and cathode, and thus effective killing of bacterial cells. However, our devices were implanted between the dermis layer and surficial muscle tissue of the rabbit. In this location, lower amounts of bodily fluids are present compared to the fluid surrounding deeper tissues, which lower the conductivity for killing biofilm cells on the device surface. The only conductive media is dermis tissue that has a conductivity of 0.2 S/m [17]. To select an appropriate internal resistor and obtain the current level at the expected range of 200 ± 30 μA, the total current levels and total impedances between the TGON anode and steel cathode were measured using the same method as described in Chapter 3. The distance between two electrodes was the same design of the prototype device, and the electrodes were submerged into 0.1 % saline solution that also has a conductivity of 0.2 S/m. It found a 10K ohm resistor could maintain the actual total current level at 195 - 210 μA and the working impedance between anode and cathode in 0.2 S/m media was approximately

15000 Ω (Figure 4). Based on this result, a 10 kΩ internal resistor was included in all prototype devices. The devices for control samples had the same structure as the devices for DC treatment although their internal circuits were cut. During the animal test, both control devices and treatment devices received the same external magnetic field while there weren't DC output from the control devices.

7.4.2 Efficacy of wirelessly delivered DC treatment *in vivo*

To evaluate the efficacy of wirelessly delivered DC treatment *in vivo*, the prototype devices that contained four PDMS coupons covered with *S. aureus* biofilm were inserted under the dermis layer. Then the biofilm samples were treated with approximately 200 μA DC corresponding to a current density of 12 $\mu A/cm^2$ generated by the prototype device wirelessly for 6 hours.

After treatment, the number of viable *S. aureus* biofilm cells on device surface was reduced by 65% ($p = 0.03$), and the number of viable *S. aureus* cells attached on the skin tissue was reduced to 80% ($p < 0.01$) compared to the DC-free control. This suggests that wirelessly delivered DC could effectively kill the biofilm cells both on the device surface and the surrounding tissue *in vivo;* however, the results were not as potent as demonstrated in *in vitro* tests. There was also some cells found in the residual liquid (from injected saline) (Figure 3). By adding all three populations together, it was found that DC treatment killed *S. aureus* biofilm cells by 66% *in vivo* ($p < 0.008$, Wilcox Signed Ranked Sum Test) (Figure 5).

7.4.3 Safety of the treatment by wirelessly delivered DC

To evaluate the safety of the wirelessly delivered DC treatment, the specimens were collected from both the skin and muscle tissues surrounding the device for the histological analysis. The result of this analysis would reveal if DC and its products during treatment could cause acute damage to the

host tissue. According to the report of histological analysis from IDEXX Bioresearch, there was no damage specific to treated samples, except for mild infiltration due to surgery that was seen on both control and treated samples. None of the muscle samples show notable changes.

The skin and muscle samples treated with wirelessly delivered DC underwent cryosection and Hematoxylin and eosin staining. According to the microscopy images of samples after staining, there was no significant change between control and treated samples (Figure 6&7).

7.5 Discussion

Electrochemical treatment has been used for orthopedic applications to stimulate the growth of osteogenic cells on the fracture site [18, 19]. Such processes are invasive and require the insertion of the electrodes to reach into the fracture site. However, electric currents have not been utilized in clinical for controlling device-associated infections. There were several animal tests on using electric current to control biofilm formation on the metallic implants, but all of them required piercing of skin to introduce the wires and deliver electric current from a potentiostat outside the body to metallic implants.

The animal study in this chapter utilized the wireless delivery technique to replace skin-piercing. The process of wireless delivering of DC depended on the inductive coupling between two electromagnetic coils. The alternating magnetic field under our setup could penetrate skin tissue up to 10 mm, which was sufficient for the *in vivo* test described here. Further development based on approach may have promising applications in treating device-associated infections.

During the animal test, it was determined that the under-dermis cavity for the device had to keep moisture by injecting extra saline solution periodically. Previous animal studies for DC treatment

were carried in the deeper tissue that had more body fluid (such as blood) that ensures good conductivity between electrodes. However, we found the cavity under the dermis layer of the rabbit was very dry. Consequently, the connection between anode and cathode was poor and the actual current level was much lower than expected. Adding the saline solution could improve the electrical connection temporarily but it was absorbed by surrounding tissue soon after injection. Hence, more the saline solution was added every 2 hours in treatment. By testing devices at deep tissue, we expect stronger antibiofilm activities.

Overall, our results showed that there were three major populations of *S. aureus* cells in the rabbit during treatment: the biofilm cells on the PDMS surface, the cells on the skin tissue that attached to the device and the cells in the residue saline solution in the cavity. For control samples, the total number of viable cells on skins tissue was almost 10 times higher than cells on PDMS surface. The number of viable biofilm cells on PDMS were reduced by 75%, and the viability of cells on the dermis tissue was also reduced by 80% after wirelessly delivered DC treatment. However, the number of *S. aureus* cells in saline solution in the cavity varied substantially between tested rabbits. The average number of these cells showed no significant killing by DC. This is not unexpected since the volume of residue saline solution was only 100 – 150 μL and stayed in the bottom of the cavity, which was away from both electrodes. The cells in this region couldn't be treated by electric current or electrochemical products. Nevertheless, by counting the total number of cells including this subpopulation, *S. aureus* biofilm cells in the rabbit was killed by 65% after wirelessly delivered DC treatment for 6 hours.

The migration of biofilm cells from PDMS surface to surrounding tissue and liquid in our study should be due to both animal model itself and the experimental design. The female rabbit skin is soft but elastic that could attach tightly on the surface of the device after implantation. Meanwhile,

breathing of the rabbit during the treatment caused “stretch-release” motion, which may generate shear force and make the skin in close contact with the biofilms. This shear force may peer the biofilm cells from the device. Another driving force is from the saline solution that was injected into the implant site. As mentioned above, to keep the cavity and device moisture, we had injected 30 mL saline solution every 2 hours to ensure a good electrical connection. The saline solution was injected directly onto the surface of the device. This may also cause shear force and wash cells off from the device’s surface. These would not be of concern if the device were implanted in deep tissues.

To overcome the barrier of conductivity and improve biofilm killing, it would be helpful to design implants with conductive material for the case/housing. This can be achieved by infiltrating conductive materials into the polymer material or coat the device surface with conductive materials.

7.6 Conclusions

In this study, a prototype device with a function of wirelessly delivered DC treatment was tested in the rabbit model. The *S. aureus* biofilm cells were treated by the device in the presence and absence of 12 $\mu A/cm^2$ wirelessly delivered DC. The most significant killing effect was found on the cells attached to the dermis tissue, which has high conductivity. The viability of biofilm cells on devices’ surface was also reduced. For our best knowledge, this is the first study to investigate the bactericidal activity of the wirelessly delivered DC treatment *in vivo* although the whole system still needs optimizing. The results show that wirelessly delivered DC has promising applications for non-invasive control of device-associated infections.

7.7 Acknowledgments

This study was supported by Gerber Endowment Funds of Syracuse University. The surgery work was done by Dr. Alex Tampio from Upstate Medical University. We also want to thank Dr. Guirong Wang and Dr. Juntao Luo from Upstate Medical University for helping us to make culture and histological analysis.

7.8 Reference

1. Blenkinsopp, S.A., Khoury, A.E. & Costerton, J.W. Electrical enhancement of biocide efficacy against Pseudomonas aeruginosa biofilms. *Appl Environ Microbiol* **58**, 3770-3773 (1992).
2. Costerton, J.W., Ellis, B., Lam, K., Johnson, F. & Khoury, A.E. Mechanism of electrical enhancement of efficacy of antibiotics in killing biofilm bacteria. *Antimicrobial Agents and Chemotherapy* **38**, 2803-2809 (1994).
3. Griffin, D.T., Dodd, N.J., Zhao, S., Pullan, B.R. & Moore, J.V. Low-level direct electrical current therapy for hepatic metastases. I. Preclinical studies on normal liver. *British journal of cancer* **72**, 31-34 (1995).
4. Stoodley, P., deBeer, D. & Lappin-Scott, H.M. Influence of electric fields and pH on biofilm structure as related to the bioelectric effect. *Antimicrob Agents Chemother* **41**, 1876-1879 (1997).
5. van der Borden, A.J., van der Werf, H., van der Mei, H.C. & Busscher, H.J. Electric current-induced detachment of Staphylococcus epidermidis biofilms from surgical stainless steel. *Appl Environ Microbiol* **70**, 6871-6874 (2004).
6. Kloth, L.C. Electrical stimulation for wound healing: a review of evidence from in vitro studies, animal experiments, and clinical trials. *Int J Low Extrem Wounds* **4**, 23-44 (2005).
7. van der Borden, A.J., van der Mei, H.C. & Busscher, H.J. Electric block current induced detachment from surgical stainless steel and decreased viability of Staphylococcus epidermidis. *Biomaterials* **26**, 6731-6735 (2005).

8. Gan, J.C. & Glazer, P.A. Electrical stimulation therapies for spinal fusions: current concepts. *European spine journal : official publication of the European Spine Society, the European Spinal Deformity Society, and the European Section of the Cervical Spine Research Society* **15**, 1301-1311 (2006).
9. Niepa, T.H.R., Wang, H., Gilbert, J.L. & Ren, D. Eradication of Pseudomonas aeruginosa cells by cathodic electrochemical currents delivered with graphite electrodes. *Acta Biomater* **50**, 344-352 (2017).
10. Ehrensberger, M.T. et al. Cathodic voltage-controlled electrical stimulation of titanium implants as treatment for methicillin-resistant Staphylococcus aureus periprosthetic infections. *Biomaterials* **41**, 97-105 (2015).
11. Canty, M., Luke-Marshall, N., Campagnari, A. & Ehrensberger, M. Cathodic voltage-controlled electrical stimulation of titanium for prevention of methicillin-resistant Staphylococcus aureus and Acinetobacter baumannii biofilm infections. *Acta Biomater* **48**, 451-460 (2017).
12. Nodzo, S.R. et al. Cathodic Voltage-controlled Electrical Stimulation Plus Prolonged Vancomycin Reduce Bacterial Burden of a Titanium Implant-associated Infection in a Rodent Model. *Clin Orthop Relat Res* **474**, 1668-1675 (2016).
13. Niepa, T.H.R. in Chemical Engineering, Vol. Ph.D (Syracuse University, 2014).
14. van der Borden, A.J. et al. Prevention of pin tract infection in external stainless steel fixator frames using electric current in a goat model. *Biomaterials* **28**, 2122-2126 (2007).
15. Giladi, M. et al. Microbial growth inhibition by alternating electric fields in mice with Pseudomonas aeruginosa lung infection. *Antimicrob Agents Chemother* **54**, 3212-3218 (2010).

16. Schwartzman, D. et al. An off-the-shelf plasma-based material to prevent pacemaker pocket infection. *Biomaterials* **60**, 1-8 (2015).

17. Peters, M., Stinstra, J. & Hendriks, M. Estimation of the electrical conductivity of human tissue. *Electromagnetics* **21**, 545-557 (2001).

18. Gan, J.C. & Glazer, P.A. Electrical stimulation therapies for spinal fusions: current concepts. *Eur Spine J* **15**, 1301-1311 (2006).

19. Brighton, C.T. et al. A multicenter study of the treatment of non-union with constant direct current. *J Bone Joint Surg Am* **63**, 2-13 (1981).

7.9 Figures

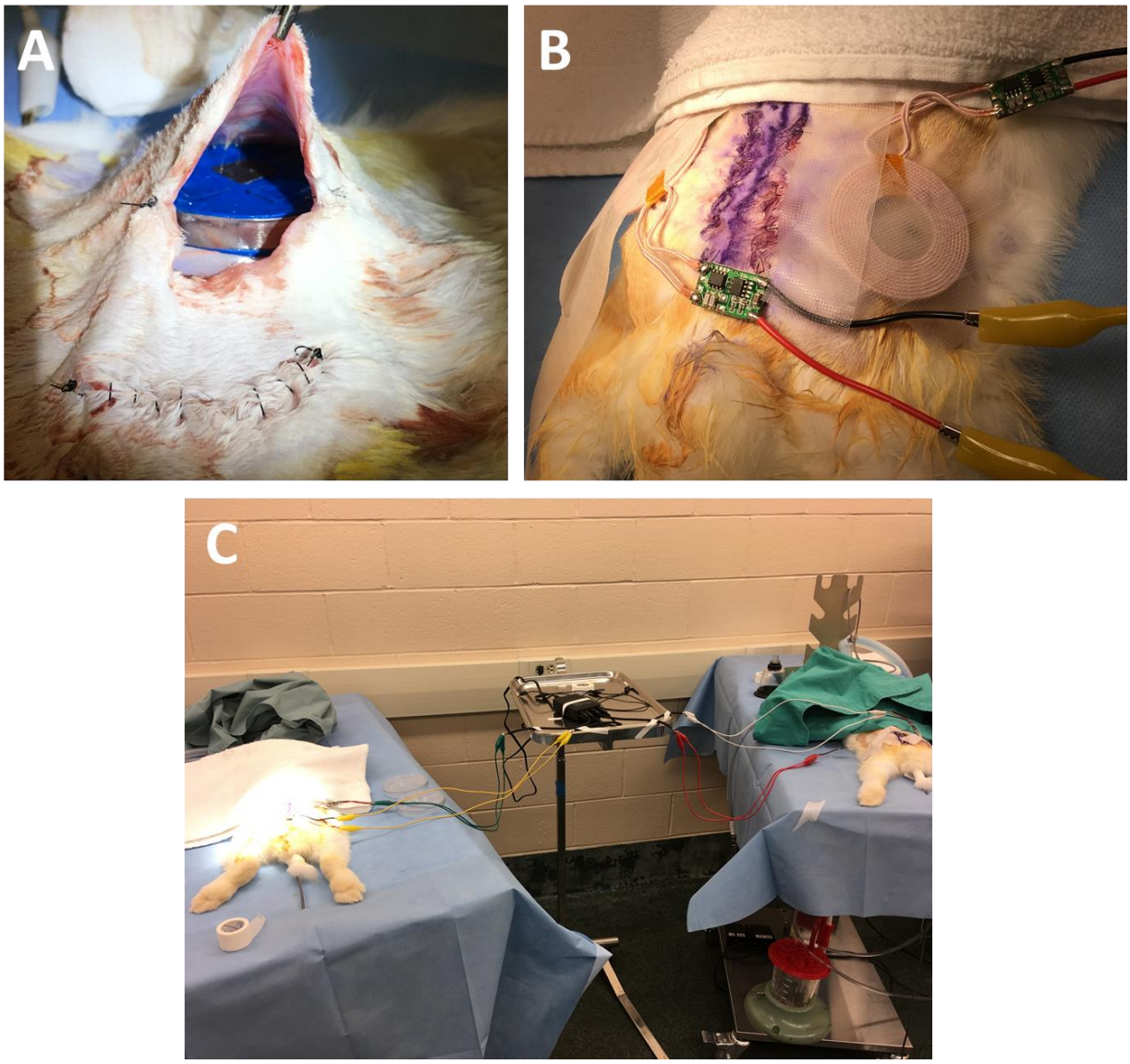

Figure 1. The setup of the wirelessly delivered DC treatment in the rabbit model. (A): The prototype device was placed in the pocket under the dermis layer of the rabbit. (B): A transmitter coils were put on the skin to deliver DC wirelessly. (C): Two rabbits were tested in parallel.

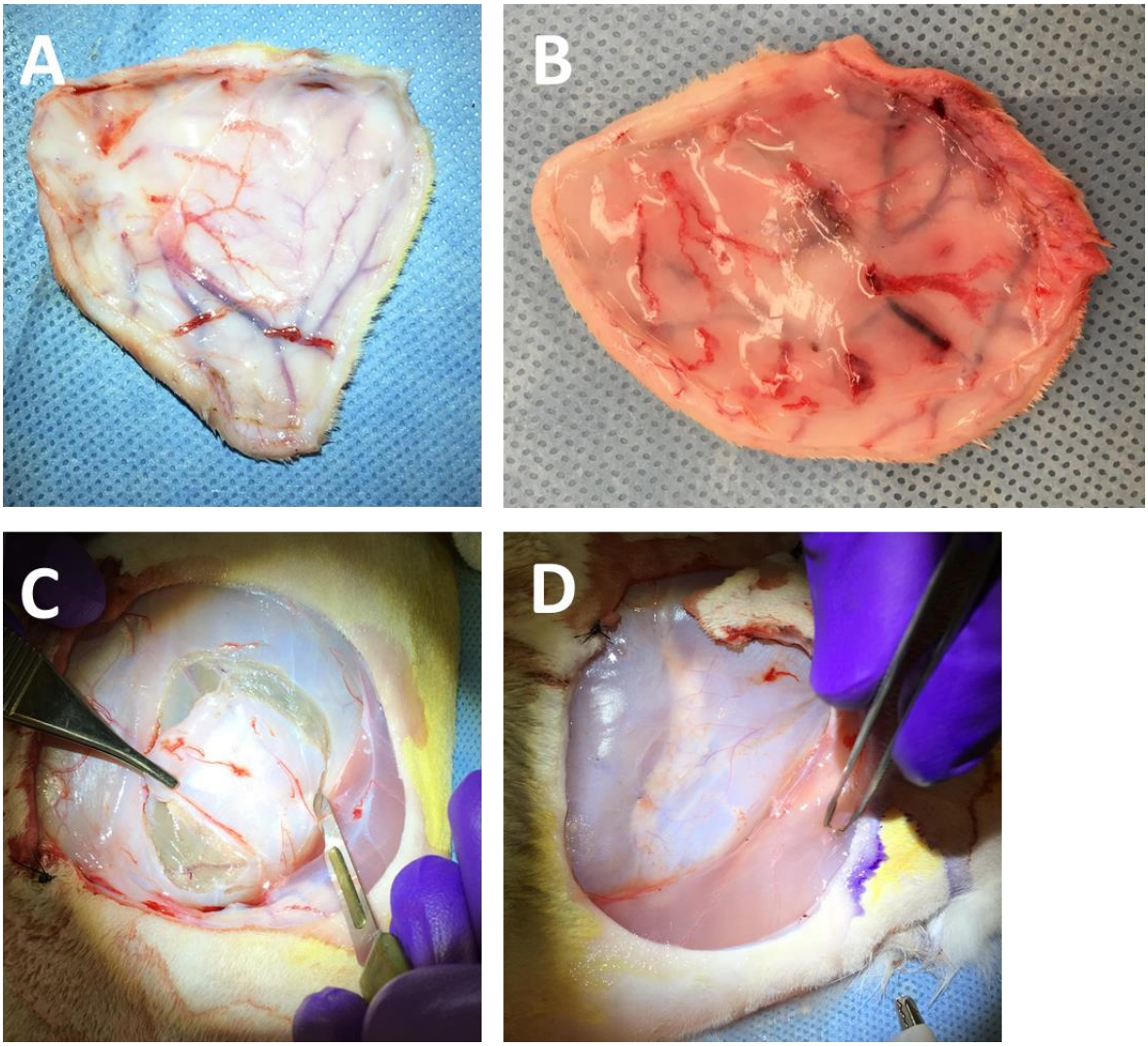

Figure 2. Representative pictures of the rabbits that were in direct contact with the prototype device. (A): The skin tissue without DC treatment. (B): A dermis tissue treated with wirelessly delivered DC for 6 h. (C): The surficial muscle tissue without DC treatment. (D): The surficial muscle tissue treated with 12 μA/cm^2 of wirelessly delivered DC for 6 h.

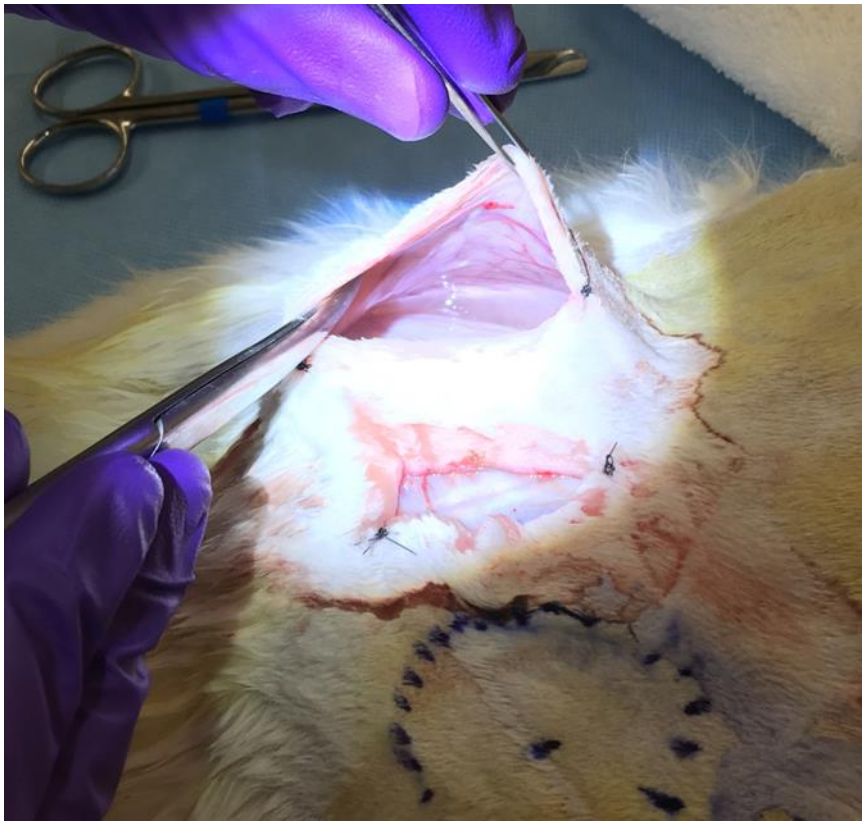

Figure 3. Representative picture showing the residue saline solution.

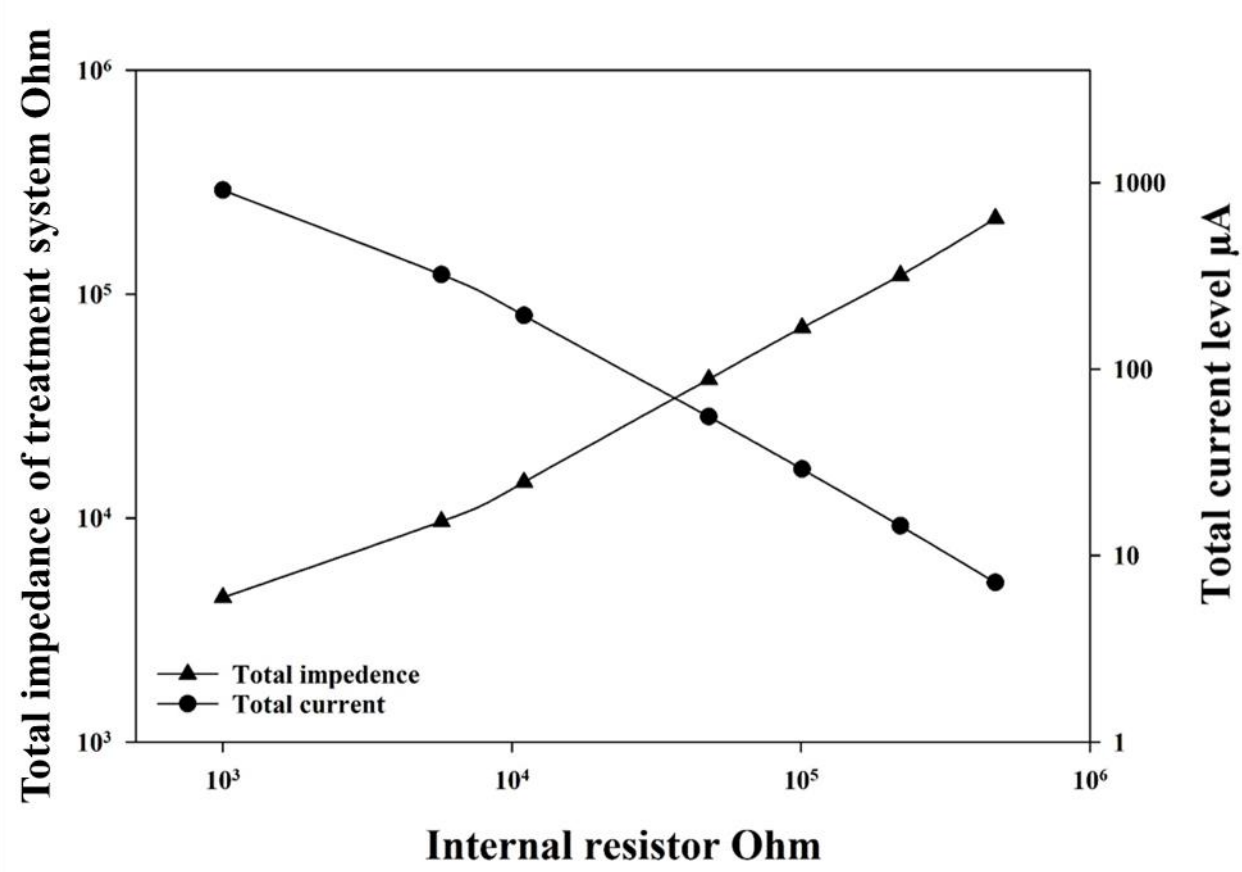

Figure 4. The total impedances and total current level between anode and cathode in 0.1% saline solution with different internal resistors.

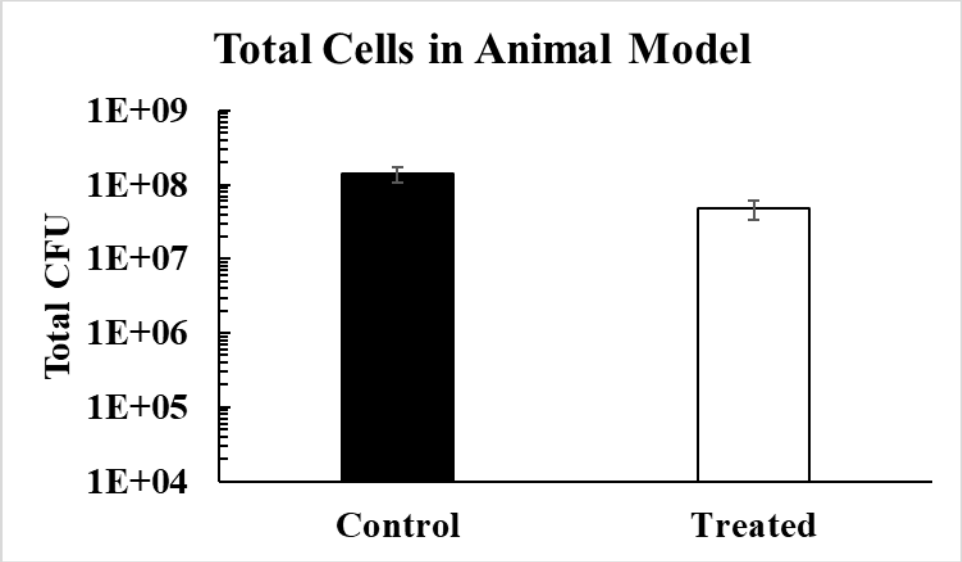

Figure 5. Viability of total *S. aureus* cells in the rabbits after 12 μA/cm^2 wireless delivered DC treatment for 6 h.

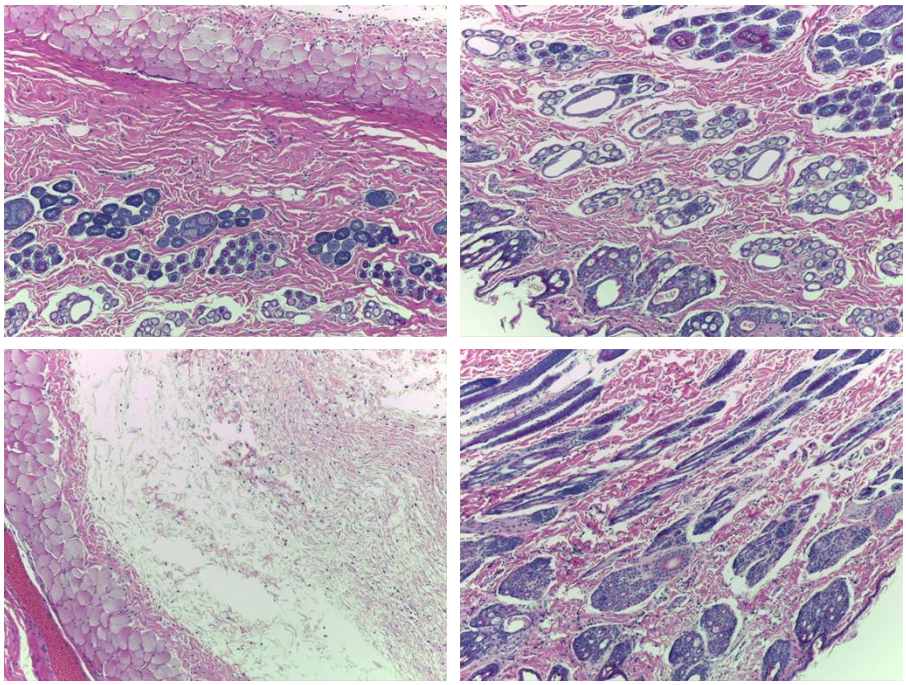

(A)

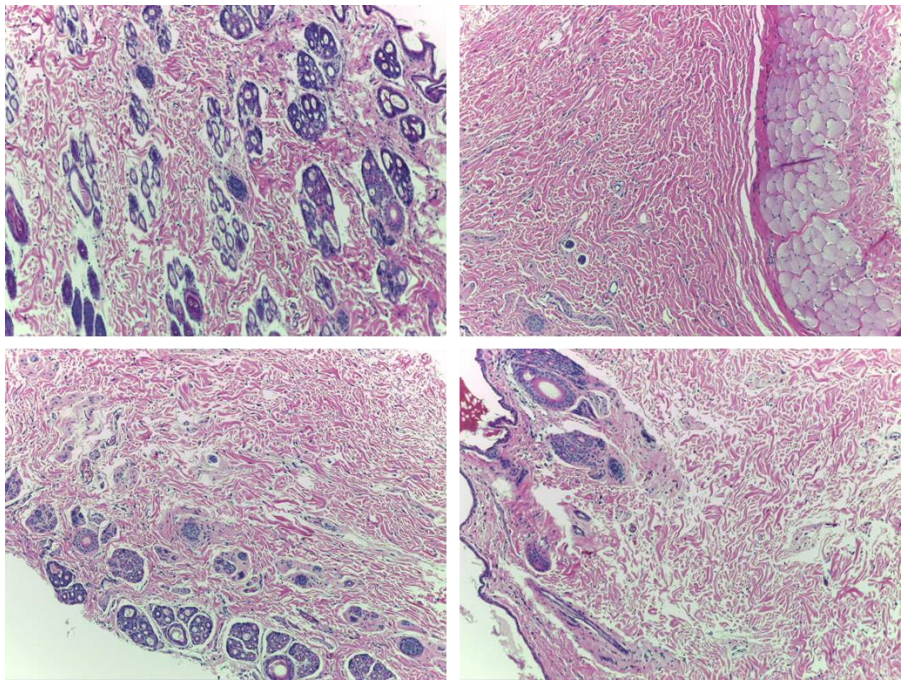

(B)

Figure 6. HE staining of the dermis tissues in direct contact with the devices. The specimen was collected, and undergone cryosection. H &E staining was performed to evaluate the histology of the untreated (A) and treated (B) specimen with 12 μA/cm^2 DC wirelessly delivered for 6 h.

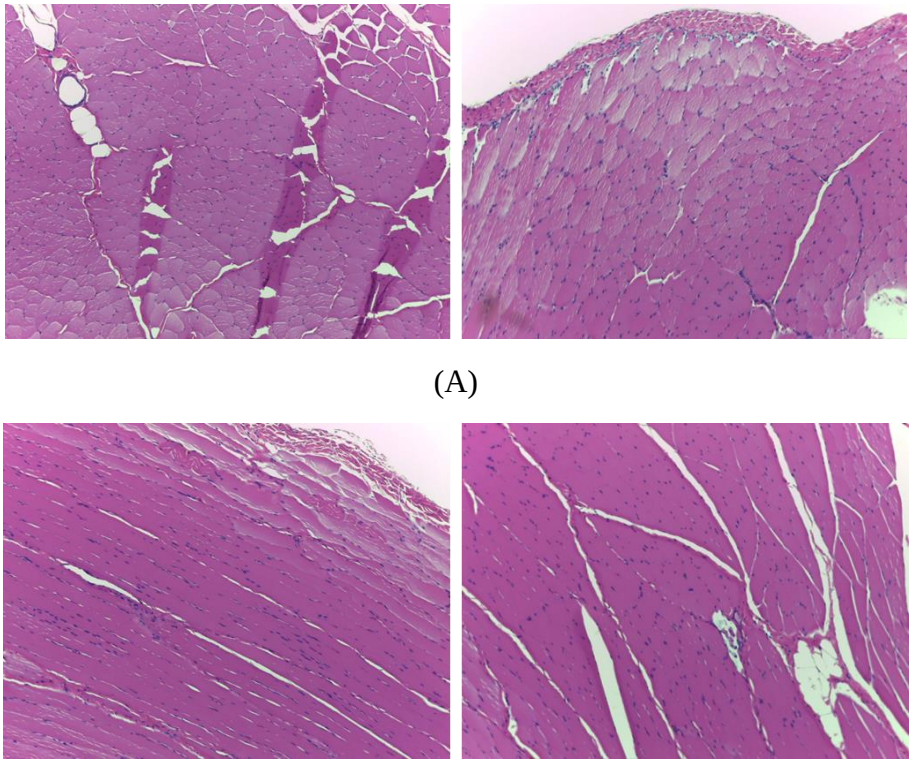

(A)

(B)

Figure 7. HE staining of the surficial muscle tissues in direct contact with the devices. The specimen was collected, and undergone cryosection. H &E staining was performed to evaluate the histology of the untreated (A) and treated (B) specimen with 12 μA/cm^2 DC wirelessly delivered for 6 h.

Chapter 8

Conclusions and Future work

8.1 Conclusions

Device-associated infections are not only a serious challenge to affected patients but also a heavy burden for the healthcare system and risk for the development of antibiotic bacteria. Previous studies discovered the promising killing effects of μA level DC on bacterial biofilms. However, the approach of DC delivery by wires requires skin piercing and thus limits the application of DC treatment *in vivo*. Motivated by this, we conducted this study to investigate the possibility of applying wirelessly delivered DC treatment to control pathogenic biofilms on the surface of implanted biomaterial devices. *P. aeruginosa* and *S. aureus* were chosen as model pathogens, and the PDMS was chosen as the substrate for biofilm growth to mimic the contaminated surfaces of implanted devices. Our results demonstrated for the first time that both *P. aeruginosa* and *S. aureus* biofilm could be effectively eradicated by wirelessly delivered DC. For example, 60 μA/cm^2 of wirelessly delivered DC-mediated with 316L stainless steel electrodes reduced the viability of *P. aeruginosa* and *S. aureus* biofilm cells by 3.6 logs and 2.5 logs, respectively. When using graphite-based electrodes (TGON), similar levels killing effects were obtained with the 30 μA/cm^2 of wirelessly delivered DC. The treatment condition was found safe to lung epithelial cells and fibroblast cells *in vitro*.

The killing results based on CFU were corroborated by SEM analysis, which showed that *P. aeruginosa* and *S. aureus* biofilm cells were deformed/lysed after wirelessly delivered DC treatment. This is consistent with the results of previous researches using wired delivery of DC. Synergies between wirelessly delivered DC and antibiotics (tobramycin and chlorhexidine) in killing biofilm cells were also observed.

To evaluate the potential of wirelessly delivered DC in biofilm control related to commercial medical implants, we engineered a prototype device with the wireless delivery and treatment system integrated into prototype device. Different shapes and electrodes layouts of the prototype device were compared using COMSOL simulation to obtain the best killing effects. *In vitro* and *ex vivo* tests demonstrated good killing effects of the prototype device on both *P. aeruginosa* and *S. aureus* biofilms on the surface of the prototype device. For example, the number of viable *S. aureus* biofilm was reduced by 2.3 and 2.1 logs after treatment *in vitro* and *ex vivo* for 6 h. These results demonstrated showed the feasibility of applying the same wirelessly delivered DC treatment in commercial implant devices (such as cochlear implant, pacemaker, GI tract stimulator, deep brain stimulator, et al.), which have similar dimension as our prototype device (4.5 cm diameter, 1 cm thickness).

Although the animal tests showed less killing (65%) effect on *S. aureus* biofilm cells on the surface of the device than *in vitro* and *ex vivo* tests, because of the low conductivity under the dermis layer, the wirelessly delivered DC was effective in eradicating *S. aureus* cells especially those attached on the dermis tissue without noticeable cytotoxicity. Many researchers reported that the biofilm on the contaminated implant device could release free cells to the surrounding environment by shear force and caused secondary infections [1-3]. Our results showed that the device of wirelessly delivered DC treatment could protect both devices and surrounding host tissues from biofilm-associated infections.

Through mechanism study, we found that the products of electrochemical reactions have stronger effects in biofilm killing than the flow of ions during DC treatment. The killing mechanisms between the stainless steel electrode and graphite-based electrode appeared to be different. For example, bacterial killing by DC using graphite electrodes depends on the concentration of sodium

chloride in the solution. This concentration-dependent killing effect was also observed when treating biofilms with different concentrations of the sodium hypochlorite solution. Because the graphite anode could oxidize the chloride ions to chlorine and hypochlorous acid, the killing effect of graphite electrodes may be due to its oxidation products during DC treatment. In contrast, steel electrodes didn't show any concentration-dependent killing effect, and the hydrogen peroxide produced by steel electrodes wasn't enough to cause the killing effects to biofilm. Interestingly, the killing effect of stainless steel electrode was only observed in the single chamber system. This indicates that stainless steel electrode has bactericidal agents from the secondary electrochemical reaction between the products from the anode and cathode, which is completely different from graphite electrode.

In summary, this study demonstrated that wirelessly delivered DC treatment is a promising approach for controlling device-associated infections caused by pathogenic biofilms. More research is needed to further develop this technology for clinical applications.

8.2 Future work

8.2.1 Optimizing the prototype device

The prototype device used in this study has a volume of 25 cm^3 that shares a similar size as Oreo cookie. However, it still seems oversize compared to the latest generation of electronic pacemaker that is only 1 cm^3 [4]. The smaller size of the device could be more feasible for *in vivo* applications. The bottleneck to minify our devices is the rectifier chips and the internal resistor that reduces the total current to micro-amp levels. The rectifier chip we used is derived from the commercial wireless electric receiver with several large circuit components and fixed power output (5 V). It is

necessary to design a new rectifier chip with minimized components to reduce the size and power output to so that the internal resistor will be unnecessary.

Additionally, the surface conductivity of the device is a critical issue that needs to be considered. In *in vitro* and *ex vivo* tests, the device was perfectly surrounded with a saline solution that promised good conductivity between the anode and cathode. However, when the device was implanted in the pocket cavity under the epidermis of the rabbit, it had a drier environment with only little body fluid. This lead to a poor connection between electrodes, and relating less killing in the *in vivo* tests. To address this challenge, the conductive particles (such as carbon black nanotube and nanoparticle [5, 6]) could be mixed with PDMS monomer to increase the electric conductivity, and thus the capability of biofilm control by the engineered device.

8.2.2 Roles of the electrochemical products in bacterial killing by DC

Our data indicated that different electrochemical reactions played a significant role in low-level DC treatment, and the movement of ions does not appear to be important. For example, DC treatment using graphite electrodes could generate chlorine and hypochlorite, while the steel electrodes may have secondary electrochemical reactions between anode and cathode products (Fenton reaction) and produce free radicals. The next step should be using specific assays to measure the actual concentration of these products in the electrolysis solution. This will provide deeper insight into the killing mechanism of electric current as well as the information about long-term cytotoxicity.

8.2.3 Wireless electric impendency scanning

The electric impendency scanning (EIS) technique can detect tiny changes in redox property of the electrode. Thus, it is a perfect approach to monitoring biofilm formation on the surface of an

implant device. However, conventional EIS also needs wires to connect the potentiostat with electrodes. If we can modify our system of wirelessly delivered DC treatment to achieve wireless communication between potentiostat and *in vivo* electrodes, the device will be able to both detect the biofilm formation and conduct DC treatment on demand. This would be a new generation of implanted devices with both self-diagnosing and self-cleaning functions.

8.3 References

1. Kostakioti, M., Hadjifrangiskou, M. & Hultgren, S.J. Bacterial biofilms: development, dispersal, and therapeutic strategies in the dawn of the postantibiotic era. *Cold Spring Harb Perspect Med* **3**, a010306 (2013).
2. Ymele-Leki, P. & Ross, J.M. Erosion from Staphylococcus aureus biofilms grown under physiologically relevant fluid shear forces yields bacterial cells with reduced avidity to collagen. *Appl Environ Microbiol* **73**, 1834-1841 (2007).
3. McConoughey, S.J. et al. Biofilms in periprosthetic orthopedic infections. *Future Microbiol* **9**, 987-1007 (2014).
4. Cingolani, E., Goldhaber, J.I. & Marbán, E. Next-generation pacemakers: from small devices to biological pacemakers. *Nat Rev Cardiol* **15**, 139-150 (2018).
5. Kim, J.H. et al. Simple and cost-effective method of highly conductive and elastic carbon nanotube/polydimethylsiloxane composite for wearable electronics. *Sci Rep* **8**, 1375 (2018).
6. Han, C.J., Chiang, H.P. & Cheng, Y.C. Using Micro-Molding and Stamping to Fabricate Conductive Polydimethylsiloxane-Based Flexible High-Sensitivity Strain Gauges. *Sensors (Basel)* **18** (2018).

Appendix A. Growing *S. aureus* biofilm on the PDMS surface of different stiffness

In all the study of this dissertation, we grew the S. aureus biofilm on the stiff PDMS with Young's modulus of 2 MPa. The actual stiffness of PDMS used in implant device the could be varied. We reported that the stiffness of PDMS could affect the formation of *P. aeruginosa* biofilm on early stage although there was no obvious difference for mature biofilm. To investigate if there was also such phenomena for *S. aureus* biofilm, we compared the attachment and growth of S. aureus biofilm on both stiff and soft PDMS surfaces.

Method:

1. The *S. aureus* overnight culture was made in the LB medium and then washed by 1X PBS solution as the same procedure mentioned in Chapter 3. The PDMS surfaces were also prepared as the same procedure, the ratio of between monomer and crosslinker were 40:1, 20:1 and 5:1 for soft, medium and stiff PDMS, respectively.

2. The cells' solution was diluted by 500 times with PBS and then added into petri dish contained soft, medium and stiff PDMS.

3. The PDMS surfaces were kept in the cells' solution at 37°C for 2 h.

4. The PDMS surfaces were gently washed with PBS solution and then transported to LB medium at 37°C.

5. After 2, 5 and 24 hours, the PDMS surfaces were taken out from LB followed by CFU counting and Living/Dead staining to evaluate the number of viable S. aureus cells.

Result:

The growth curve of the *S. aureus* biofilm on PDMS demonstrated that the biofilm on stiff surface grew obviously slower (Figure 1) in the first 5 hours compared to soft and medium surfaces, although the numbers of the initially attached cells were same (Figure 2). After 6 hours, the total cells' numbers of biofilms on three surfaces were closed, and there was no significant difference among mature (24 h) biofilms on soft, medium and stiff PDMS surfaces.

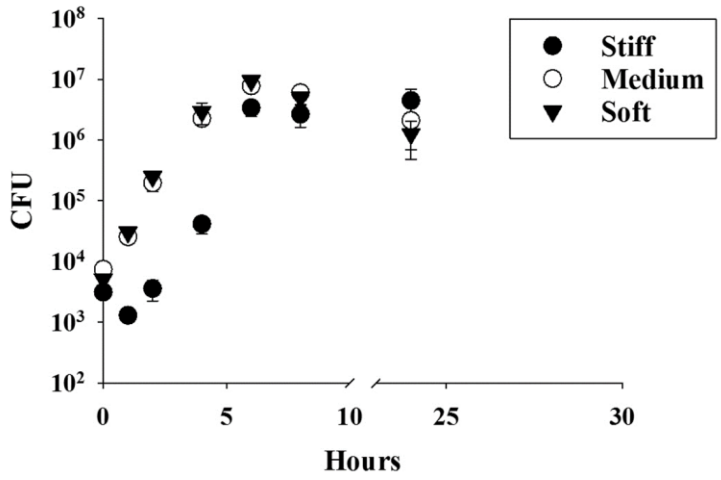

Figure 1. The growth curve of *S. aureus* biofilm on stiff, medium and soft PDMS substrates.

The images of Living/Dead staining were in consistent with the CFU results. For example, there were noticeably more cells on the soft and medium PDMS surfaces than the stiff one after 2 hours incubation in LB medium although the initially attached cells were almost equal (Figure 3). After 5 hours' incubation, the soft and medium surfaces had multiple layers of biofilm cells while the cells' number of the stiff surface was still closed to initial attachment (Figure 3). After 24 hours' growth, all three kinds of PDMS surface had similar coverage of biofilm cells.

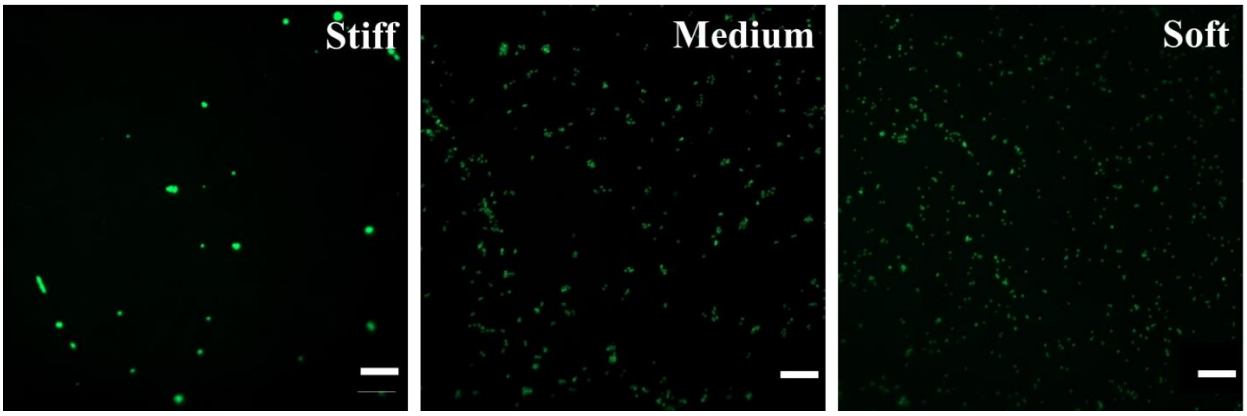

Figure 2. The SYTO9 stained *S. aureus* cells attached on stiff (5:1), medium (20:1) and soft (40:1) PDMS substrates after inoculation in PBS solution for 2 hours. Scale bars = 20 μm.

In all the studies of this dissertation, the *S. aureus* biofilms were grown in 22 – 24 hours in LB medium for 24 hours. At this stage, we didn't find the significant difference *S. aureus* biofilm on soft and stiff PDMS surfaces, which was in consistent with the *P. aeruginosa* biofilm reported before. Therefore, the interfere of the substrate's stiffness could be excluded.

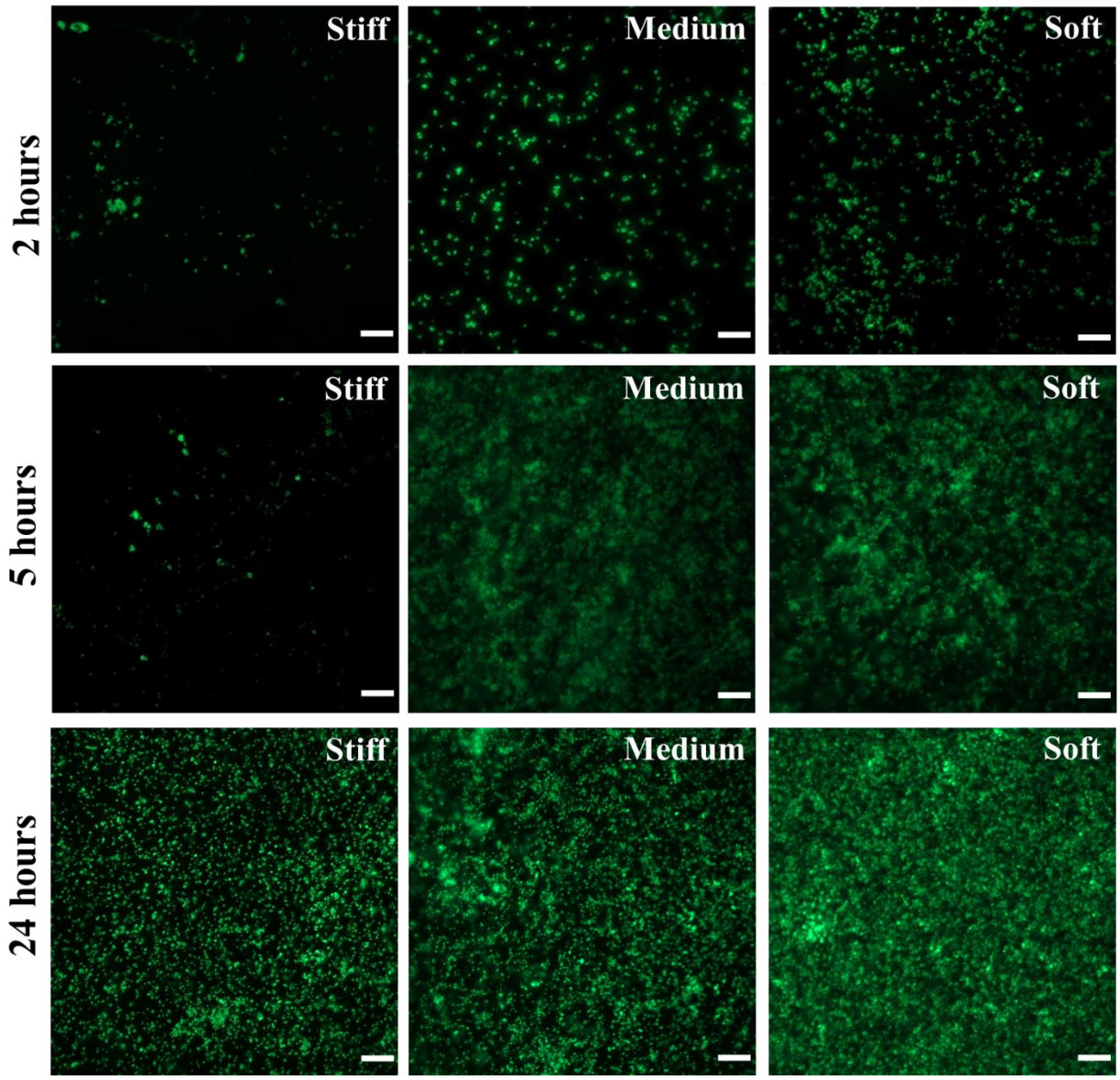

Figure 3. The SYTO9 stained *S. aureus* biofilm cells on stiff (5:1), medium (20:1) and soft (40:1) PDMS substrates during biofilm growth in LB medium. Scale bars = 20 μm.

Appendix B. Supplementary data Chapter 3: The proof-of-concept study of wirelessly delivered DC treatment on biofilm cells

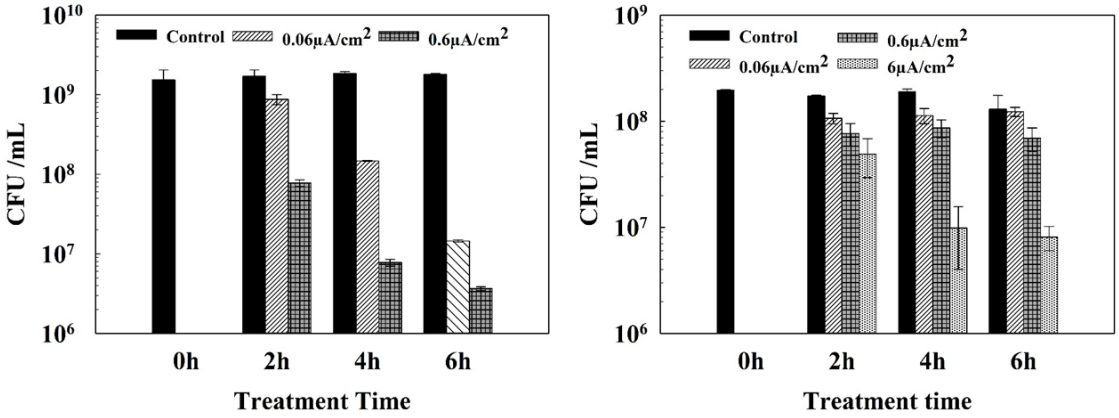

Figure S1. The viability of *P. aeruginosa* (left) and *S. aureus* (right) planktonic cells after treatment with 0.06, 0.6 or 6μA/cm^2 DC in 0.85 % NaCl for 2, 4 or 6 h.

Name: Hao Wang
Cell: (937) 760-9989
Email: hwang50@syr.edu

EDUCATION

06/2014 **-** Present Syracuse University, Syracuse, NY
PhD. Candidate in Chemical Engineering
Advisor: Dacheng Ren, Ph.D.
Thesis: Eradicating Bacterial Biofilm by Wireless Electrostimulation.

08/2008 – 05/2013 University of Dayton, Dayton, OH
M.S. Chemical Engineering, August 2011
Advisor: Donald Comfort, Ph.D.
Thesis: The Study of Microbial Fuel Cell with *Pseudomonas aeruginosa* as Individual Catalyst.

08/2002-06/2006 Southeast University. Nanjing, China PR.
B.S. Pharmaceutical Engineering, June 2006
Advisor: Songqin Liu, Ph.D.
Thesis: Utilizing Prussian blue modified electric chip to monitor the concentration of hemoglobin in samples.

RESEARCH EXPERIENCE

Controlling pathogen biofilm on biomaterial surface with wireless electrostimulation. (*04/2017 - present*)

- Firstly reported using wirelessly delivered electric current (DC) to eradicate the pathogen biofilm on biomaterial surface and the effect to mammalian cells in *in vitro*, *ex vivo* and animal model.
- Invented the prototype model with the function of self-disinfection via wirelessly delivered electric current.
- Reported the new killing mechanism of graphite and steel electrodes in DC treatment to biofilm.
- Two papers are in preparation.
- Parts of the results will be summarized as my Ph.D. thesis.

Effects of material stiffness on bacterial adhesion and biofilm infection. *(06/2016 - 04/2017)*

- Found that the effects of surface stiffness on the physiology of attached gram-positive bacteria, and possible pathway of bacteria sensing stiffness of biomaterial surface.
- Three papers have been published in Frontiers in Microbiology, ACS Applied Materials and Interfaces and Applied Microbiology and Biotechnology, respectively.

Difference of glucose metabolism process between *Pseudomonas aeruginosa* biofilm and planktonic cells *(05/2016 - 09/2017)*

- Found that the difference in metabolism pathway of glucose between *P. aeruginosa* biofilm and planktonic cells.
- One paper is in reviewing (Frontiers in Microbiology).

Controlling dental plaque with direct current and chlorhexidine. *(05/2015 - 05/2016)*

- Found the synergy treatment effect between low level direct current and chlorhexidine to two dental plaque strains, *Streptococcus mutans* and *Staphylococcus aureus*.
- One paper has been published in AMB Express.

Effect of direct current to *Pseudomonas aeruginosa* biofilm (*08/2014 - 06/2016*)

- Firstly reported the synergic affinition between chromium ions and tobramycin to RNA molecule.
- Found the different effects of DC treatment to *P. aeruginosa* biofilm with anode and cathode.

- Three papers have been published in Biomaterials and Acta Biomaterialia, respectively.

Reducing initial period of microbial electrolysis cell (MEC) by improving biofilm growth on electrodes (*08/2013 - 04/2014*)

- Transferred mature environmental biofilm to the electrodes of MEC, reduced the lag phase of system initiation, enhanced the degradation efficiency of organic waste in MEC. Immobilizing Geobacter sulfurreducens biofilm on the anode and improving the current generation in MEC.

Utilizing *Pseudomonas aeruginosa* to generate electric current in microbial fuel cell system (MFC) (*01/2010 – 04/2013*)

- Used *P. aeruginosa* planktonic and biofilm cells as anodic catalyst to covert glucose into electric power in the dual chamber microbial fuel cell system, optimized the system structure to get maximum and long-term power output.
- The results were summarized as my master thesis.

Looking for optimized synthesis methods of drug intermediates compounds (*06/2006 – 06/2008*)

- Optimized industrial manufacturing process of Allopurinol. Developed a new protocol for synthesizing (+)-Bornyl Chloromethylether.
- One paper has been published in Chemical Reagents (China).

Using electrochemical method to detect the concertation of blood (*01/2006 – 06/2006*)

- Used printed electrodes' chip to qualify the concentration of blood hemoglobin in the biological sample, established standard curve of measurement, developed fast detection assay of blood hemoglobin of patients.
- The results were summarized as my bachelor thesis.

WORKING EXPERIENCE

Syracuse University

06/2017 – Present **Research assistant**

08/2015 – 05/2017 **Teaching assistant**

- CEN 341 Fundamentals of Heat and Mass Transfer.
- CEN 412 Chemical Engineering Laboratory II.
- CEN 575 Process Control

06/2014 – 07/2015 **Research assistant**

07/2013 – 05/2014 **Research assistant**

University of Dayton

06/2009 – 04/2013 **Research assistant**

Jiangsu Provincial Institute of Material Medica. Nanjing, China PR.

06/2006 – 05/2008 **Technician of Medical Chemistry Lab**

PUBLICATIONS

Fangchao Song †, **Hao Wang** †, Karin Sauer and Dacheng Ren. "Cyclic-di-GMP and oprF are involved in the response of Pseudomonas aeruginosa to substrate material stiffness during attachment on polydimethylsiloxane (PDMS)." **Frontiers in Microbiology**. 9:110 (2018).

H. Wang and D. Ren. "Controlling *Streptococcus mutans* and *Staphylococcus aureus* with Direct Current and Chlorhexidine". **AMB EXPRESS**. 7 pp 204 (2017).

F. Song, M. E. Brasch, **H. Wang**, J. H. Henderson, K. Sauer, D. Ren. "How bacteria respond to material stiffness during attachment: a role of Escherichia coli flagellar motility." **ACS Applied Materials and Interfaces**. 9 (27), pp 22176–22184 (2017).

Y. Zhao, F. Song, H. Wang, J. Zhou, D. Ren. "Phagocytosis of Escherichia coli Biofilm Cells with Different Aspect Ratios: A Role of Substratum Material Stiffness". **Applied Microbiology and Biotechnology**. Volume 101, issue 16, pp 6473–6481 (2017).

T. H. R. Niepa, **H. Wang**, J. L. Gilbert, and D. Ren. "Eradication of Pseudomonas aeruginosa cells by cathodic electrochemical currents delivered with graphite electrodes". **Acta Biomaterialia**. 50: 344-352 (2017).

T. H. R. Niepa, **H. Wang**, J. C. Dabrowiak, J. L. Gilbert, and D. Ren. "Synergy between Tobramycin and Trivalent Chromium Ion in Electrochemical Control of Pseudomonas aeruginosa." **Acta Biomaterialia.** 36:286-95 (2016).

T. H. R. Niepa, L. M. Snepenger, **H. Wang**, S. Sivan, J. L. Gilbert, M. B. Jones, D. Ren. "Sensitizing *Pseudomonas aeruginosa* cells to antibiotics by electrochemical disruption of membrane functions." **Biomaterials.** 74: 267-279 (2015).

H. Wang, X. Yan, Q. Wei and P. Wang. "Synthesis of (+)-Bornyl Chloromethylether." **Chemical Reagents (China).** 7 (2008).

PAPERS IN PREPARING

H. Wang and D. Ren. "Wireless Electrostimulation to Eradicate Bacterial Biofilms." In preparation.

N. Wan, **H. Wang**, N. Kiat, M. Mukherjee, D. Ren, B. Cao, Y. Tang. "Bacterial metabolism during biofilm growth investigated by ^{13}C tracing". **Frontiers in Microbiology.** In reviewing.

PATENT

Wireless Electrostimulation to Eradicate Implanted Device Associated Biofilms. 62/543,570. Filed Aug 10, 2017

CONFERENCES' PRESENTATIONS

H. Wang, D. Ren. Wireless Electrostimulation to Eradicate Bacteria Biofilm. **2018 AIChE Annual Meeting,** October 2018.

H. Wang, D. Ren. Wireless Electrostimulation to Eradicate Bacteria Biofilm (*Poster*). **8th ASM Conference on Biofilms,** October 2018.

H. Wang, D. Ren**.** The Stiffness of Poly (dimethylsiloxane) Affects Staphylococcus aureus Biofilm Growth (*Poster*). **4th Bacteria-Material Interactions Conference**, June 2017.

M. Gerwitz, **H. Wang** and D. Ren. Synergy between Low-level Electric Current and Nystatin in Controlling Candida albicans (*Poster*). **ASM microbe**, June 2017.

H. Wang and D. Ren. Controlling Dental Plaque-causing Bacteria within Electric Current and Chlorhexidine (*Poster*). **Nunan Lecture & Research Day.** April 5, 2016.

H. Wang, R. Stoutenburg, D.F. Call. Extraction and Re-immobilization of Exoelectrogenic Biofilms (*Poster*). **North American ISMET.** May 14, 2014.

H. Wang, P.J. Shah, D.A. Comfort, J. Rowe, A.M. Sarangan. Fabrication and Flow Characterization of a micro-Laminar Flow Device for use as a Miniature Microbial Fuel Cell. **8th Annual Dayton Engineering Sciences Symposium.** October 29, 2012.

H. Wang, P.J. Shah, T.J. Gorey, J. Rowe, A.M. Sarangan, D.A. Comfort. A New Method of Generating Electricity Using *Pseudomonas aeruginosa* in a Microbial Fuel Cell. **University of Dayton, Stander Symposium**. April 13, 2011.

SKILLS

Software: SigmaPlot, AfterMath, AutoCAD, Microsoft Office.

Programming Languages: C++, Matlab

Languages: English and Mandarin.

Skills: GC, HPLC, IR, Microarrays, qPCR, Optical microscopy, Electrophoresis, SEM, Cloning, PCR, Flow cytometer, RNA isolation, Mammalian Cell cultures, Viability test, NMR.

TRAINING EXPERIENCE

Photolithography, Cornell Nanoscale Science and Technology Facility (CNF), Ithaca, NY, 01/2016

- Joined the community of CNF, learned and improved the skill of mask making and photolithography.

HONORS AND REWARDS

- Graduate Student Organization Travel Grant, Syracuse University 06/2017
- Summer Research Fellowship, University of Dayton 06/2010